

Aus dem
Institut für Schlaganfall- und Demenzforschung (ISD)
Klinikum der Ludwig-Maximilians-Universität München



Evaluating the therapeutic effects of a peptide-based inhibitor of amyloid aggregation in mouse models of Alzheimer's disease

Dissertation
zum Erwerb des Doctor of Philosophy (Ph.D.)
an der Medizinischen Fakultät
der Ludwig-Maximilians-Universität München

vorgelegt von
Hao Ji

aus
Huai'an / China

Jahr
2024

Mit Genehmigung der Medizinischen Fakultät der
Ludwig-Maximilians-Universität München

Erstes Gutachten: Prof. Dr. Jürgen Bernhagen
Zweites Gutachten: Prof. Dr. Ozgun Gokce
Drittes Gutachten: Prof. Dr. Harald Steiner
Viertes Gutachten: Priv. Doz. Dr. Florian Schöberl

Dekan: Prof. Dr. med. Thomas Gudermann

Tag der mündlichen Prüfung: 15.07.2024

Table of Contents

Abstract	4
List of figures	7
List of tables	9
List of abbreviations	10
1. Introduction	13
1.1 Alzheimer’s disease	13
1.2 Clinical aspects of Alzheimer’s disease	13
1.2.1 Epidemiology	13
1.2.2 Risk factors	14
1.2.3 Disease progression	15
1.2.4 Diagnosis and treatment.....	16
1.3 Neuropathological hallmarks of Alzheimer’s disease	18
1.3.1 Amyloid plaques	18
1.3.2 Cerebral amyloid angiopathy	19
1.3.3 Neurofibrillary tangles	21
1.3.4 Inflammation	21
1.3.5 Neuron loss.....	22
1.4 The amyloid cascade hypothesis	22
1.4.1 Definition	22
1.4.2 Amyloid-beta aggregation	23
1.5 Mouse models of Alzheimer’s disease	24
1.6 Drug development in Alzheimer’s disease	26
1.6.1 Symptomatic treatments	27
1.6.2 Disease-modifying therapies	27
1.6.3 Peptide-based inhibitors	29
1.7 Transcriptome profiling: RNA sequencing	31
1.7.1 RNA sequencing	31
1.7.2 Single-cell RNA sequencing	32
2. Aims of the study	34
3. Materials and Methods	35

3.1	Materials	35
3.1.1	Reagents.....	35
3.1.2	Assay kits.....	37
3.1.3	Antibodies	37
3.1.4	Materials	38
3.1.5	Equipment.....	39
3.2	Animals	40
3.2.1	General considerations and housing	40
3.2.2	5XFAD transgenic mice	40
3.2.3	APPNL-G-F knock-in mice	41
3.2.4	Peptide preparation and administration	41
3.2.5	Mouse plasma and cerebral spinal liquid collection.....	42
3.2.6	Preparation of mouse brain for biochemistry	42
3.2.7	Preparation of mouse brain for immunohistology	43
3.3	Behavioral tests	43
3.3.1	Open field test.....	43
3.3.2	Barnes maze.....	43
3.3.3	Elevated plus maze	44
3.4	Biochemical and molecular studies	44
3.4.1	DNA extraction from mouse tails	44
3.4.2	Nucleic acid quantitation	45
3.4.3	Protein extraction from mouse brains	45
3.4.4	Protein quantification	46
3.4.5	Immunofluorescence staining and imaging	46
3.4.6	Western blot and slot blot	47
3.4.7	Screening and validation of anti-2E antibody	48
3.4.8	Simoa NF-light assay.....	49
3.4.9	Enzyme-linked immunosorbent assay	49
3.4.10	Luminex neurodegeneration array	50
3.5	RNA sequencing of mouse brains	50
3.5.1	RNA extraction from mouse brains.....	52
3.5.2	cDNA library preparation.....	53
3.5.3	Sequencing data generation	53
3.6	Bioinformatics analysis	53
3.7	Statistical analysis	54

3.8	Software.....	55
4.	Results	56
4.1	Chronic 2E treatment alleviates A β deposition in the brains of 5XFAD mice 56	
4.2	2E changes soluble A β 42 and A β 40 levels in Alzheimer’s disease mouse models	60
4.3	2E shifts amyloid deposition in the brains of 5XFAD mice	61
4.4	2E distributes into brain after intraperitoneal injection	62
4.5	Chronic 2E treatment improves behavior deficits in 5XFAD mice.....	64
4.6	Establishment of RNA sequencing with PFA-fixed brain samples	67
4.7	2E alters 5XFAD induced gene expression changes	70
4.8	2E decreases neuronal damage in the brains of 5XFAD mice	73
4.9	2E alters disease-associated glial signatures	76
5.	Discussion.....	81
5.1	Peptide-based inhibitors for A β aggregation.....	81
5.2	Responses of microglia	83
5.3	Responses of astrocytes	86
5.4	RNA-seq with PFA-fixed tissue	88
5.5	Preclinical randomized controlled trial.....	89
5.6	Limitations.....	90
5.7	Potential future directions	91
6.	Summary.....	93
7.	List of publications	94
8.	References	96
9.	Acknowledgements	130
	Affidavit.....	132
	Confirmation of congruency.....	133

Abstract

Alzheimer's disease (AD), a predominant neurodegenerative disorder, leads to cognitive impairment stemming from extensive neuronal loss with limited disease-modifying therapies (DMTs) available. Central to AD pathology is the accumulation of amyloid-beta ($A\beta$) peptide, a key player in disease progression. In addition to the $A\beta$ -specific monoclonal antibodies, islet amyloid polypeptide (IAPP) has been found to attenuate amyloid self-assembly *in vitro* and *in vivo*. Building on IAPP's "cross-amyloid" inhibitor function, the macrocyclic 17-residue peptide 2E was designed as a mimic of the interaction surface of IAPP with $A\beta$. Encouragingly, 2E turned out to be a potent inhibitor with nanomolar affinity of $A\beta$ amyloid self-assembly *in vitro* and, in addition, it exhibited a significant proteolytic stability in human plasma and the ability to cross the blood-brain barrier (BBB) in a cell model. These favorable, drug-like, properties of 2E motivated us to test its effectiveness on amyloid pathology in AD mouse models.

In my thesis, I investigated the efficacy of two treatment paradigms of the macrocyclic peptide 2E in ameliorating amyloid pathology using both female and male 5XFAD mice, a commonly used animal model for AD. The findings revealed a significant reduction in cortical amyloid deposition, decreased plasma and CSF $A\beta_{42}$ concentration, increased $A\beta_{40}$ levels, shifted amyloid deposition from brain parenchyma to blood vessels, decreased neuronal damage, and enhanced astrocytic activation upon 2E administration. Similar effects of 2E on soluble $A\beta_{42}$ and $A\beta_{40}$ changes were observed in APPNL-G-F transgenic mice. Furthermore, treated 5XFAD mice displayed improvements in memory and motor functions without any alterations in anxiety or stress responses, as evidenced by various behavioral tests. Notably, I established a novel method to perform high-resolution RNA sequencing from PFA-fixed microscopy slices. RNA-seq analyses highlighted 2E's ability to bolster astrocytic activation while reversing AD-associated neuronal gene expression changes. Importantly, following intraperitoneal (i.p.) injection, 2E's presence in the brain attests to its biodistribution capability. Thus, the macrocyclic peptide 2E, either as a standalone or combined with other anti-amyloid strategies, emerges as a promising drug candidate to combat $A\beta$ -driven AD pathogenesis.

Zusammenfassung

Die Alzheimer-Krankheit (AD), eine vorherrschende neurodegenerative Störung, führt zu kognitiven Beeinträchtigungen, die auf einen umfassenden Verlust von Nervenzellen zurückzuführen sind, wobei nur begrenzte krankheitsmodifizierende Therapien (DMTs) zur Verfügung stehen. Zentraler Bestandteil der Alzheimer-Pathologie ist die Anhäufung von Amyloid-beta (A β)-Peptiden, die eine Schlüsselrolle beim Fortschreiten der Krankheit spielen. Zusätzlich zu den A β -spezifischen monoklonalen Antikörpern wurde festgestellt, dass das Insel-Amyloid-Polypeptid (IAPP) die Amyloid-Selbstorganisation *in vitro* und *in vivo* abschwächt. Aufbauend auf der "Cross-Amyloid"-Hemmfunktion von IAPP wurde das makrozyklische Peptid 2E mit 17 Residuen als Nachahmung der Interaktionsfläche von IAPP mit A β entwickelt. Erfreulicherweise erwies sich 2E als potenter Inhibitor mit nanomolarer Affinität der A β -Amyloid-Selbstorganisation *in vitro* und zeigte darüber hinaus eine hohe proteolytische Stabilität in menschlichem Plasma und eine Durchlässigkeit der Blut-Hirn-Schranke (BHS) in einem Zellmodell. Diese vorteilhaften, arzneimittelähnlichen Eigenschaften von 2E motivierten uns, seine Wirksamkeit auf die Amyloid-Pathologie in AD-Mausmodellen zu testen.

In meiner Dissertation untersuchte ich die Wirksamkeit von zwei Behandlungsparadigmen des makrozyklischen Peptids 2E bei der Verbesserung der Amyloid-Pathologie an weiblichen und männlichen 5XFAD-Mäusen, einem häufig verwendeten Tiermodell für AD. Die Ergebnisse zeigten eine signifikante Verringerung der kortikalen Amyloidablagerung, eine verringerte A β 42-Konzentration im Plasma und im Liquor, erhöhte A β 40-Spiegel, eine Verlagerung der Amyloidablagerung vom Hirnparenchym zu den Blutgefäßen, eine verringerte neuronale Schädigung und eine verstärkte astrozytäre Aktivierung nach der Verabreichung von 2E. Ähnliche Wirkungen von 2E auf die Veränderungen von löslichem A β 42 und A β 40 wurden bei APPNL-G-F transgenen Mäusen beobachtet. Darüber hinaus zeigten behandelte 5XFAD-Mäuse Verbesserungen im Gedächtnis und in der Motorik, ohne dass es zu Veränderungen bei Angst- oder Stressreaktionen kam, wie verschiedene Verhaltenstests zeigten. Insbesondere habe ich eine neue Methode zur hochauflösenden RNA-Sequenzierung von PFA-fixierten Mikroskopschnitten entwickelt. RNA-seq-Analysen unterstrichen die Fähigkeit

von 2E, die astrozytäre Aktivierung zu verstärken und gleichzeitig AD-assoziierte neuronale Genexpressionsänderungen umzukehren. Wichtig ist, dass nach einer intraperitonealen (i.p.) Injektion das Vorhandensein von 2E im Gehirn seine Fähigkeit zur Biodistribution beweist. Somit erweist sich das makrozyklische Peptid 2E, entweder als Einzelwirkstoff oder in Kombination mit anderen Anti-Amyloid-Strategien als vielversprechender Arzneimittelkandidat zur Bekämpfung der A β -bedingten AD-Pathogenese.

List of figures

Figure.1: Global prevalence trends of dementia, 2019-2050

Figure.2: Two major senile plaques in Alzheimer's disease: diffuse plaques and dense core plaques

Figure.3: Cerebral amyloid angiopathy in Alzheimer's disease

Figure.4: IAPP-A β cross-amyloid nanomolar peptide inhibitors of A β aggregation

Figure.5: Schematics of in vivo experimental plan and summary

Figure.6: 2E has no side effects on bodyweight

Figure.7: Chronic 2E treatment alleviates A β deposition in the brains of 5XFAD mice

Figure.8: 2E changes soluble A β 42 and A β 40 levels in 5XFAD mouse model

Figure.9: 2E changes soluble A β 42 and A β 40 levels in APP-NL-G-F mouse model

Figure.10: 2E shifts amyloid deposition in the brains of 5XFAD mice

Figure.11: Anti-2E 26A12 monoclonal antibody validation and 2E detection using spike-in assays

Figure.12: 2E distributes within the brain after i.p. injection

Figure.13: 2E improves behavior deficits in 5XFAD mice.

Figure.14: 2E improves behavior deficits without changing the anxiety levels in 5XFAD mice.

Figure.15: 2E has no effects on the anxiety levels of young 5XFAD mice.

Figure.16: Workflow of the main steps of the RNA extraction protocol from PFA-fixed tissue.

Figure.17: Isolation of brain tissue for RNA-seq through microdissection

Figure.18: Purify and elute mRNA using oligo dT25 magnetic beads

Figure.19: Quality check of cDNA libraries before sequencing

Figure.20: Quality assessment of the sequencing data

Figure.21: RNA-seq experiment summary and differential gene expression analysis.

Figure.22: 2E alters 5XFAD induced gene expression changes.

Figure.23: Functional analysis of the differentially expressed genes.

Figure.24: 2E mitigates neuronal damage in the brains of 5XFAD mice

Figure.25: 2E mitigates dystrophic neurites in the brains of 5XFAD mice

Figure.26: 2E decreased the biomarkers of neurodegeneration in 5XFAD mice

Figure.27: 2E activates astrocytes in the brains of 5XFAD mice.

Figure.28: 2E partially activates microglia in the brains of 5XFAD mice.

Figure.29: 2E preferentially activates astrocytes rather than microglia.

Figure.30: 2E has no effects on glial cell numbers in the brains of 5XFAD mice.

Figure.31: 2E increases phagocytic activity of microglia in the brains of 5XFAD mice.

List of tables

Table.1: Key reagents

Table.2: Critical Commercial assays

Table.3: Antibodies

Table.4: Materials

Table.5: Equipment

Table.6: Sample and grouping list for RNA-seq

Table.7: Software

List of abbreviations

A β	Amyloid-beta
AD	Alzheimer's disease
ALS	Amyotrophic lateral sclerosis
APP	Amyloid precursor protein
APOE	Apolipoprotein E
ApoE4	Apolipoprotein E ϵ 4 allele
ARIAs	Amyloid-related imaging abnormalities
BBB	Blood-Brain Barrier
BCA	Bicinchoninic acid
BSA	Bovine serum albumin
CA	Cornu ammonis
CAA	Cerebral amyloid angiopathy
CAMCOG	Cambridge Cognitive Examination
CDT	Clock Drawing Test
CNS	Central Nervous System
CSF	Cerebral spinal fluid
CT	Computed Tomography
ddH ₂ O	double-distilled water
DEA	Diethylamine
DMTs	Disease-Modifying Therapies
DNA	Deoxyribonucleic Acid
Dox	Doxycycline
EC	Entorhinal cortex
EDTA	Ethylenediaminetetraacetic acid
ELISA	Enzyme-linked immunosorbent assay
ERCC	External RNA Controls Consortium
FA	Formic acid
FAD	Familial AD

FELASA	Federation of European Laboratory Animal Science Association
FDA	Food and Drug Administration
GFAP	Glial fibrillary acidic protein
GSEA	Gene Set Enrichment Analysis
GV-SOLAS	Society for Laboratory Animals Science
HB	Hybridization buffer
HRP	Horseradish peroxidase
IAPP	Islet amyloid polypeptide
i.p.	Intraperitoneal
MCI	Mild cognitive impairment
MMSE	Mini-mental state examination
MRI	Magnetic resonance imaging
NfL	Neurofilament light
NfM	Neurofilament medium
NfH	Neurofilament heavy
NFTs	Neurofibrillary tangles
NMDA	N-methyl-D-aspartate
NPs	Neuritic plaques
PBS	Phosphate-buffered saline
PBST	Phosphate-buffered saline with Tween
PCA	Principle component analysis
PD	Parkinson's disease
PET	Positron Emission Tomography
PFA	Paraformaldehyde
PHFs	Paired helical filaments
PKD	Phosphate-potassium dextrose
pRCT	Preclinical randomized multicenter trial
PSEN	Presenilin
RIPA	Radioimmunoprecipitation

RNA	Ribonucleic Acid
RNA-seq	RNA sequencing
RT	Room temperature
scRNA-seq	single-cell RNA sequencing
SEM	Standard error of the mean
TBIs	Traumatic brain injuries
TBST	Tris-buffered saline with Tween
TE	Tris-EDTA
TRE	Tetracycline (Tet) response element
tTA	Tetracycline-controlled transactivators
UMIs	Unique molecular identifiers
WHO	World Health Organization
WT	Wild type

1. Introduction

1.1 Alzheimer's disease (AD)

AD (named after the German psychiatrist Alois Alzheimer) is defined as a slowly progressive neurodegenerative disease defined by the depositions of amyloid plaques and neurofibrillary tangles (NFTs) within the brain (Alzheimer et al., 1995; Breijyeh & Karaman, 2020). AD represents the predominant form of dementia, a broad term for the decline in memory and other cognitive functions, constituting the majority of dementia cases (DeTure & Dickson, 2019). The most significant risk factor identified for AD is advancing age or aging, with the majority of AD patients being 65 years of age or older. However, AD is not considered to be a normal part of aging. AD can affect persons under 65, referred to as younger-onset or early-onset AD (YOAD or EOAD) (Mendez, 2019). People with YOAD can be at any stages of the disease, including the early, middle, or late stages. AD worsens over time since it's a progressive condition, leading to a gradual worsening of dementia symptoms over several years (Tarawneh & Holtzman, 2012). At the onset of AD, memory loss is mild, but as the disease progresses to its late stages, individuals lose the capacity to engage in normal conversation and to react to their surroundings. On average, individuals diagnosed with AD can live between 4 to 8 years, though some may live up to 20 years, depending on various other factors.

1.2 Clinical aspects of Alzheimer's disease

1.2.1 Epidemiology

As reported by the World Health Organization (WHO), over 55 million people globally were living with dementia in 2020 (Figure 1). As a result of the global rise in the aging population, the number of individuals living with AD dementia is projected to nearly double every 20 years, approaching 78 million by 2030 and 139 million by 2050, with a significant portion of this increase from the developing countries (Shin, 2022). Currently, approximately 1.8 million people are diagnosed with dementia in Germany, with around 400 thousand new dementia cases per year (Blotenberg et al., 2023). To date, it is estimated that more than 6 million aged 65 and older are living with Alzheimer's

dementia in America, making it the 5th leading cause of death (“2023 Alzheimer’s Disease Facts and Figures,” 2023). According to an updated report, over 15 million individuals in China aged 60 or older are afflicted with dementia, with approximately 10 millions of these cases attributed to AD (Ren et al., 2022).

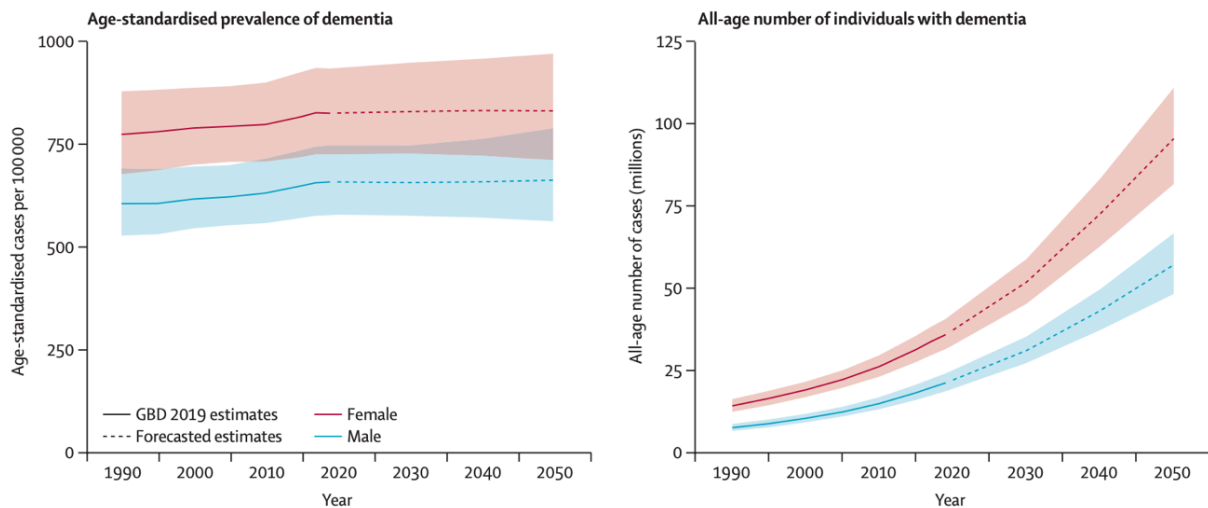


Figure. 1 | Global prevalence trends of dementia, 2019-2050. Age-standardized prevalence of dementia (left panel), and all-age number of individuals with dementia (right panel) with 95% uncertainty intervals. GBD: Global Burden of Diseases, Injuries, and Risk Factors Study. Modified and cited from (GBD 2019 Dementia Forecasting Collaborators, 2022).

1.2.2 Risk factors

AD is linked to various risk factors, including age, gender, genetic factors, lifestyle choices, and concurrent health conditions (Armstrong, 2019). Firstly, age is a significant risk factor as the chance of developing AD increases when people get older, particularly after 65 years old. Statistics show that the risk of AD doubles roughly every five years past this age (Guerreiro & Bras, 2015). Secondly, gender plays a role in AD. Women over 65 are approximately twice as likely to develop AD compared to men, a disparity partly attributed to women’s longer life expectancy. Intriguingly, even after 80, women still exhibit a marginally higher risk than men of the same age (Mielke, 2018). Medical research indicates that early menopause induced by medical treatments may elevate the risk, although it remains uncertain whether natural menopause carries the same implications (Shuster et al., 2010). Thirdly, genetic factors play a crucial role in the development of AD, particularly in early-onset or familial AD (FAD) (Bekris et al., 2010). FAD is often linked to specific gene mutations, including those in

the amyloid precursor protein (APP) and presenilin (PSEN1/2) genes (Lanoiselée et al., 2017). These mutations, if inherited, can be strong indicators of the disease. However, the exact mechanisms by which family genetics influence AD risk remain largely unknown, with many factors likely contributing to its complexity. Notably, FAD is relatively rare and typically appears before the age of 60 (Bird, 2008). Apart from familial genes, risk genes also contribute to Alzheimer's susceptibility. These genes are more common than familial genes but do not guarantee the development of the disease. A prominent example is a variant of the apolipoprotein E (APOE) gene, particularly the APOE e4 allele. This allele is found in approximately 25% to 30% of the population and is linked to an elevated risk of developing AD (Liu et al., 2013).

In addition to above mentioned un-controllable risk factors, some risk factors can be controlled, like lifestyle and health conditions. Adopting a healthy lifestyle, particularly from mid-life (ages 40-65), can significantly decrease the likelihood of developing AD (Livingston et al., 2020). Key aspects of this include avoiding smoking, moderating alcohol consumption, and maintaining a balanced diet. Engaging in regular physical, mental, and social activities also plays a crucial role in reducing AD risk (Meng et al., 2020). Such activities keep the brain and body active and connected, potentially warding off the onset of the disease. Moreover, traumatic brain injuries (TBIs), which result from blows or jolts to the head and often lead to unconsciousness, are known to increase AD risk (Ahmed et al., 2017). Therefore, consistent head protection throughout life may help in lowering this risk. Various health conditions can heighten the risk of developing AD and vascular dementia. Key risk factors include diabetes, stroke, heart issues, cardiovascular risk factors (such as mid-life hypertension, elevated cholesterol, and obesity), age-related hearing loss, and depression (Gottesman et al., 2017; Leszek et al., 2021). Each of these conditions either directly affects brain health or contributes to its decline, thereby increasing the likelihood of AD.

1.2.3 Disease progression

AD is a gradually progressive neurodegenerative disorder. It primarily affects memory and cognitive abilities, frequently leading to alterations in mood and personality ("2023 Alzheimer's Disease Facts and Figures," 2023). Typically, patients transition from mild to severe AD within a timeframe of 7 to 10 years (Holtzman et al., 2011a). Revised

guidelines by the Alzheimer's Association and the National Institute on Aging introduced a three-stage classification for AD: preclinical AD, mild cognitive impairment (MCI) due to AD, and dementia due to AD (Budson & Solomon, 2012; Croisile et al., 2012). During the preclinical phase, individuals show no symptoms, but brain changes may start up to 20 years before clinical diagnosis (Dubois et al., 2016). MCI is characterized by a noticeable, albeit mild, cognitive decline, with 10-15% of cases annually advancing to AD (Petersen et al., 2014; Vega & Newhouse, 2014). In the final phase of AD, characterized by dementia, individuals experience profound memory decline, communication barriers, alterations in personality, motor skill deterioration, and challenges with spatial orientation (Cipriani et al., 2020). In the terminal stage, patients become completely dependent on caregivers, losing basic motor functions, such as swallowing. AD is ultimately a fatal disease, often resulting in death due to complications such as pneumonia (Manabe et al., 2019).

1.2.4 Diagnosis and treatment

1.2.4.1 Diagnosis

Currently, a definitive AD diagnosis is confirmed post-mortem through neuropathological examination, focusing on amyloid plaques and NFTs in the brain (DeTure & Dickson, 2019). However, cognitive, and behavioral changes and family history are used for a probable AD diagnosis during life. Diagnosing early-stage AD, particularly for mild cognitive impairment (MCI), focuses on detecting physical and cognitive shortfalls. This includes memory loss and challenges in recognition (agnosia), language use (aphasia), motor activities (apraxia), or decision-making (executive functioning) that significantly affect daily life (Vega & Newhouse, 2014). Various tests, like the minimal state examination (MMSE), clock drawing test (CDT), and Cambridge cognitive examination (CAMCOG), assess mental status throughout the disease (Cecato et al., 2010; Jonker et al., 2000). Neuroimaging methods such as magnetic resonance imaging (MRI), computed tomography (CT), and positron emission tomography (PET) scans are crucial in diagnosing MCI due to AD and its progression, as well as ruling out other dementia causes (Croisile et al., 2012; Perrin et al., 2009). Additionally, cerebral spinal fluid (CSF) biomarkers, including reduced $A\beta_{x-42}$ and increased tau and phosphorylated tau levels, have shown promise in diagnosing MCI and AD (Fiandaca et al., 2015; Paterson et al., 2018).

1.2.4.2 Treatment

The U.S. Food and Drug Administration (FDA) has authorized several prescription medications for AD management and treatment. These medications are most efficacious during the early to middle stages of AD. Notably, AD remains incurable at present, but these medications help in managing symptoms for those with mild to moderate AD, enhancing their quality of life and aiding caregivers.

The primary class of drugs approved are cholinesterase inhibitors, including rivastigmine, galantamine, and donepezil, applicable to all AD stages. These drugs prevent the breakdown of acetylcholine, a neurotransmitter crucial for memory and thinking (Grossberg, 2003; Khoury et al., 2018). However, as AD progresses, the brain's acetylcholine production diminishes, reducing these drugs' effectiveness. Individual responses to these inhibitors vary, so trialing different drugs can be beneficial. For moderate to severe stages of Alzheimer's, memantine, an N-methyl-D-aspartate (NMDA) antagonist, is recommended (Olivares et al., 2012; Reisberg et al., 2003). This medication helps manage symptoms and potentially allows patients to maintain certain daily functions for a longer duration, such as using the bathroom independently. Memantine operates by regulating glutamate, a brain chemical that, in excess, can cause brain cell death (Reisberg et al., 2003). Because NMDA antagonists and cholinesterase inhibitors function differently, they are often used in combination.

For immunotherapies, lecanemab and aducanumab have been introduced for early-stage AD (Sevigny et al., 2016a; van Dyck et al., 2023). Lecanemab targets beta-amyloid peptides to decrease amyloid plaques, a key AD's feature. Clinical trials have shown that lecanemab can slow cognitive decline in early-stage patients. Aducanumab, also targeting beta-amyloid, has been granted accelerated approval by the FDA but requires additional studies to fully confirm its clinical benefits (Mafi et al., 2022). Brexpiprazole, an atypical antipsychotic, has been approved for treating Alzheimer's-related agitation (Lee et al., 2023). This medication adds to the options for managing behavioral symptoms in Alzheimer's patients.

1.3 Neuropathological hallmarks of Alzheimer's disease

1.3.1 Amyloid plaques

Amyloid plaques are a primary neuropathological characteristic in AD. These extracellular deposits mainly consist of amyloid beta ($A\beta$) peptides, which result from the enzymatic breakdown of amyloid precursor protein (APP) (Hampel et al., 2021; O'Brien & Wong, 2011). There are two distinct categories of amyloid plaques: diffuse plaques (Figure 2A) and dense core plaques (Figure 2B) (Dickson, 1997; Serrano-Pozo et al., 2011). Diffuse plaques are composed of non-fibrillar $A\beta$ deposits with minimal neuritic dystrophy (Selkoe & Hardy, 2016) and range in size from 50 μm to hundreds μm (Figure 2A). These plaques are not exclusive to AD patients but can also be found in the cerebral cortex of cognitively normal elderly people (Serrano-Pozo et al., 2011). Characteristically, diffuse plaques form initially in the neuropil and demonstrate weak staining with thioflavin S and other dyes that bind to amyloid substances. Conversely, dense core plaques feature compact, dense amyloid formations that exhibit strong positivity under thioflavin S fluorescent microscopy and Congo red staining (Figure 2B), indicating the presence of more fibrillogenic $A\beta$ forms (Koronyo et al., 2017; Kumar-Singh et al., 2002). Notably, a specific group of dense core plaques includes neuritic components (Figure 2C-D). These cored neuritic plaques (NPs) often surrounded by tau-positive or dystrophic neurites, identifiable using various markers such as synaptic and APP immunohistochemistry (Dickson, 1997). Dense-cored NPs are linked to synaptic degradation and the presence of activated microglia and reactive astrocytes (Serrano-Pozo et al., 2011; Yasuhara et al., 1994).

Conversely, diffuse plaques generally lack neuritic components, although diffuse NPs can occur in advanced AD (Dickson, 1997). Diffuse plaques, detectable through $A\beta$ immunohistochemistry, encompass filamentous $A\beta$ at the ultrastructural level. However, it is unclear whether they signify a component of pathological aging or represent an initial phase in the formation of neuritic $A\beta$ plaques (DeTure & Dickson, 2019). Plaques primarily composed of dense cores without neuritic components are referred to as "burnt-out" plaques (Perl, 2010). Crucially, neuritic plaques (NPs) characterized by dense amyloid accumulation and tau-positive neurites are thought to have a direct association with neuronal loss and cognitive deterioration in AD (Knowles et al., 1999; Malek-Ahmadi et al., 2016).

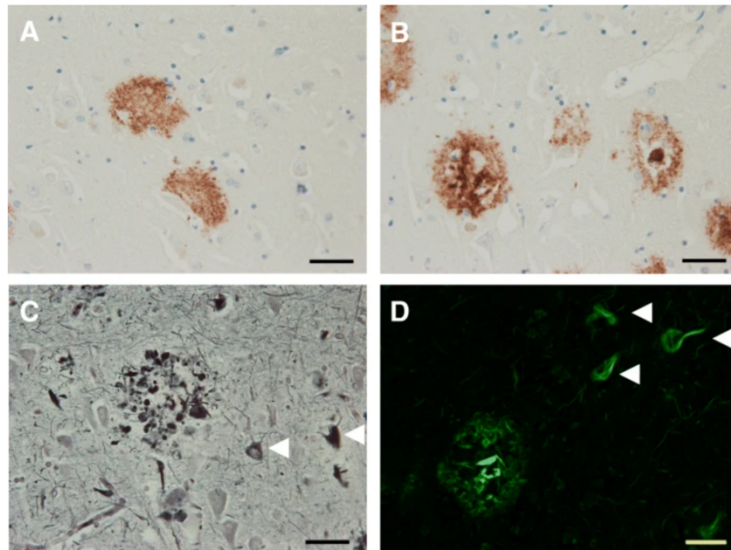


Figure. 2 | Two major senile plaques in AD: diffuse plaques and dense core plaques. A/B. Immunohistochemical analysis of AD brain tissues using A β peptide-specific antibodies reveals the existence of both diffuse (A) and dense core (B) senile plaques. These dense core plaques frequently co-occur with neuritic components, which are identifiable through filamentous tau staining, and are closely linked with the progression of AD. **C/D.** The presence of neuritic AD plaques is also clearly visible with the application of Bielchowsky silver stain (C) and Thioflavin S stain (D), techniques that additionally mark NFTs, as highlighted by the arrowheads. Scale bars are 40 μ m. Modified and cited from (DeTure & Dickson, 2019).

1.3.2 Cerebral amyloid angiopathy

Amyloid-beta (A β) peptides accumulate not just in the form of amyloid plaques within the brain parenchyma but also inside cerebral blood vessels. It's estimated that a vast majority of AD cases, between 85-95%, exhibit varying levels of cerebral amyloid angiopathy (CAA). According to the Mayo Brain Bank, moderate-to-severe CAA is present in 13% of confirmed AD cases. These cases can be identified through A β immunohistochemistry or thioflavin S fluorescent microscopy (Figure 3 A-B) (Charidimou et al., 2017). Notably, amyloid deposition in CAA is rich in A β 40 peptides, distinct from parenchymal deposits that predominantly contain A β 42 species. These deposits impact small arteries, arterioles, and capillaries within the gray matter of cerebral cortices and leptomeningeal vessels (Perl, 2010; Serrano-Pozo et al., 2011).

Two distinct types of CAA have been distinguished. Type 1 CAA has a quadruple increased likelihood of association with APOE4 and affects capillaries, arterioles, and

small arteries. Type 2 CAA, twice as likely to be linked with APOE2, influences arterioles and small arteries but spares capillaries (Attems et al., 2010; Thal et al., 2002). Intriguingly, it's noteworthy that the parietal and occipital cortices exhibit greater susceptibility to CAA compared to the frontal and temporal lobes. Additionally, leptomeningeal arteries demonstrate higher vulnerability than parenchymal vessels (Serrano-Pozo et al., 2011). Severe CAA can lead to blood flow impairment, resulting in ischemic lesions or small infarcts. In more extreme cases, it can precipitate lobar hemorrhages, predominantly impacting the frontal and occipital lobes (Perl, 2010).

CAA's prevalence in AD, coupled with its association with an earlier onset of the disease, underscores its significant role in the AD process, contributing independently to clinical presentations of AD (Charidimou et al., 2017; Smith, 2018; Vidoni et al., 2016). Several methods for scoring the severity of CAA burden have been proposed, with imaging methods being established to distinguish CAA from plaque amyloid within the brain parenchyma (Charidimou et al., 2017). Notably, immunization therapies focusing on A β peptides may reduce amyloid accumulation with a potential risk of exacerbating amyloid deposition in CAA, sometimes leading to inflammation and hemorrhage (Bales et al., 2016; Boche et al., 2010). Animal model studies indicate that capillary CAA originates from neuronal A β , impairing perivascular clearance and leading to peri-capillary A β deposits and eventually CAA (Calhoun et al., 1999). The association of the APOE4 allele with capillary CAA is attributed to potentially diminished transendothelial clearance of A β -apolipoprotein complexes compared to individuals harboring APOE2 (Attems et al., 2010). Furthermore, a correlation has been observed between the severity of perivascular neuritic tau pathology and perivascular A β accumulation, suggesting that amyloid deposition may drive dystrophic neurites (Bales et al., 2016).

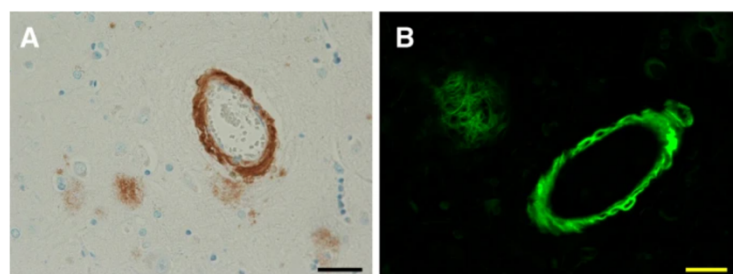


Figure. 3 | Cerebral amyloid angiopathy in AD. A/B. CAA can be observed in frontal cortical sections via A β -directed immunohistochemistry (A) or Thioflavin S staining (B) similar to the methods used for

detecting senile plaques in AD. Scale bars are 40 μm . Modified and cited from (DeTure & Dickson, 2019).

1.3.3 Neurofibrillary tangles

NFTs represent a critical neuropathological signature of AD, initially characterized by Alois Alzheimer in 1907 as intracellular filamentous inclusions predominantly situated in the perikaryal area of pyramidal neurons. Further research, incorporating ultrastructural analyses, has elucidated that the primary structural elements of NFTs are paired helical filaments (PHFs), primarily composed of excessively phosphorylated tau protein (Castellani et al., 2008; Goedert & Spillantini, 2006). Tau, a phosphoprotein abundant within neuronal structures and synthesized by all nucleated cells, ordinarily functions to facilitate the assembly and stabilization of microtubules. However, in the context of AD, tau is subject to abnormal hyperphosphorylation, which not only diminishes its microtubule-binding capacity but also promotes the aggregation of PHFs within neuronal cell bodies and dystrophic neurites (Alonso et al., 1996; Holtzman et al., 2011a). Despite ongoing research, the exact role and impact of tau pathology in the pathogenesis of AD remain unclear. There is a consensus that tau-related abnormalities manifest subsequent to A β deposition in the disease's progression. Nevertheless, it is imperative to acknowledge that the extent of neurofibrillary tangle formation exhibits a more robust correlation with the severity of cognitive deficits in AD, as opposed to plaque pathology (Holtzman et al., 2011b).

1.3.4 Inflammation

Inflammation is another notable pathological feature observed in AD. This inflammatory response in the brain involves activation of microglia, astrocytes, the complement system, as well as the release of various cytokines and chemokines (Rubio-Perez & Morillas-Ruiz, 2012). Notably, activated astrocytes and microglia are frequently observed adjacent to NPs in AD, indicating that A β plays a key role in triggering glial activation (Fakhoury, 2018; Itagaki et al., 1989; Krause & Müller, 2010). Once activated, these glial cells release a range of pro-inflammatory signaling molecules, including complement factors, cytokines, and chemokines (Rubio-Perez & Morillas-Ruiz, 2012; Tuppo & Arias, 2005).

1.3.5 Neuron loss

Neuronal loss, alongside plaques and tangles, constitutes a fundamental pathological characteristic of AD. This loss predominantly manifests in the pyramidal layers of the hippocampus, the layer II of the entorhinal cortex (EC), and specific regions of the temporal, parietal, and frontal neocortex (Holtzman et al., 2011b; Serrano-Pozo et al., 2011). For instance, significant neuron loss in the entorhinal cortex of individuals diagnosed with mild AD was demonstrated through stereology (Gómez-Isla et al., 1996). While preclinical AD stages show no neuron loss in the *cornu ammonis* (CA) region, marked neuron loss in AD patients has been reported (Schmitz et al., 2004). Early investigations suggested a correlation between NFTs and neuronal loss within the corresponding region (Cras et al., 1995). Unbiased stereological analysis uncovered neuronal cell loss in the superior temporal sulcus, partially correlating with NFTs formation but exceeding it significantly (Gómez-Isla et al., 1997). Recent findings propose that intraneuronal or oligomeric A β may play a pivotal role in neuronal loss observed in AD. (Jawhar et al., 2011; Larson & Lesné, 2012).

Cortical atrophy in AD, primarily attributed to neuronal loss, is visibly evident macroscopically, particularly in the hippocampus, amygdala, and EC, and is measurable by MRI (A. T. Du et al., 2004). Diagnosing AD can be achieved with 80 to 90% accuracy by assessing hippocampal atrophy using MRI (Jagust et al., 2006). Hippocampal atrophy also serves as a predictive marker for the progression from MCI to AD (Mueller et al., 2005). The loss of synapses contributes significantly to the cortical atrophy observed in AD, with the extent of loss exceeding neuronal reduction. This indicates that synapse loss likely precedes neuronal loss (Serrano-Pozo et al., 2011). Synaptic density correlates more closely with AD severity and cognitive decline than NFTs or neuron loss (DeKosky & Scheff, 1990; Scheff et al., 1993).

1.4 The amyloid cascade hypothesis

1.4.1 Definition

The amyloid cascade hypothesis, proposed over two decades ago suggests that the accumulation and deposition of A β are central to the etiology and pathogenesis of AD (Hardy & Higgins, 1992). This hypothesis posits that either an elevation in A β production or a decrease in its clearance leads to the deposition of A β 40 and A β 42 peptides,

resulting in the formation of insoluble extracellular plaques. These plaques are believed to initiate a series of detrimental changes, including synapse loss, neuronal death, brain atrophy, and dementia (Pimplikar, 2009; Selkoe & Hardy, 2016). Genetic studies of FAD, showing mutations in APP, PSEN-1, and PSEN-2 that affect A β levels and result in increased plaque deposition, provide strong evidence (Bertram et al., 2010; Lanoiselée et al., 2017; Pimplikar, 2009). AD mouse models carrying familial mutations replicate numerous features of AD pathology, including the presence of A β plaques, gliosis, and memory deficits (Duyckaerts et al., 2008; Pimplikar, 2009). The apolipoprotein E ϵ 4 allele (ApoE4), a significant risk factor for late-onset AD, is linked to increase A β deposition and diminished its clearance (Bickeböller et al., 1997; Castellano et al., 2011; C.-C. Liu et al., 2013). Conversely, mutations in the tau protein lead to tauopathies such as frontotemporal dementia rather than AD, implying that NFTs follow, rather than initiate, AD pathology (Goedert & Jakes, 2005; Hutton et al., 1998; Samudra et al., 2023). Moreover, recent progress on anti-amyloid therapies have provided substantial support to the amyloid cascade hypothesis (Zhang et al., 2023). These therapies, aimed at reducing A β accumulation or promoting its clearance, have shown promising results, further validating the theory that A β plays a central role in the pathogenesis of AD. However, the amyloid cascade hypothesis has notable limitations. The extent of plaque pathology does not consistently correlate with dementia severity (Nelson et al., 2009). Notably, some cognitively normal individuals display significant plaque pathology without signs of dementia (Zolochovska & Tagliavola, 2016). In numerous AD mouse models, memory impairment and pathological alterations occur before the formation of plaques (S. Lesné et al., 2008; S. E. Lesné et al., 2013).

1.4.2 Amyloid-beta aggregation

Soluble A β monomers, with a molecular weight of around 4 kDa, have a high propensity for polymerization and aggregation. The transition from these monomers to insoluble A β fibrils, which form plaques, is a complex process. A β monomers can aggregate into various oligomeric forms, ranging from dimers to octamers, most commonly appearing as lower oligomers. These soluble A β oligomers, which are non-fibrillar in structure, maintain their stability in water-based solutions, even after undergoing rigorous centrifugation (Walsh & Selkoe, 2007). It is believed that A β monomers exist in

a state of equilibrium with multiple oligomeric configurations. Upon achieving a specific concentration level, they start to polymerize into paranuclei. These paranuclei then self-associate to form protofibrils, eventually forming the fibrils that are the main components of amyloid plaques. Protofibrils could also break down into simpler structures (Roychaudhuri et al., 2009). The critical role of the formation and accumulation of neurotoxic A β oligomers in the onset and development of AD is widely recognized (Tolar et al., 2021). Research indicates that soluble oligomeric A β 42 is more strongly associated with synaptic deterioration and cognitive impairment in AD patients than plaques (Haass & Selkoe, 2007; Lue et al., 1999). A β 's amphiphilic nature facilitates its aggregation into larger oligomers *in vitro*, and such oligomers have been detected in extracts from AD patients' brains as well as in AD mouse models (Pimplikar, 2009; Viola & Klein, 2015).

1.5 Mouse models of Alzheimer's disease

In order to advance AD research, a range of transgenic mouse models have been developed, which are based on genetic mutations associated with FAD, particularly those associated with early-onset cases. Broadly categorized into amyloidopathy models that mimic A β pathology, tauopathy models focusing on tau protein abnormalities, and combined models that display both pathologies, they provide critical insights into the disease mechanisms and have been key in exploring novel therapeutic approaches (Cavanaugh et al., 2014).

Diverse mutations in the APP gene, including the Swedish (K670N/M671L), London (V717I), Indiana (V717F), and Florida (I716V) mutations, are linked to amyloid pathogenesis in FAD. These mutations were named after the locations of their discovery (Eckman et al., 1997; Goate et al., 1991). From this, researchers have developed several transgenic mice that express human APP proteins with such mutations. These mice typically exhibit extracellular A β deposits, neuroinflammation, impairments in cognitive or memory functions, and various behavioral changes across different life stages.

The initial generation of these AD mouse models comprises monogenic mice, each carrying either a single mutation or multiple mutations. The AD mouse model *PDAPP*, was developed in 1995, featuring mice expressing APP with the Indiana mutation,

displaying significant memory loss and synaptic deficits (Games et al., 1995). Following this, the *Tg2576* mouse model was developed, which carries the Swedish mutation under the hamster prion protein promoter. *Tg2576* mice show normal cognition in their early life, followed by cognitive deficits as they age, with memory impairments becoming evident between 12 and 18 months. They develop amyloid plaques in the CA1 region of hippocampus but no neuronal loss or NFTs (Hsiao et al., 1996). Currently, the *Tg2576* mouse model is recognized as one of the most thoroughly studied and extensively utilized mouse models for AD research.

The next generation of transgenic mouse models for AD research includes those expressing both APP and PSEN mutations, such as M233T, L235P, M146L, and L286V. Notable models like *APPSLPS1-M146L*, *APPSLPS1-ki*, and *5XFAD* (Tg6799) have been developed (Casas et al., 2004; Langui et al., 2004; Oakley et al., 2006). These models, characterized by biogenic or polygenic mutations, exhibit early and severe amyloid pathology. The *5XFAD* mouse begins showing AD-like symptoms around 2 months old, with widespread plaques in the brain by 6 months and associated synaptic and neuronal loss by 4 months, affecting spatial learning abilities.

Researchers introduced an innovative approach to enable inducible expression of transgenic proteins, leading to the creation of the third generation of AD mouse models. A notable example of this generation is the *rTg4510* model, established in 2005 (Santacruz et al., 2005). It represents a tauopathy model that uses a repressible form of the human tau gene carrying the P301L mutation. This inducible setup allows researchers to explore the duration and reversibility of FAD-related phenotypes. In the *rTg4510* model, cognitive impairments start as early as 3 months, with NFTs appearing by 4 months old, and synaptic loss by 6 months (Santacruz et al., 2005; Spire-Jones et al., 2007). This AD model is beneficial for studying the dynamic nature of tau pathology and how it affects cognitive abilities.

The fourth generation of AD mouse models, including the *APPNL-G-F* model, utilizes a knock-in approach (Saito et al., 2014). This method offers more precise expression patterns and levels of the APP, avoiding the artifacts typically associated with generalized APP overexpression and potential disruptions of unknown genomic loci (Onos et al., 2016). The *APPNL-G-F* mice express APP at wild-type levels, incorporating three specific APP mutations: KM670N/M671L (Swedish), I716F (Florida), and E693G

(Arctic). These mutations contribute to early amyloid plaque formation and gliosis by the age of 3 months, synaptic degradation by 4 months, and cognitive decline associated with aging by 6 months (Saito et al., 2014). AD mouse models play essential roles in the drug discovery process, facilitating the identification and validation of drug targets, as well as in conducting preclinical studies. This process begins with identifying and validating potential drug targets, followed by extensive high-throughput screening, optimization of lead compounds and eventually, preclinical and clinical trials. AD mouse models are invaluable for advancing our understanding and development of its treatments (Hall & Roberson, 2012).

1.6 Drug development in Alzheimer's disease

Developing effective therapies for AD remains a vital focus in medical research, with efforts centered on developing medications that can prevent the disease's onset, decelerate its progression, or enhance the cognitive and behavioral symptoms linked to AD. These treatments are generally categorized into two types: "symptomatic" and "disease-modifying." Symptomatic treatments are designed to enhance cognitive function or manage neuropsychiatric symptoms without necessarily addressing the underlying biological causes of AD (Cummings et al., 2023). Their primary aim is to alleviate the symptoms and improve the quality of life for patients.

DMTs target the biological processes of AD with the intent to slow down or alter the disease's progression (Cummings & Fox, 2017). DMTs are further subdivided into: **Biologics:** This category includes treatments like monoclonal antibodies, vaccines, antisense oligonucleotides, gene therapy, etc. These are typically large molecules or complex biological products. **Small Molecules:** These are generally orally administered drugs with a molecular weight less than 500 Daltons, designed to interact with specific biological targets. By 2023, there were 187 clinical trials in various stages, evaluating 141 distinct treatments for AD (Cummings et al., 2023). Among these, the majority of the agents being studied are DMTs, accounting for 78% (111 agents) of all drugs in these trials. Symptomatic agents, which include cognitive enhancers and psychotropic drugs, make up 21% (30 agents) of the pipeline, with each of these two subcategories representing 11% of all agents in the current clinical trials. These statistics underline the significant research efforts being directed towards finding effective treatments for AD, with a strong focus on disease-modifying strategies. However, it also highlights

the complexity and challenges involved in developing treatments that can effectively alter the course of this neurodegenerative disease.

1.6.1 Symptomatic treatments

Symptomatic treatments for AD primarily focus on alleviating symptoms and temporarily slowing cognitive decline, enhancing the life quality of both patients and their caregivers. These treatments are critical, especially given the challenges in developing DMTs. For mild to moderate AD dementia, cholinesterase inhibitors such as donepezil, galantamine, and rivastigmine are commonly prescribed (Yiannopoulou & Papageorgiou, 2020). These drugs work on similar principles, but patients may respond differently to each. They are developed based on the cholinergic hypothesis, which posits that the loss of cholinergic innervation within the brain is key to the cognitive decline in AD (Hempel et al., 2018). By increasing acetylcholine availability at synapses, these inhibitors have shown clinical efficacy in delaying cognitive deterioration. However, gastrointestinal symptoms and sleep disorders are common side effects, affecting 5-20% of patients. For moderate to severe AD dementia, memantine, which is a non-competitive NMDA receptor antagonist with low-to-moderate affinity, is frequently administered (Olivares et al., 2012). Memantine targets the NMDA receptor-operated calcium channels, helping to mitigate the harmful effects of elevated glutamate levels, which can lead to neuronal dysfunction. The FDA has also approved Namzaric[®], a combination of donepezil and memantine, which is particularly effective for moderate to severe AD dementia (Guo et al., 2020). This combination therapy has shown to cause fewer gastrointestinal symptoms, although it may increase the occurrence of headaches. Overall, while these symptomatic treatments don't cure AD, they play a vital role in managing its symptoms and improving the daily lives of those affected by the disease.

1.6.2 Disease-modifying therapies

Recent clinical trials of anti-A β passive immunization therapies, like lecanemab and donanemab, indicate a potential new era in AD treatment, demonstrating the possibility of slowing cognitive decline in individuals with MCI and mild dementia due to AD (Budd Haeberlein et al., 2022; Sevigny et al., 2016b; van Dyck et al., 2023). While these treatments offer some clinical benefits, their modest impact and safety concerns

highlight the need for a deeper understanding of neurodegeneration mechanisms to improve outcomes.

The trials reveal that monoclonal antibodies targeting soluble A β species, such as solanezumab and crenezumab, did not significantly affect amyloid plaque clearance or cognitive changes (Doody et al., 2014; Ostrowitzki et al., 2022). However, aducanumab showed mixed results, with notable amyloid plaque removal but inconsistent cognitive improvements (Budd Haeberlein et al., 2022). Lecanemab and donanemab trials demonstrated clinical efficacy, slowing cognitive decline, and reducing amyloid plaque burden. Benefits were most consistent 18 months after treatment initiation, correlating with amyloid plaque removal. However, the extent of potential long-term disease modification and the need for continued treatment to sustain cognitive benefits are still unclear, necessitating long-term follow-up studies.

Safety concerns with these therapies, especially amyloid-related imaging abnormalities (ARIA), have been noted (Antolini et al., 2021; Honig et al., 2023; Reish et al., 2023). Instances of intracerebral hemorrhage have been reported post-trial in lecanemab-treated patients, with APOE ϵ 4 carriers at higher risk for ARIAs (Honig et al., 2023). Amyloid β may also deposit in brain blood vessels, leading to CAA, which can be exacerbated by anti-A β antibody treatments. A potential future strategy is targeting other amyloid plaque components, like APOE, to remove both CAA and plaque pathology without adverse effects, as evidenced in mouse models (Xiong et al., 2021).

The observed cognitive decline slowing in symptomatic AD patients supports testing anti-amyloid therapies in preclinical AD stages. However, trials in this area face challenges due to the lengthy period required to observe clinical AD progression. Recent prevention trials in autosomal dominant AD haven't shown success in slowing cognitive decline, possibly due to few participants experiencing decline during the study (Salloway et al., 2021). Ongoing trials are assessing anti-amyloid therapies in cognitively unimpaired individuals with amyloid deposition. The optimal design for preventive treatment trials in asymptomatic individuals, especially considering the risk of ARIAs, remains a significant concern (Joseph-Mathurin et al., 2022). The recent approval of lecanemab and other potential A β -monoclonal antibodies will likely fuel further research in AD prevention, exploring novel approaches like active A β vaccines or A β -production modulators with safer profiles.

1.6.3 Peptide-based inhibitors

Peptide-based inhibitors for AD have been developed based on four primary strategies: 1) The creation of inhibitors grounded in the molecular recognition principles of amyloid self-assembly, 2) The study of cross-amyloid interactions, 3) The exploration of interactions with chaperones or other non-amyloidogenic polypeptides, and 4) The identification through combinatorial libraries and subsequent refinement using peptide chemistry techniques (Armiento et al., 2020). Early in the field of peptide-based inhibitors, a small fragment A β (16-20) or (KLVFF) was shown to bind to full-length A β and block its aggregation into amyloid fibrils (Tjernberg et al., 1997). Other classes of inhibitors include β -Wrapins, which are engineered binding proteins derived from phage-display libraries, and peptides modeled after naturally A β -binding proteins, like transthyretin (J. Du & Murphy, 2010; Orr et al., 2016).

IAPP, or amylin, is another peptide involved in AD pathology (Kayed et al., 1999; Westermark et al., 2011). Produced by the β -cells in the pancreas, IAPP easily passes through the BBB and mediates various brain functions. It shares several features with A β peptide, including comparable β -sheet secondary structures (Lim et al., 2008) and binding to the same receptor (Fu et al., 2012). The cross-amyloid interaction between A β and IAPP was utilized to design and create the cross-amyloid inhibitors (Figure 4A) (O'Nuallain et al., 2004; Yan et al., 2007). Given the remarkable similarities in sequence and structure between these two peptides, the N-methylated IAPP analogs, effective against IAPP's amyloid formation, were explored if they could similarly impact A β 's aggregation process (Figure 4A) (Andreetto et al., 2010; Yan et al., 2007, 2013). Indeed, these analogs, including IAPP-GI, emerged as potent nanomolar-level inhibitors against the toxic aggregation of A β 40, making the IAPP-GI as the first cross-amyloid peptide inhibitor of A β and IAPP (Yan et al., 2007, 2013). This inhibition process involved the formation of non-toxic hetero-oligomers between the inhibitor and A β 40, along with the disruption and remodeling of existing fibrils, a mechanism paralleled in its inhibitory action on IAPP aggregation (Yan et al., 2006).

Recent developments in the field of cross-amyloid inhibition have introduced a novel class of compounds known as "interaction surface mimics" or ISMs (Andreetto et al., 2015). These peptides, comprising 21 residues derived from IAPP, are engineered to replicate potential interaction sites between IAPP itself and A β , facilitating cross-inhibition (Figure 4B). Demonstrating nanomolar efficacy, ISMs selectively target

A β 40(42) and IAPP, with some variants effectively blocking the cross-seeding of IAPP via A β 40 fibrils, suggesting a mechanistic link between AD and Type 2 diabetes (O'Nuallain et al., 2004; Oskarsson et al., 2015). ISMs represent promising candidates for therapeutic intervention in both conditions (Verdile et al., 2015). Their innovative design leverages critical "hot segments" of IAPP, known for engaging in both self- and cross-amyloid interactions with A β 40(42), connected via specially designed linkers that influence both the potency and specificity of these inhibitors (Figure 4B) (Andreetto et al., 2010, 2015). The mechanism of action primarily involves the binding of ISMs to early, prefibrillar forms of A β 40(42) or IAPP, redirecting these molecules into non-toxic, amorphous aggregates, thereby mitigating their pathogenic assembly (Figure 4B).

In the latest research, ISM R3-GI served as a template for developing a new class of macrocyclic peptides, known as macrocyclic inhibitory peptides (MCIPs), aimed at effectively inhibiting amyloid formation (Figure 4C) (Bakou et al., 2017; Spanopoulou et al., 2018). These MCIPs are crafted to replicate the inhibitory interaction surfaces of IAPP, incorporating the minimal essential elements derived from IAPP to maintain target specificity. Through a streamlined design process and employing advanced peptide chemistry techniques, a particular 17-residue peptide, 2b, emerged as a potent nanomolar-level inhibitor against the toxic aggregation processes of both A β 40(42) and IAPP, maintaining only four residues from IAPP (Figure 4C) (Spanopoulou et al., 2018). However, its susceptibility to rapid degradation by serum proteases presented a challenge. A strategic alteration in the peptide structure through l-/d-residue exchange produced MCIP 2e, or 2E, enhancing its stability and preserving its inhibitory efficacy against A β 40(42) in human serum (Figure 4C). Significantly, 2E demonstrated the ability to penetrate the BBB in cellular models, marking it as a highly promising candidate for the development of anti-amyloid therapies for AD (Spanopoulou et al., 2018), with its in vivo inhibitory effects to be confirmed. This progress in peptide-based drug development underscores the potential of peptides as dynamic and potent tools in combating complex conditions like AD, merging the strengths of biopharmaceuticals with the convenience of small molecule therapies, thereby offering promising avenues for future therapeutic strategies.

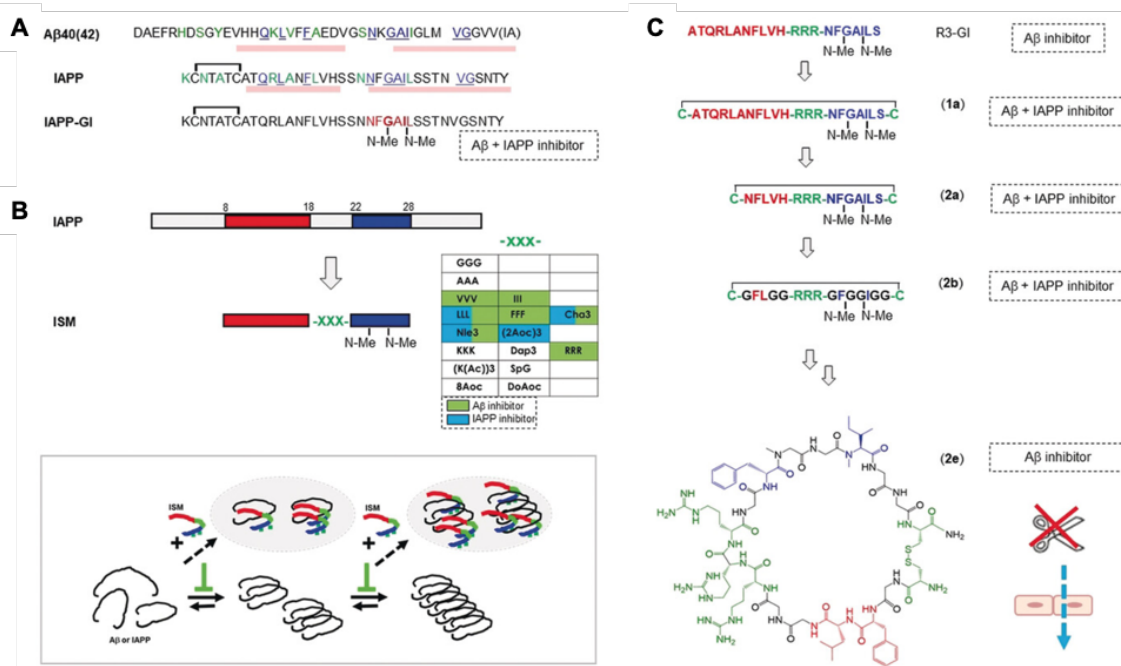


Figure. 4 | IAPP-Aβ cross-amyloid nanomolar peptide inhibitors of Aβ aggregation. A. The sequence alignment of Aβ40(42) and IAPP, where shared residues are marked in green, identical residues in blue and underlined, and residues forming β-strands are highlighted with pink bars. The core amyloidogenic sequence of IAPP, NFGAIL, pivotal in amyloid formation, is indicated in red within the IAPP-GI structure. **B.** The concept of design, effects of inhibition, and potential inhibitory mechanism of ISMs. **C.** Principle of design, sequences, structures, and functions of the MCIPs. Modified and cited from (Armiento et al., 2020).

1.7 Transcriptome profiling: RNA sequencing

1.7.1 RNA sequencing

RNA sequencing (RNA-seq) is a critical genomic method for analyzing messenger RNA in biological samples, pivotal for cellular response studies (Haque et al., 2017; Z. Wang et al., 2009). Initially, its scope was limited to large samples, restricting single-cell analysis. The introduction of single-cell RNA sequencing (scRNA-seq) in 2009, has expanded its capabilities of RNA-seq (Tang et al., 2009). Advances in both technology and bioinformatics have made scRNA-seq broadly accessible, fostering significant breakthroughs across various research and clinical fields (Jaitin et al., 2014; Picelli et al., 2014). Furthermore, spatial transcriptomics, emerging in 2016, refines RNA-seq by detailing the location of cell types and mRNA within tissue sections (Ståhl

et al., 2016). These continuous improvements in RNA-seq technology, from bulk, single-cell to spatial RNA-seq, are crucial in advancing biomedical research, offering new possibilities for scientific exploration and discovery (Li & Wang, 2021).

1.7.2 Single-cell RNA sequencing

Since its introduction in 2009, scRNA-seq has significantly impacted diverse research areas, including cancer biology, stem cell biology, and immunology (Tang et al., 2009). It offers a distinct advantage over traditional RNA-seq of bulk tissues by enabling detailed analysis of tissue composition, cellular state diversity, and the detection of rare cell types. Advances in sequencing technologies have made scRNA-seq more robust and widely accessible for comprehensive transcriptome analysis. Among the scRNA-seq platforms, *Smart-seq2* and *10X Genomics Chromium (10X)* are particularly prominent.

Smart-seq2, a notable advancement in scRNA-seq, significantly enhances the sensitivity and accuracy of gene expression analysis at the individual cell level (Picelli et al., 2014). This method improves upon earlier techniques by introducing an optimized protocol for synthesizing cDNA, ensuring a more thorough and representative capture of the entire transcriptome, including the crucial 5' and 3' ends of mRNA molecules. The use of microtiter plates in *Smart-seq2* is a key feature, allowing for the effective isolation and processing of mRNA from single cells, which leads to a more focused and efficient analysis. A significant advantage of *Smart-seq2* is its wider availability to research labs, as it doesn't demand specialized equipment, making it a practical choice for various genomic studies. Its application in diverse areas of biological research has been crucial in yielding deeper insights into the complexities of cellular processes, thereby advancing our understanding of single-cell biology, including the neurodegeneration (Safaiyan et al., 2021). With its capability to provide detailed gene expression profiles, *Smart-seq2* has become an essential tool in the dynamic field of genomic research.

10X Genomics (*10X*) single-cell RNA-sequencing (scRNA-seq) is an innovative and powerful technology in the field of genomics, offering detailed insights into the complexities of cellular biology (X. Wang et al., 2021). This technology is based on a droplet-based microfluidic system that encapsulates individual cells, each with a unique barcode, enabling researchers to track and sequence mRNA from each specific cell.

This approach allows for the high-throughput analysis of thousands of cells in a single experiment, making it an invaluable tool for large-scale genomic studies. The precision and sensitivity of the *10X* platform are particularly beneficial in uncovering cell-to-cell variations within a sample, thus revealing the diversity of cell types and states, including rare and previously undetected cell populations (Androvic et al., 2023; Kaya et al., 2022). The use of unique molecular identifiers (UMIs) further refines the accuracy of gene expression measurements by reducing technical noise, ensuring that the observed variability is biologically relevant. The versatility and comprehensive nature of *10X* make it a cornerstone technology in genomic research, driving forward our understanding of complex biological systems and disease mechanisms at an unprecedented single-cell resolution.

2. Aims of the study

In the realm of neurodegenerative diseases, AD poses a significant challenge due to cognitive decline and limited therapeutic options. A key aspect of AD pathology is the accumulation of amyloid-beta ($A\beta$) peptide, driving disease progression. Islet amyloid polypeptide (IAPP) has shown promise in inhibiting amyloid self-assembly, prompting the development of the macrocyclic 17-residue peptide 2E, designed to mimic IAPP's interaction with $A\beta$. Encouragingly, 2E demonstrated potent inhibitory effects on $A\beta$ amyloid self-assembly *in vitro*, along with stability in human plasma and the ability to cross the BBB in cell models.

It was my aim to investigate the efficacy of the macrocyclic peptide 2E in ameliorating amyloid pathology in early and middle symptomatic AD mouse models. My objective was to assess the impacts of 2E treatment on cortical amyloid deposition and distribution, soluble $A\beta_{42}$ and $A\beta_{40}$ levels, neuronal damage, glial cell responses and behavioral performance. A novel method for high-resolution RNA sequencing from PFA-fixed microscopy sections was established to elucidate the 2E's impacts on the AD-associated gene expression changes. Through this systematic investigation of the underlying mechanisms of 2E, the goal was to gain a comprehensive understanding of its potential therapeutic effects in Alzheimer's disease.

3. Materials and Methods

3.1 Materials

3.1.1 Reagents

Table 1. Key reagents

Reagents	Identifier	Supplier
2E peptide	-	Kapurniotu Lab (TUM)
AMPure bead	GE45152105050250	Sigma
Betaine	B0300	Sigma
Bovine serum albumin (BSA)	8076.4	Roth
Diethylamine (DEA) buffer	34064	Thermo
Dithiothreitol (DTT)	15508013	Thermo
DPBS (DPBS-CMF)	14190144	Thermo
Ethanol, Pure (200 Proof, anhydrous)	E7023-500ML	Millipore Sigma
ERCC RNA Spike-In Mix	4456740	Ambion /Thermo
Fetal bovine serum (FBS)	10270-106	Thermo
Formic acid (FA)	85178	Thermo
Gel aqua mount media	G0918	Sigma
Glycerin (glycerol), 50% (v/v) Aqueous Solution	3290-32	Ricca Chemical
Hoechst	34580	Thermo
Heparin-Natrium-25000	PZN:03029843	Ratiopharm
IAPP peptide	-	Kapurniotu Lab (TUM)
Isotonic saline (0.9%)	00808765	Die Pharmazentralnummer (PZN)
KAPA HiFi Hotstart ReadyMix	KK2602 07958935001	Roche
Lambda Exonuclease	M0262L	New England Biolabs
msR4M-L1 peptide	-	Kapurniotu Lab (TUM)
Low TE buffer	12090-015	Thermo
Methoxy-X04	4920	TOCRIS

MgCl ₂	M1028	Sigma
Nuclease-free water	10977035	Invitrogen
Intercept (PBS) blocking buffer	927-70001	LI-COR
Oligo dT25 magnetic beads	61005	Invitrogen
Optimal cutting temperature (O.C.T.) Compound	4583	Sakura Finetek
Paraformaldehyde (PFA)	J19943.K2	Thermo
Ponceau S staining solution	A40000279	Thermo
Phosphate-buffered saline (PBS)	10010023	Thermo
Proteinase K	EO0491	Thermo
Protease inhibitor	A32965	Thermo
Phosphate-potassium dextrose (PKD) buffer	1034963	Qiagen
Qiagen Buffer EB	19086	Qiagen
Radioimmunoprecipitation (RIPA) buffer	89901	Thermo
Recombinant RNase inhibitor	2313B	Takara Clontech
SMARTScribe reverse transcriptase	639538	Takara Clontech
Saline-sodium phosphate-EDTA (SSPE) buffer	Cat#15591-043	Life Technologies
Sodium chloride (NaCl)	J21618.A1	Thermo
SPRIselect Reagent	B23318	Beckman Coulter
Sucrose	15503022	Thermo
Sodium-dodecyl sulfate (SDS)	28312	Thermo
Tris	17926	Thermo
Tris-EDTA (TE) buffer	93283	Sigma
Tris-HCl	15506017	Thermo
Triton-X100	93443	Sigma
Typan blue stain (0.4%)	T10282	Thermo
Tween-20 (10%)	1610781	Bio-Rad
X-34	SML1954	Sigma

3.1.2 Assay kits

Table 2. Critical Commercial assays

Reagents	Identifier	Supplier
2100 Bioanalyzer high sensitivity DNA kit	5067-4626	Agilent
Amyloid beta 40 human ELISA kit	KHB3481	Thermo
Amyloid beta 42 human ELISA kit, ultrasensitive	KHB3544	Thermo
Novex™ 10 to 20% Tricine mini protein gels	EC6625BOX	Thermo
Pierce™ BCA protein assay kits	23225	Thermo
ProcartaPlex™ human neurodegeneration panel 1, 9plex	EPX090-15836-901	Thermo
Qubit dsDNA HS assay kit	Q32854	Thermo
Simoa® NfL assay	103186	Quanterix
SuperSignal™ West Dura extended duration substrate	34075	Thermo

3.1.3 Antibodies

Table 3. Antibodies

Antibodies	Identifier	Supplier
Anti-GFAP (GA5) mouse mAb	3670S	CST
Anti-CD68 rat mAb	MA5-13324	Abcam
Anti-Y188 rabbit mAb	ab32136	Abcam
Anti-6E10 mouse mAb	803001	BioLegend
Anti-Ki67 biotin mAb	13-5698-82	Invitrogen
Anti-SMA- α mouse mAb	14-9760-82	Invitrogen
Anti-Iba1 rabbit mAb	SAB5702256	Wako
Anti-2E mouse mAb (26A12)	/	Feederle Lab (DZNE Munich)
Anti-actin (C4) Mouse mAb	G0918	Sigma

Goat anti-mouse IgG crossed-absorbed secondary antibody, Alexa Fluor 488	A-11001	Invitrogen
Goat anti-mouse IgG crossed-absorbed secondary antibody, Alexa Fluor 555	A-21422	Invitrogen
Goat anti-mouse IgG crossed-absorbed secondary antibody, Alexa Fluor 647	A-21235	Invitrogen
Goat anti-rabbit IgG crossed-absorbed secondary antibody, Alexa Fluor 488	A-11008	Invitrogen
Goat anti-rabbit IgG crossed-absorbed secondary antibody, Alexa Fluor 555	A-21428	Invitrogen
Goat anti-rabbit IgG crossed-absorbed secondary antibody, Alexa Fluor 647	A-21244	Invitrogen
Donkey anti-rat IgG crossed-absorbed Secondary antibody, Alexa Fluor 555	A48270	Invitrogen
Streptavidin, Alexa Fluor™ 555 conjugate	S21381	Invitrogen
Streptavidin, Alexa Fluor™ 488 conjugate	S11223	Invitrogen
Goat anti-mouse IgG2b secondary antibody, HRP	M32407	Invitrogen
Goat anti-rabbit IgG secondary antibody, HRP	7074S	CST
Goat anti-mouse IgG secondary antibody, HRP	31430	Invitrogen

3.1.4 Materials

Table 4. Materials

Materials	Identifier	Manufacturer
Low-Profile 96-well PCR plates	HSP9601	Bio-Rad
Qubit assay tubes	Q32856	Invitrogen
PCR Tubes 0.2 ml 8-tube strips	951010022	Eppendorf
DNA LoBind Tubes, 1.5 ml	022431021	Eppendorf
Tips LTS 200UL filter RT-L200FLR	30389240	Rainin
Tips LTS 1ML filter RT-L1000FLR	30389213	Rainin
Tips LTS 20UL filter RT-L10FLR	30389226	Rainin
Microseal 'F' Foil	MSF1001	Bio-Rad
Microseal 'B' Film	MSB1001	Bio-Rad

3.1.5 Equipment

Table 5. Equipment

Equipment	Identifier	Manufacturer
Confocal microscope	LSM 880	Carl Zeiss
Cell counter	TC20	Bio-Rad
DynaMag™-2 magnet	12321D	Thermo
DynaMag™-96 Side skirted magnet	12027	Invitrogen
EnSpire multimode plate reader	23001395	Perkin Elmer LAS
Leica dissection microscope	Leica M125C	Leica Microsystems
Leica DMI8 fluorescent microscope	S/N 425074	Leica Microsystems
NanoDrop one microvolume UV- Vis spectrophotometer	AZY1602185	Thermo
MACS MultiStand	130-042-303	Miltenyi Biotec
Odyssey Fc imaging system	OFC-0976	LI-COR Biosciences
C1000 Touch thermal cycler	1851196	BIO-RAD
96-Deep well reaction module	1840197	BIO-RAD
S1000 thermal cycler	1852196	BIO-RAD
Qubit 4.0 Fluorometer	Q33226	Thermo
2100 Bioanalyzer Laptop Bundle	G2943CA	Agilent
Vortex Genie 2 Mixer	5429121	Omnilab
LightCycler® 480 Instrument II	05015243001	Roche
Mantis Liquid Dispenser	-	FORMULATRIX
Pipet-Lite LTS Pipette L-2XLS+	17014393	Rainin
Pipet-Lite LTS Pipette L-10XLS+	17014388	Rainin
Pipet-Lite LTS Pipette L-20XLS+	17014392	Rainin
Pipet-Lite LTS Pipette L-200XLS+	17014391	Rainin
Pipet-Lite LTS Pipette L-1000XLS+	17014382	Rainin
Pipet-Lite Multi Pipette L8-10XLS+	17013802	Rainin
Pipet-Lite Multi Pipette L8-200XLS+	17013805	Rainin

Pipet-Lite Multi Pipette L8-50XLS+	17013804	Rainin
------------------------------------	----------	--------

3.2 Animals

3.2.1 General considerations and housing

The animal experiments conducted for this study were reviewed and agreed by the institutional animal use and care committee in Center for Stroke and Dementia Research (CSD) at Ludwig Maximilian University of Munich (LMU). In our study, mice were grouped and housed in threes in Greenline IVC GM500 plastic cages. The housing environment was carefully regulated, maintaining a stable temperature of $21 \pm 2^\circ\text{C}$ and adhering to a consistent 12-hour light/dark cycle, ensuring optimal living conditions for the mice. Additionally, food and water were provided ad libitum to the mice. Adhering to rigorous ethical standards, all procedures involving animals were conducted in strict compliance with the established guidelines of both the Society for Laboratory Animals Science (GV-SOLAS) and the Federation of European Laboratory Animal Science Association (FELASA). These guidelines are critical in ensuring the humane and ethical treatment of laboratory animals. Our research team made every effort to minimize animal suffering and to decrease the number of animals utilized, aligning with the principles of ethical animal research. The study included both genders of in all tests, except in specific instances where differentiation between genders was necessary for the validity of the experimental outcomes.

3.2.2 5XFAD transgenic mice

In this research, we utilized *5XFAD* mice with a B6/SJL genetic background (34840-JAX, Tg6799), characterized by the expression of human APP and PSEN1 transgenes containing five mutations linked to AD (Oakley et al., 2006). These include the Swedish (K670N/M671L), Florida (I716V), and London (V717I) mutations in the APP gene, along with the M146L and L286V mutations in PSEN1 gene. We employed a breeding strategy where heterozygous male *5XFAD* mice were mated with female B6/SJL mice. This approach ensured the transmission of the same transgene from the heterozygous fathers to their offspring. In the context of this study, both female and male *5XFAD* mice, with their WT littermates used as specified indicated in the results section.

3.2.3 APPNL-G-F knock-in mice

In addition to the *5XFAD* mice who overexpress APP, we also introduced another AD mouse model in this project, the *APPNL-G-F* knock-in mice, which are on a C57BL/6J background (Saito et al., 2014). The *APPNL-G-F* model was specifically designed to mitigate potential artifacts that could arise from the overexpression of APP, commonly seen in other AD models. In this model, while APP itself is not overexpressed, the concentrations of pathogenic A β are increased owing to the synergistic effects of three mutations linked to FAD, which allows for a more accurate representation of the disease's pathogenic mechanisms. The *APPNL-G-F* knock-in model is characterized by three FAD-associated mutations: the Swedish "NL", the Iberian "F", and the Arctic "G" mutations. In our experiments, both female and male *APPNL-G-F* knock-in mice were employed, with specific details of their use outlined in the results section.

3.2.4 Peptide preparation and administration

In our study, several *in vivo* experiments were conducted to evaluate the effects of the 2E peptide in AD models. 2E peptide were produced and provided by Prof. Dr. Aphrodite Kapurniotu, Dr. Beatrice Dalla Volta and with the help of other lab members from the Division of Peptide Biochemistry at Technical University of Munich (TUM).

Experiment A - Chronic treatment of *5XFAD* mice (cohort 1): All female *5XFAD* mice were allocated into two experimental groups (treatment and control) utilizing block randomization. The treatment group (n=8) received i.p. injections of 2E peptide solution every other day, starting at 3 months of age, at a dosage of 5 mg/kg for the first 6 weeks, followed by 2.5 mg/kg until 6 months. The saline group (n=9) and WT littermates (n=10) received equivalent volumes of saline. All mice were sacrificed at 6 months of age. Experiment B - Chronic treatment of *5XFAD* mice (cohort 2): Conducted by the independent researchers who were blinded to the treatments, this experiment followed a similar protocol. Three female *5XFAD* mice were given 5 mg/kg of 2E peptide via i.p. injection every other day from 3 to 6 months of age. The vehicle group (n=4) received saline. All mice were sacrificed at 6 months. Experiment C - Chronic treatment of *5XFAD* mice (cohort 3): Conducted by the independent researchers who were blinded to the treatments, this experiment followed a similar protocol. 11 female and male

5XFAD mice were given 100 µg of 2E peptide via i.p. injection every other day from 2 to 4 months of age. The vehicle group (n=11) received saline. All mice were sacrificed at 6 months. Experiment D - Acute treatment in *APPNL-G-F* mice: In this acute experiment, symptomatic 10-month-old male and female *APPNL-G-F* mice (n=8) were intracerebrally injected with 2 µL of 2E peptide (1 µg/µL). The vehicle group mice (n=10) received an equal volume of saline. All mice were sacrificed 4 days post-injection. Experiment E - 2E detection experiment: To detect 2E peptide in the brains, 6 months old female WT mice were treated with varying doses of 2E peptide (0, 100, 200, and 500 µg) via i.p. injection. All mice were sacrificed 4 hours post-injection.

3.2.5 Mouse plasma and cerebral spinal liquid collection

Before perfusion, the blood and cerebrospinal fluid (CSF) were collected from the mice, which were under a terminal dose of anesthesia. The whole blood was collected into anticoagulant-treated tubes, such as those treated with Ethylenediaminetetraacetic acid (EDTA). To separate plasma, the blood samples were centrifuged at approximately 2000 g for 15 mins at room temperature using a refrigerated centrifuge. This process removed cells and platelets, and the resulting supernatant (plasma) was then stored at -80°C for subsequent analysis. The extraction of CSF was performed following a well-established protocol (Kaur et al., 2023), conducted prior to both perfusion and blood collection. From each mouse, approximately 10 µL of CSF was carefully extracted and then transferred into a 0.5 ml protein low-binding tube. Like the plasma, the CSF samples were also preserved at -80°C until needed for further experiments.

3.2.6 Preparation of mouse brain for biochemistry

Following blood collection, mice underwent transcatheterial perfusion with ice-cold phosphate-buffered saline (PBS) for 10 minutes at a flow rate of 10 ml/min, or they were first perfused with PBS followed by a 10-minute perfusion with 4% paraformaldehyde (PFA). For each cohort of mice, the same perfusion strategy was taken. For biochemical analysis: brains from mice (either PBS-perfused or not perfused) were removed and immediately frozen in liquid nitrogen, then preserved at -80°C for future analysis.

3.2.7 Preparation of mouse brain for immunohistology

For histological analysis: brains from mice (perfused with PBS or PBS-PFA) were harvested and submerged in a 4% PFA solution for post-fixation for 24 h at 4°C, followed by immersion in a 30% sucrose solution at 4°C for approximately 24-36 h. The brains were then encapsulated in optimal cutting temperature compound (O.C.T.), rapidly frozen with dry ice, and preserved at -80°C until they were sectioned. Consecutive coronal brain slices of 14 µm were produced using a cryostat (CryoSTAR NX70, Thermo Scientific) and kept at -80°C for subsequent analysis.

3.3 Behavioral tests

All behavioral experiments were done and analyzed by experimenters who were blind to the treatments and the genotypes of the mice.

3.3.1 Open field test

The open field test, a broadly acknowledged method for assessing locomotion, exploratory behavior, and anxiety levels in rodents (Seibenhener & Wooten, 2015), was utilized in our study. The mice underwent this test at either 4 or 6 months old. For the experiment, each mouse was placed inside a brightly illuminated, transparent Plexiglas enclosure, located within a secluded cabinet to maintain a regulated environment. The procedure began with a 1-minute habituation period to allow the mice to acclimate to the new surroundings. Following this, their exploratory behavior in the open field was recorded for 10 minutes using video monitoring, specifically with EthoVision®XT software from Noldus Information Technology, Netherlands. This setup allowed for precise and detailed tracking of the mice's movements and behaviors, providing valuable insights into their locomotor capabilities and anxiety-related responses in an open and novel environment.

3.3.2 Barnes maze

The Barnes maze is a behavioral test used to evaluate spatial learning and memory in rodents (Pitts, 2018). For the spatial memory test, spatial markers were positioned around the maze, remaining unchanged throughout the study. Mice were consecutively subjected to Barnes maze at 5 months and 6 months of age. This maze features a round table equipped with circular openings along its circumference. The objective

is for the animal to locate the box placed under one of the openings, guided by visual signals. During the trials, the table's surface is intensely illuminated, acting as an unpleasant stimulus that encourages the mouse to find the target box. The location of the goal box remained unchanged throughout all testing sessions. The mouse memorizes the position of the box, and the amount of time it takes for the mouse to locate the correct hole within the 180s is automatically assessed through video tracking (EthoVision®XT, Noldus Information Technology, Netherlands). To assess spatial memory, a spatial probe test was conducted 24 hours following the final training session. During the probe test, each mouse performed the tests three times, and was allowed to search for the goal box on the platform for 180 s. Each test was stopped once the mouse found the goal box or failed to find it within 180 s.

3.3.3 Elevated plus maze

The elevated plus maze is a commonly recognized behavioral assay employed to evaluate anxiety-related behaviors in mice, which can influence their performance in other tests (Kraeuter et al., 2019). Mice was tested on the elevated plus maze either at 4 or 6 months of age. The apparatus consists of two enclosed arms with walls and two open arms without walls, elevated above the floor. Entries into both the arms, as well as the percentage of time spent in the arms, were quantified through video monitoring with EthoVision®XT software. Each mouse was initially placed in the left closed arm and given 1 minute to acclimate. Subsequently, their exploratory behavior was recorded over a 5-minute session, providing insights into their anxiety levels based on their arm preference and locomotion.

3.4 Biochemical and molecular studies

3.4.1 DNA extraction from mouse tails

Before being used in the experiments, all mice underwent genotyping to confirm their genetic profiles. Deoxyribonucleic Acid (DNA) was isolated from biopsies of mouse tails as a part of the genotyping process. A 0.5 mm section of the tail is placed into a microfuge tube with 0.5 ml of digestion buffer containing 0.5 mg/ml proteinase K. The DNA digestion buffer is composed of 50 mM Tris-HCl at pH 8.0, 100 mM EDTA, 100

mM NaCl, and 1% SDS, ensuring optimal conditions for DNA release. After an overnight incubation at 50-55°C with gentle shaking, the sample is centrifuged post-phenol/chloroform extraction. The 0.5ml supernatant is then transferred to a new tube, and DNA is precipitated with ethanol, washed, and centrifuged. The dried DNA pellet is then resuspended in Tris-EDTA (TE) buffer and warmed to 65°C to ensure complete dissolution. The final preparation, yielding about 20-50 µg of DNA, is suitable for analyses such as restriction enzyme digestion.

3.4.2 Nucleic acid quantitation

The purity and concentration of DNA and RNA samples were measured using a Spectrophotometer (NanoDrop). Prior to sample measurement, the NanoDrop was calibrated with 2 µL of nuclease-free water, establishing a baseline for analysis. Concentrations were determined by the instrument based on absorbance at 260 nm. Additionally, for DNA samples, the NanoDrop provided a purity ratio (A260/A280), while for RNA samples, both A260/A280 and A260/A230 ratios were obtained. Generally, a DNA sample is considered pure with a ratio of approximately 1.8, and for RNA, a ratio of around 2.0 is indicative of purity.

3.4.3 Protein extraction from mouse brains

Protein was isolated from isolated from fresh-frozen brains and PFA-fixed OCT-embedded frozen brain sections according to previous, well-established methods with some modifications.

For fresh-frozen brains, we took an established protocol which includes a buffer-dependent extraction of protein according to protein solubility in each buffer: diethylamine (DEA) extraction for soluble proteins, followed by radioimmunoprecipitation (RIPA) assay extraction for membrane, nuclei, mitochondrial and cytosolic proteins. Brain hemispheres from -80 °C were taken and put on dry ice to keep them frozen. 1 ml of DEA buffer + protease inhibitor (PI) mix was added into Precellys tubes and placed on ice. Each tube was then transferred one frozen hemisphere, and the cap was securely closed. The brain tissues were homogenized using the Precellys machine at 6500 rpm for 30 seconds at 8 °C. Subsequently, the homogenized mixture was centrifuged at 4 °C for 10 minutes at 4000 g to pellet membranes, nuclei, and mitochondria. The supernatant (same amount from each sample) was carefully transferred from Precellys

tubes into ultra-centrifuge 1.5 mL tubes without disturbing the pellet. The supernatant was ultracentrifuged at 4 °C for 30 minutes at 100 000 g. The DEA fraction from the ultracentrifuge tubes was collected without disturbing the pellet, followed by the addition of 10% ice-cold 0.5M Tris (pH=6.8) to adjust the pH. After thorough mixing, the DEA extraction was stored at -80°C for further use. The pellet from was resuspended with 1 mL ice-cold RIPA buffer by brief shaking and homogenizing with the Precellys machine at 5000 rpm for 12 seconds at 8 °C. The mixture was then centrifuged at 4 °C for 10 minutes at 4000 g to remove insoluble material. The supernatant from the RIPA fraction and the pellet from the ultracentrifuge were collected in 0.1 mL ice-cold RIPA buffer and subjected to ultracentrifugation at 4 °C for 60 minutes at 100 000 g. The supernatant was collected as the RIPA extraction and stored at -80°C for further use.

For PFA-fixed brain sections: the frozen brain sections (14 µm) were rinsed with PBS, then incubated at RT for 10 min. Target brain sections were scratched and collected the brain lysates (in PBS) into 1.5 ml tubes by pipetting with 200 µl tips. The samples were centrifuged for 3 min at 14000 g at 4°C, then the pellet was resuspended with 200 µL lysis buffer. Samples were incubated at 4°C for 5 min and boiled at 100°C for 20 min, followed by a 2 h incubation at 80°C. The supernatant after centrifugation at 4°C for 20 min at 14000 g was collected and stored at -80°C.

3.4.4 Protein quantification

The Bicinchoninic acid (BCA) assay is a colorimetric technique for quantifying total protein that relies on copper. It depends on the creation of a Cu²⁺-protein complex under alkaline conditions, followed by the reduction of Cu²⁺ to Cu⁺. Experiment was performed according to the manufactory instructions using a Pierce™ BCA Protein Assay Kit and Multimode plate reader.

3.4.5 Immunofluorescence staining and imaging

Before the staining procedure, non-fixed mouse brains sections (fresh-frozen) were taken out of the -80°C and were fixed with 4% PFA at 4°C for 15 min. Then the brain sections were rinsed 3 times with 1xPBS at RT. Then all brain sections (both non-fixed and fixed) can be rinsed with the double-distilled water (ddH₂O) followed by 10 min incubation in PBS with 0.1% tween (PBST) at room temperature. After two rinses in

PBS, slides were preincubated in blocking solution (3% (vol/vol) bovine serum albumin (BSA) and 0.4% (vol/vol) Triton-X100 in PBS for 45 min at room temperature. The slides were then incubated overnight at 4°C in blocking solution with the following primary antibodies: mouse anti-GFAP (1:500), rabbit anti-Iba1 (1:500), rat anti-CD68 (1:500), rabbit anti-Y188 (1:500), mouse anti-6E10 (1:500), Biotin anti-Ki67 (1:1000), mouse anti-SMA- α (1:500). After primary antibody incubation overnight at 4°C, brain sections were washed three times with 1xPBS and incubated with appropriate fluorophore-conjugated secondary antibodies together with fluorescent amyloid β (A β) dye Methoxy-X04 (10 μ M) or nuclei dye Hoechst (1:1000) for one hour at room temperature (RT). Brain sections were subsequently washed two times with 1xPBS and ddH₂O, then affixed to glass slides (Thermo Scientific), allowed to dry in darkness for at least 30 minutes, and mounted with Gel Aqua Mount media (Sigma Aldrich) and analyzed by Dmi8 fluorescent microscopy (Leica) and confocal microscopy (LSM880 AiryScan, Zeiss). For X-34 staining, the brain slide was permeabilized with 0.25% Triton X-100 for 30 minutes and stained with X-34 dye (100 μ M) dissolved in a solution of 40% ethanol in PBS, for around 20 minutes. Brain slide was then rinsed with distilled water and mounted. All imaging and quantifications were done by experimenters who were blind to the treatments and the genotypes of the mice.

3.4.6 Western blot and slot blot

Samples were prepared and separated with Novex™ 10 to 20% Tricine mini protein gels and transferred onto nitrocellulose membranes. For A β detection, boil the membrane for 5 min with a microwave before blocking. Block the membranes with 10-15ml Intercept Blocking Buffer (LI-COR) for 60 min at RT on a shaker. Prepare the primary antibodies in 5% BSA in TBST. Incubate the membranes with primary antibodies overnight at 4°C. Primary antibodies were used as follows: mouse anti-2E (26A12), mouse anti-GFAP, mouse anti-actin (C4). Wash the membranes 3x10 min at RT in TBST, then incubate with secondary antibodies at RT for one hour. Secondary antibodies were used as follows: anti-mouse IgG 2b, anti-rabbit IgG, anti-mouse IgG horseradish peroxidase (HRP) - conjugated Abs. Then the membranes were washed 3x15 min at RT in TBST.

The dot blot method is a technique used for the detection, analysis, and identification of proteins. It shares similarities with the western blot technique; however, it differs in

that the protein samples are not separated via electrophoresis. Instead, they are directly spotted onto the membrane or paper substrate through circular templates. Re-suspend 2E or IAPP peptide powder with ddH₂O, and put on ice for the later usage. Transfer peptide solution onto nitrocellulose membranes with Minifold I 96-well system via a vacuum pump. Rinse the blot transfer membrane with water three times. The membrane was stained with Ponceau S stain for 2 mins, and then scanned the membrane after 3 rounds of washing. Wash the membrane on a shaker with 1X TBST buffer for 3 times, 10 mins for each wash. Block the membrane on a shaker with the blocking buffer (1% BSA in PBS) at RT for 60 mins. Then remove the blocking buffer, and incubate the membrane with primary antibody at 4°C overnight. Wash the membrane on a shaker with 1X TBST buffer for 3 times, 10 mins for each wash at RT. Incubate with secondary antibody at RT for 60 mins, then wash with TBST buffer for 3 times, 10 mins for each wash at RT. Target proteins/peptides were then identified with the enhanced chemiluminescence method using Luminol enhancer and peroxide solutions. Visualization of these protein bands was achieved with an Odyssey Fc imager from LI-COR.

3.4.7 Screening and validation of anti-2E antibody

Mouse anti-2E antibodies were designed by Prof. Aphrodite Kapurniotu (TUM), Prof. Jürgen Bernhagen (LMU), and Dr. Regina Feederle (Helmholtz Center Munich). Antibodies were then produced and provided by Dr. Feederle at Helmholtz Center Munich. In brief, IBalb/c mice received subcutaneous and intraperitoneal immunizations with a concoction of 50 µg of ovalbumin-linked 2E in 200 µl PBS, 5 nmol CpG2006, and 200 µl of Incomplete Freund's adjuvant (Sigma-Aldrich). 11 weeks post-immunization, a booster shot, excluding Freund's Adjuvant, was administered both intraperitoneally and subcutaneously 3 days before the fusion process. This involved merging the P3X63-Ag8.653 myeloma cell line with immunized mouse spleen cells using polyethylene glycol 1500 (Köhler & Milstein, 1975). The fused cells were then cultured in 96-well plates in RPMI 1640 medium supplemented with 20% fetal calf serum, glutamine, pyruvate, non-essential amino acids, and HAT media supplement.

After 10 days, screening of the hybridoma supernatants was conducted via a flow cytometry assay (iQue, Intellicyt; Sartorius) against biotinylated 2E affixed to streptavidin

beads, treated for 90 minutes with hybridoma supernatant and Atto-488-labeled isotype-specific monoclonal rat-anti-mouse IgG secondary antibodies. Antibody adherence was scrutinized using ForeCyt software (Sartorius). Subsequent validations for promising supernatants were carried out through dot blot and Western blot techniques. Selected hybridoma clones are in the process of sub-cloning via limiting dilution to secure stable monoclonal cell lines. This investigation utilized primary oligoclone anti-2E 26A12 (mouse IgG2b/k) hybridoma supernatant.

3.4.8 Simoa NF-light assay

Neurofilament light (NfL), a 68 kDa protein found in the cytoskeleton of neurons, plays a key role in the structural integrity of neurons. NfL works in conjunction with the 125 kDa Neurofilament medium (NfM) and the 200 kDa Neurofilament heavy (NfH) proteins to construct neurofilaments, crucial elements of the neuronal cytoskeleton. These proteins are primarily responsible for providing structural support to axons and regulating their diameter. Significant release of neurofilaments can occur as a result of axonal damage or during the process of neuronal degeneration. NfL, in particular, has been linked with various neurological conditions, including traumatic brain injury, multiple sclerosis, frontotemporal dementia, and other neurodegenerative diseases. The measurement of NfL in serum is conducted through the SR-X immunoassay analyzer by Simoa (Quanterix Corp, Boston, MA). This method utilizes an ultrasensitive paramagnetic bead-based enzyme-linked immunosorbent assay (ELISA), which has been extensively documented in prior research (Preische et al., 2019). In total, 16 qualified serum samples were included for the Simoa assays, which received full support from Brigitte Nuscher at the German Center for Neurodegenerative Diseases (DZNE) Munich.

3.4.9 Enzyme-linked immunosorbent assay

The Amyloid beta 40 and 42 ELISA kits are the specific and sensitive biochemical assay used primarily for the quantification of amyloid beta peptides (A β 1-40 and A β 1-42) in blood. Experiment was performed according to the manufactory instructions using Amyloid beta 40/42 Human ELISA Kit and Multimode plate reader.

3.4.10 Luminex neurodegeneration array

The ProcartaPlex 9-Plex Neurodegeneration Panel 1 (Human) (Invitrogen, EPX090-15836-901) is a sophisticated tool designed for neurological research, particularly in the context of neurodegenerative diseases like amyotrophic lateral sclerosis (ALS), AD, and Parkinson's disease (PD). This panel utilizes Luminex xMAP technology to simultaneously analyze nine different protein targets in a single well, providing a comprehensive and efficient approach for studying the complex protein interactions and pathways involved in these conditions. The experiment was performed according to the manufacturer's instructions using ProcartaPlex 9-Plex Neurodegeneration Panel 1 (Human), with support from Dr. Omar El Bounkari at the Institute for Stroke and Dementia Research (ISD) University Hospital, LMU Munich.

3.5 RNA sequencing of mouse brains

For the RNA-seq analysis of mouse brains, our study initiated with a bulk RNA-seq experiment on PFA-fixed, OCT-embedded frozen mouse brain sections from cohort 1. This was conducted using a modified Smart-seq2 method, which was established as a new method (Ji et al., 2023). The list of samples subjected to RNA-seq is detailed in Table 6 for reference.

Table 1: Sample and grouping list for RNA-seq.

Sample ID	Animal	Region	Treatment
P8C10	2E_08	Brain_stem	2E
P8D4	2E_01	Brain_stem	2E
P8D5	2E_03	Brain_stem	2E
P8H4	2E_02	Brain_stem	2E
P8H5	2E_04	Brain_stem	2E
P8H7	2E_05	Brain_stem	2E
P8H8	2E_06	Brain_stem	2E
P8H9	2E_07	Brain_stem	2E
P8B10	2E_08	Cortex	2E
P8B4	2E_01	Cortex	2E
P8B5	2E_03	Cortex	2E
P8F4	2E_02	Cortex	2E
P8F5	2E_04	Cortex	2E
P8F7	2E_05	Cortex	2E
P8F8	2E_06	Cortex	2E

P8F9	2E_07	Cortex	2E
P8C4	2E_01	Hippocampus	2E
P8C5	2E_03	Hippocampus	2E
P8D10	2E_08	Hippocampus	2E
P8G4	2E_02	Hippocampus	2E
P8G5	2E_04	Hippocampus	2E
P8G7	2E_05	Hippocampus	2E
P8G8	2E_06	Hippocampus	2E
P8G9	2E_07	Hippocampus	2E
P8A10	2E_08	Hippocampus_Cortex	2E
P8A5	2E_03	Hippocampus_Cortex	2E
P8E4	2E_02	Hippocampus_Cortex	2E
P8E5	2E_04	Hippocampus_Cortex	2E
P8E7	2E_05	Hippocampus_Cortex	2E
P8E8	2E_06	Hippocampus_Cortex	2E
P8E9	2E_07	Hippocampus_Cortex	2E
P8D1	AD_01	Brain_stem	AD
P8D2	AD_02	Brain_stem	AD
P8D3	AD_04	Brain_stem	AD
P8D6	AD_06	Brain_stem	AD
P8H2	AD_03	Brain_stem	AD
P8H3	AD_05	Brain_stem	AD
P8B1	AD_01	Cortex	AD
P8B2	AD_02	Cortex	AD
P8B3	AD_04	Cortex	AD
P8B6	AD_06	Cortex	AD
P8F2	AD_03	Cortex	AD
P8F3	AD_05	Cortex	AD
P8C1	AD_01	Hippocampus	AD
P8C2	AD_02	Hippocampus	AD
P8C3	AD_04	Hippocampus	AD
P8C6	AD_06	Hippocampus	AD
P8G2	AD_03	Hippocampus	AD
P8G3	AD_05	Hippocampus	AD
P8A2	AD_02	Hippocampus_Cortex	AD
P8A3	AD_04	Hippocampus_Cortex	AD
P8A6	AD_06	Hippocampus_Cortex	AD
P8E2	AD_03	Hippocampus_Cortex	AD
P8E3	AD_05	Hippocampus_Cortex	AD
P8D7	WT_03	Brain_stem	WT
P8D8	WT_04	Brain_stem	WT

P8D9	WT_05	Brain_stem	WT
P8F6	WT_02	Brain_stem	WT
P8B7	WT_03	Cortex	WT
P8B8	WT_04	Cortex	WT
P8B9	WT_05	Cortex	WT
P8F1	WT_01	Cortex	WT
P8H6	WT_02	Cortex	WT
P8C9	WT_05	Hippocampus	WT
P8E6	WT_02	Hippocampus	WT
P8G1	WT_01	Hippocampus	WT
P8A7	WT_03	Hippocampus_Cortex	WT
P8A8	WT_04	Hippocampus_Cortex	WT
P8A9	WT_05	Hippocampus_Cortex	WT
P8E1	WT_01	Hippocampus_Cortex	WT
P8G6	WT_02	Hippocampus_Cortex	WT

3.5.1 RNA extraction from mouse brains

RNA was extracted from PFA-fixed, OCT-embedded frozen mouse brain sections using a previously established method that enzymatically digests proteins to release crosslinked RNA (Ji et al., 2023). Briefly, 14 μm brain sections were taken from -80°C storage and allowed to equilibrate at room temperature for 5 minutes, ensuring they remained hydrated. RNA isolation buffer, comprising 40 μl of phosphate -potassium dextrose (PKD) buffer and 10 μL of proteinase K solution, was pre-prepared and chilled. This buffer (50 μL) was then applied to the brain sections, which were incubated at room temperature for 30 seconds. The sections were subsequently scraped, and the lysate was collected using pipette tips, immediately frozen in liquid nitrogen, and stored at -80°C .

For RNA purification, the samples were thawed for 3 minutes at room temperature, then vortexed, spun down, and incubated at 56°C for 4 hours in a thermal cycler with a 66°C lid temperature, with periodic checks for sample dissolution. Post-incubation, the samples were vortexed, spun down, and transferred to chilled 1.5 mL tubes. Oligo dT25 magnetic beads (Invitrogen) were prepared by performing three washes with 1x hybridization buffer (HB), consisting of 2x saline-sodium phosphate-EDTA (SSPE) buffer, 0.05% Tween-20, and 0.05% RNase Inhibitor. The beads were then resuspended to half of the initial volume with 2x HB for subsequent use. For each sample, 10 μL of the pre-washed dT25 beads (0.1 mg) were added, and the mixture was

heated at 56°C for one minute to reverse crosslinking. Following a 10-minute room temperature incubation for mRNA hybridization, the beads were washed twice with 100 µL of ice-cold 1x HB and once with ice-cold 1x PBS containing 0.1% RNase Inhibitor. After removing the PBS, the beads were resuspended in 15 µL of RNase-free water. To elute the mRNA, the bead-sample mixture was incubated at 80°C for two minutes and then quickly placed on a room temperature magnet to pellet the beads. The supernatant, rich in mRNA, was immediately transferred to a new tube and stored at -80°C for future analysis.

3.5.2 cDNA library preparation

For Smart-seq2: 0.1-0.5 ng mRNA from each sample were taken and continued with a modified Smart-seq2 protocol (Ji et al., 2023), involving reverse transcription and pre-amplification steps to prepare cDNA for library construction. The samples were thawed, subsequently heated for 3 minutes at 72°C, and then immediately cooled by placing them on ice. After reverse transcription, the pre-amplification of cDNA was conducted to generate enough cDNA. The amplification cycles were determined by the sample quality and quantity. cDNA libraries were then cleaned using the AMPure bead. Qualities of libraries were evaluated with a Bio-analyzer, utilizing the High Sensitivity DNA analysis kit. Fluorometric assessments were also performed using Qubit's DNA HS assay kits along with a Qubit 4.0 Fluorometer for concentration measurements. The samples were normalized to a concentration of 160 pg/mL. The sequencing libraries were prepared using an in-house produced Tn5 transposase. These libraries were then barcoded, pooled, and subjected to three rounds of AMPure bead cleanup, using a bead-to-library ratio of 0.8:1.

3.5.3 Sequencing data generation

For Smart-seq2: libraries were sequenced 2x150 reads base pairs (bp) paired-end on DNBSEQ Sequencing System (BGI) to a depth of 1×10^6 - 3×10^6 reads/sample.

3.6 Bioinformatics analysis

RNA-sequencing data analysis was performed with support from Dr. Peter Androvic at the Institute for Stroke and Dementia Research (ISD) University Hospital, LMU Munich. Sequencing data were demultiplexed using bcl2fastq (Illumina). Quality control

of reads was performed using FastQC and adaptor sequences were trimmed using TrimGalore. Reads were then aligned to GRCm38 (mm10) genome with added External RNA Controls Consortium (ERCC) sequences using STAR. Aligned reads were counted using the parameter “quantMode GeneCounts” in STAR and unstranded values were used for subsequent downstream analysis. Samples were further controlled for quality, leading to 71 QC-passing samples used in all downstream analyses (Table 1). Differential gene expression was analyzed using DESeq2 v1.30.153 and pair-wise contrasts between experimental groups within region and across all regions were then obtained. Principle component analysis (PCA) was performed on the top 500 variable genes using prcomp function in R v4.0.3. Functional enrichment analysis was performed with fGSEA v1.16.054 using gene sets obtained from Molecular Signature Database v7.2.1 and/or collected from published studies. Networks of enriched gene sets were constructed with Enrichment Map v3.3.255 in Cytoscape v3.8.2. Cell type proportion estimates were based on expression of high-confidence cell-type marker genes obtained by intersecting various resources. Significance was tested by linear mixed model via lmerTest package v3.156 on DESeq2-normalized and variance-stabilized expression values, treating experimental group and region as fixed effects and animal and gene as random effects. Post-hoc Tukey’s tests were performed using Estimated Marginal Means (emmeans) package v 1.6.1.

3.7 Statistical analysis

The specifics of the statistical analysis, including methodologies and parameters, are detailed in the respective sections accompanying the results. Where applicable, the number of biological replicates (n) is indicated at the bottom of figures. Significance levels are provided in the sections where the data are presented. Unless specified otherwise, data are presented as means \pm the standard error of the mean (SEM). All statistical analyses were conducted using GraphPad Prism 9. For comparisons between two groups with normally distributed data, a two-tailed Student's t-test was employed to assess statistical significance. In cases involving three or more groups, a one-way analysis of variance (ANOVA) was utilized, followed by either Tukey's or Dunnett's post hoc test to ascertain statistical significance.

3.8 Software

Table 7. Software

Software
Adobe Illustrator 2020
Adobe Photoshop 2021
Microsoft Office for Mac
GraphPad Prism V9.4.1
RStudio 2023.03.0
Zotero 6.0.30
ImageJ software/Fiji software (Version 64-bit Java 1.8.0_172)
Leica application suite X (Version 3.0.15878.1)
Carl Zeiss ZEN 2010 (Version 2.3.64.0)
BioRender (BioRender.com)

4. Results

4.1 Chronic 2E treatment alleviates A β deposition in the brains of 5XFAD mice

In my thesis, I employed the 5XFAD mouse model, which is genetically engineered to exhibit amyloid deposits from as early as 2 months of age (Oakley et al., 2006), a key characteristic of AD. To better mimic a clinical scenario where therapeutic interventions are introduced after the formation of amyloid plaques, we chose to administer the 2E peptide intraperitoneally three doses per week to a cohort of female 5XFAD mice aged between 3 to 6 months as cohort 1. This treatment timeframe was strategically chosen, aligning with the crucial phase of plaque accumulation in this model. For comparison, age-matched wild-type (WT) mice were given saline injections, allowing us to assess the specific impact of 2E in the context of established amyloid pathology (Figure 5). Furthermore, an additional exploratory study was conducted, administering 2E earlier in the disease course, from 2 to 4 months, involving a mixed cohort of male and female 5XFAD mice as cohort 2 (Figure 5). This experimental approach aimed to evaluate the therapeutic potential of 2E in modifying the course of AD, offering valuable insights into optimal treatment timelines for clinical application.

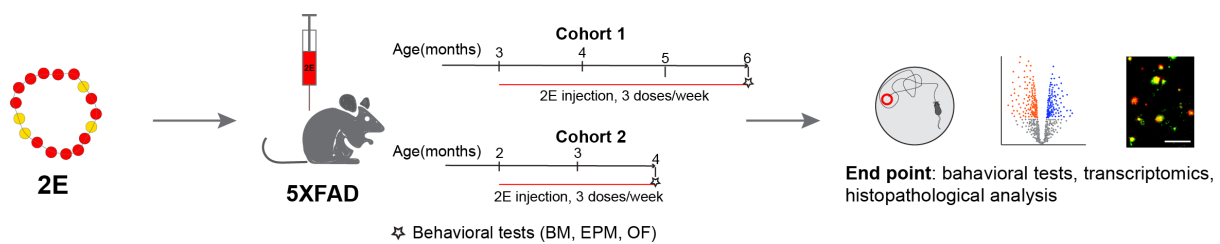


Figure. 5 | Schematics of *in vivo* experimental plan and summary. BM, Barnes Maze; EPM, Elevated Plus Maze; OF, Open Field.

It's noteworthy that a substantial difference in body weight was observed between WT mice and 2E-treated 5XFAD mice before and after treatment in cohort 1, without any notable weight changes attributable to the 2E peptide treatment within the 5XFAD groups (Figure 6A). Furthermore, from the ages of 3 to 6 months, 5XFAD mice exhibited less weight gain compared to their WT counterparts (Figure 6B). Interestingly, a

distinct upward trend in body weight gain was observed in 5XFAD mice following the 2E treatment (Figure 6B). We also investigated whether early-stage administration of the 2E peptide would yield similar outcomes in cohort 2. Here, male mice consistently outweighed their female counterparts at two separate measurements, and there was a noticeable increase in bodyweight among 2E-treated 5XFAD mice in comparison to their control counterparts (Figure 6C-D). Collectively, these findings indicate that 2E-treated 5XFAD mice experienced improved growth conditions relative to controls, without any apparent side effects being identified.

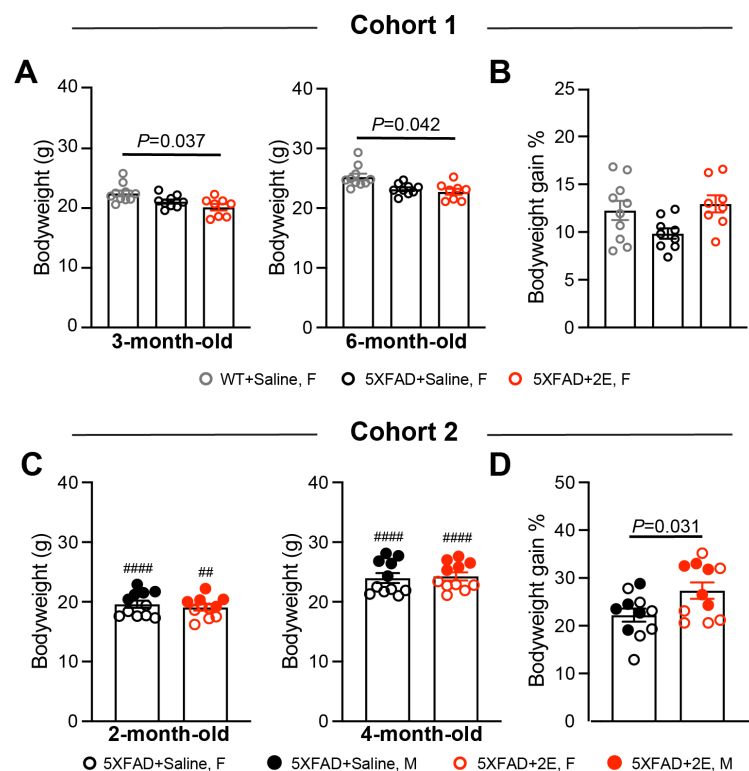


Figure. 6 | 2E peptide has no side effects on bodyweight. **A.** Quantification of female 5XFAD and WT mice bodyweight at 3- and 6-month-old before and after treatment (cohort 1). **B.** Quantification of percentage of bodyweight gain between two experimental time points. **C.** Quantification of female 5XFAD and WT mice bodyweight at 2- and 4-month-old before and after treatment (cohort 2). **D.** Quantification of percentage of bodyweight gain between two experimental time points. Each dot represents one mouse. Data are means \pm SEM. Bodyweight comparison between gender: ####, $p < 0.0001$; ##, $p < 0.01$.

Compared to controls in cohort 1, treatment with 2E peptide significantly reduced A β plaque deposition in the cortex, where reduction was most pronounced for the number of small plaques ($<20 \mu\text{m}^2$ in area), suggesting that after the start of treatment lowered

formation of new plaques in the 2E group (Figure 7A-C). Immunostaining with the 6E10 antibody against human A β 1-16 showed similar results, supporting the notion that treatment with 2E peptide led to a reduction of A β plaques deposition in the brain (Figure 7B). In cohort 2, female 5XFAD mice have significantly more amyloid plaque deposition than their male littermates (Figure 7D), which is consistent with previous study (Manji et al., 2019). Of note, 4-month-old 5XFAD mice from cohort 2 developed 60-70% less amyloid plaque burden in the cortex compared to 6-month-old ones in cohort 1 (Figure 7B, D). Consistent with cohort 1, 5XFAD mice developed significant less amyloid plaque in both genders after 2E peptide treatment compared to control group (Figure 7D), with small plaques decreased the most pronounced which is consistent with the cohort 1 mice (Figure 7E). 6E10 antibody staining showed similar decreasing trends which supported the notion that treatment with 2E peptide led to a reduction of A β plaques in the brain (Figure 7D). Together, these findings demonstrated that two treatment paradigms of 2E peptide alleviated A β plaque burden in the brains of 5XFAD mice.

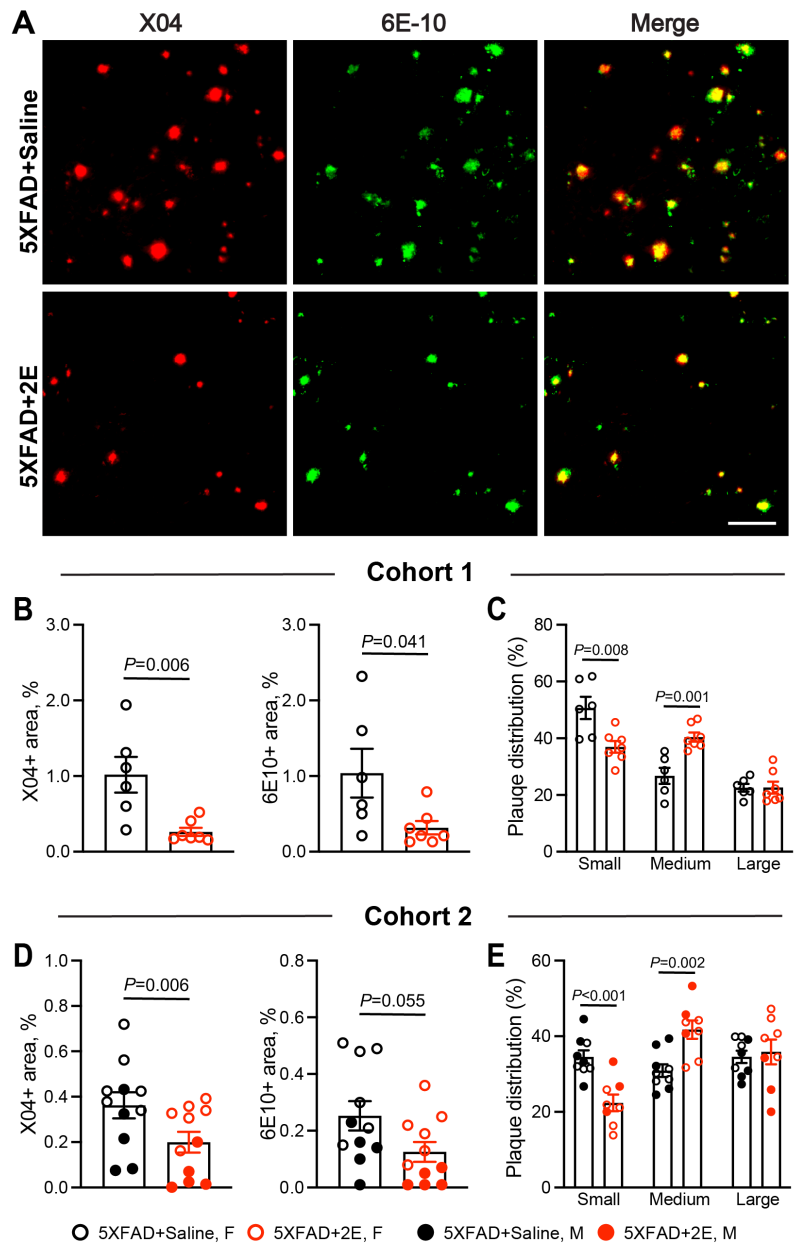


Figure 7 | Chronic 2E treatment alleviates A β deposition in the brains of 5XFAD mice. **A.** Representative confocal images of immunostaining of β -amyloid plaque with methoxy-X04 dye (red), and 6E10 antibody (green) in the brains of saline-treated (upper) or 2E-treated (bottom) 5XFAD mice. Scale bar = 100 μ m. X04: methoxy-X04. **B.** Quantification of the percentage of methoxy-X04-positive (left) and 6E10-positive (right) A β plaque coverage of 6-month-old 5XFAD mice (cohort 1). X04: methoxy-X04. **C.** Quantification of methoxy-X04-positive A β plaque size distribution of cohort 1 mice. Small: plaque size below 20 μ m²; Medium: plaque size between 20-100 μ m²; Large: plaque size above 100 μ m². **D.** Quantification of the percentage of methoxy-X04-positive (left) and 6E10-positive (right) A β plaque coverage of 4-month-old 5XFAD mice (cohort 2). X04: methoxy-X04. **E.** Quantification of methoxy-X04-positive A β plaque size distribution of cohort 2 mice. Small: plaque size below 20 μ m²; Medium: plaque size between 20-100 μ m²; Large: plaque size above 100 μ m². Each dot represents one mouse.

4.2 2E changes soluble A β 42 and A β 40 levels in Alzheimer's disease mouse models

Amyloid-beta peptides, particularly A β 42 and A β 40, are key biomarkers for Alzheimer's disease. A β 42 is more hydrophobic and more prone to aggregate than A β 40 (Sgourakis et al., 2007). A higher A β 42 to A β 40 ratio is often associated with increased formation of amyloid plaques, a hallmark of Alzheimer's disease pathology. Thus, I evaluated the concentrations of A β 42 and A β 40 in the plasma and CSF of 5XFAD mice using ELISA. In the first cohort, 2E peptide administration resulted in a partial reduction of A β 42 levels in both plasma and CSF of 5XFAD mice, compared to controls (Figure 8A, C), while A β 40 levels showed an upward trend (Figure 8B, D). In the second cohort of 5XFAD mice, there was a significant decrease in plasma A β 42 levels after 2E treatment (Figure 8E). Remarkably, 4-month-old 5XFAD mice in the second cohort exhibited a 60-70% reduction in plasma A β 42 levels compared to 6-month-old ones in the first cohort (Figure 8A, E). This reduction in A β 42 levels and A β 42/40 ratio aligns with the observed differences in amyloid plaque deposition between the two cohorts of 5XFAD mice, suggesting a consistent effect of 2E treatment across different measures of AD pathology.

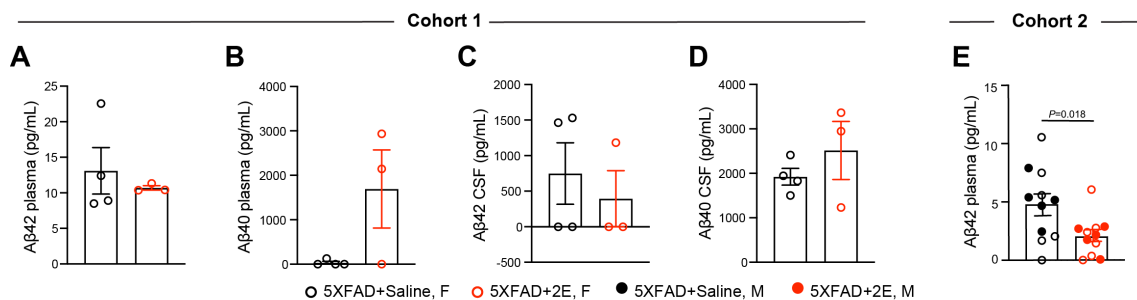


Figure. 8 | 2E changes soluble A β 42 and A β 40 levels in 5XFAD mouse model. **A.** Quantification of plasma A β 42 (left) and A β 40 (right) concentration in 6-month-old 5XFAD mice (cohort 1). **B.** Quantification of CSF A β 42 (left) and A β 40 (right) concentration in 6-month-old 5XFAD mice (cohort 1). **C.** Quantification of plasma A β 42 (left) concentration in 4-month-old 5XFAD mice (cohort 2). Each dot represents one mouse.

To further elucidate the physiological effects of 2E peptide, we performed 2E intracerebral injections in the APP-NL-G-F mouse model, a novel APP knock-in model of AD

(Figure 9A). Four days post-injection, all mice were euthanized for evaluation via ELISA assay. Consistent with the results seen in 5XFAD mice, treatment with 2E in APP-NL-G-F mice led to a significant reduction in plasma A β 42 levels, while A β 40 levels were observed to increase, leading to a decreasing A β 42/40 ratio (Figure 9B-C). These outcomes collectively indicate that 2E peptide treatment regimens effectively modify soluble A β 42 and A β 40 concentrations in the plasma and CSF, leading to a reduction of A β 42/40 ratio across different AD mouse models, showcasing the less new amyloid plaque formation post 2E treatment.

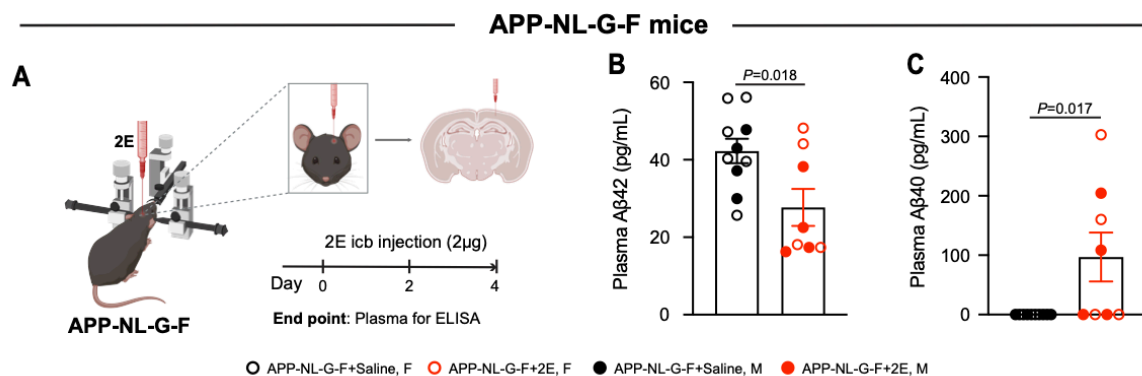


Figure. 9 | 2E changes soluble A β 42 and A β 40 levels in APP-NL-G-F mouse model. A. Schematical experimental outline of 2E intracerebral injection with 10-month-old APP-NL-G-F mice. **B.** Quantification of plasma A β 42 (left) and A β 40 (right) concentration in 10-month-old APP-NL-G-F mice. Each dot represents one mouse.

4.3 2E shifts amyloid deposition in the brains of 5XFAD mice

We next investigated amyloid deposition in various brain regions using X-34 and smooth muscle actin (SMA- α) staining to assess fibrillar A β accumulation. Our findings reveal a noticeable trend toward reduced total fibrillar A β deposition in both cortical areas and the hippocampus following 2E treatment (Figure 10A-B). Conversely, 2E led to a significant increase in fibrillar A β within blood vessels, as evidenced by areas staining positive for both X-34 and SMA- α (Figure 10C). There was a significantly increase in the proportion of vasculature showing A β + staining (Figure 10D), indicating an enhanced A β accumulation in vascular structures post treatment. Additionally, consistent with certain amyloidosis mouse models that display a sex-dependent effect on A β plaque accumulation (Manji et al., 2019), we noted sex-specific differences in amyloid deposition; female 5XFAD mice exhibited a higher cortical fibrillar amyloid load

compared to male counterparts (Figure 7D, 10B). Collectively, these data suggest that 2E peptide treatment facilitates a shift in amyloid deposition from the brain parenchyma to the vasculature.

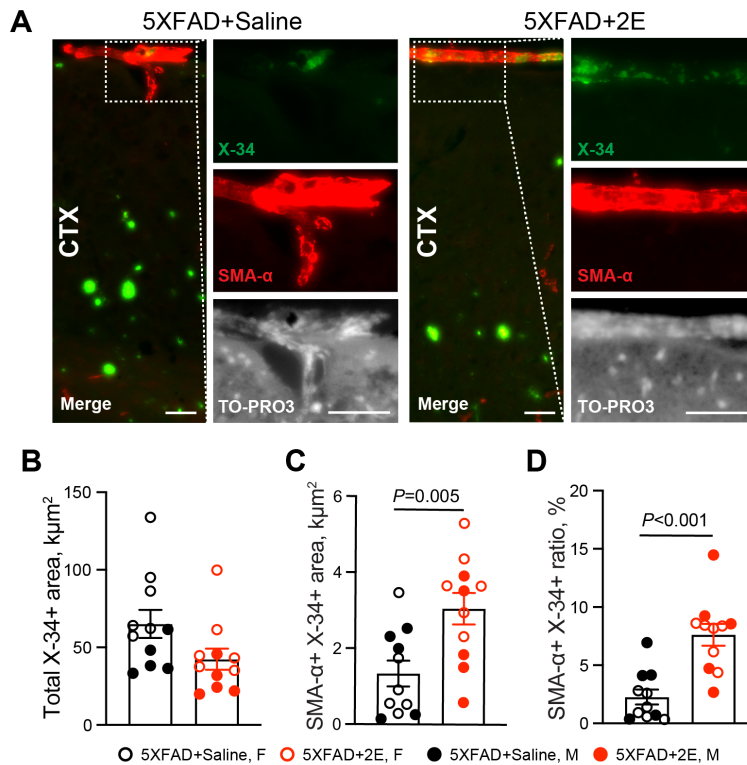


Figure. 10 | 2E shifts amyloid deposition in the brains of 5XFAD mice. A. Representative confocal images of immunostaining of fibrillar plaques/CAA with X-34 (green), smooth muscle of blood vessels with SMA-α (red) and nucleus with TO-PRO3 (white) in the brains of saline-treated (left) or 2E-treated (right) 5XFAD mice. Scale bar = 50μm. **B.** Quantification of the total X-34 positive area of 4-month-old 5XFAD mice (cohort 2). **C.** Quantification of the total SMA-α/X-34 positive area of 4-month-old 5XFAD mice. **D.** Quantification of the ratio of SMA-α/X-34 positive area out of total X-34 area of 4-month-old 5XFAD mice. Each dot represents one mouse.

4.4 2E distributes into brain after intraperitoneal injection

To better characterize the functions and potential mechanisms of 2E peptide, the development of a specific anti-2E monoclonal antibody was needed. Through a meticulous screening and validation process, the anti-2E 26A12 antibody, a mouse IgG2a monoclonal antibody (mAb), emerged as highly sensitive and dose-responsive specifically to the 2E peptide, demonstrating remarkable selectivity over other peptides such as the parent peptide IAPP or msR4M-L1, a completely unrelated peptide sequence of similar length (Kontos et al., 2020) (Figure 11A-B). Of note, anti-2E 26A12 antibody

effectively detected 2E in a spike-in assay within brain homogenates, identifying it at approximately 2-3 kDa, while showing no cross-reactivity with the full-length IAPP peptide (Figure 11C). Interestingly, this antibody also revealed 2E immunopositivity at higher molecular weights, ranging from 15-30 kDa (Figure 11C), suggesting the presence of 2E peptide aggregates or possibly its interaction with other brain proteins.

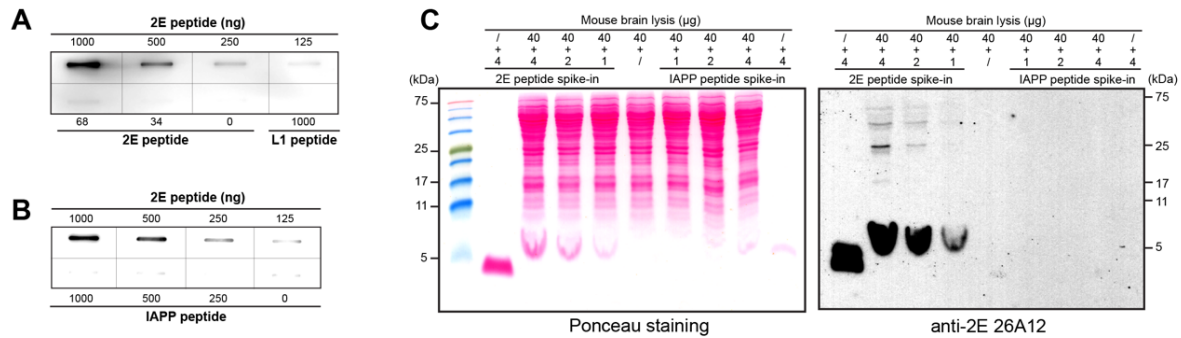


Figure. 11 | Anti-2E 26A12 monoclonal antibody validation and 2E detection using spike-in assays. A. Slot-blot assays for the validation of anti-2E 26A12 antibody with 0, 34, 68, 125, 250, 500 and 1000 ng of 2E peptide, and 1000 ng of msR4M-L1 peptide (L1) as negative control (Kontos et al., 2020). **B.** Slot-blot assays for the validation of anti-2E 26A12 antibody with 0, 125, 250, 500, 1000 ng of 2E peptide, and 250, 500, 1000ng of IAPP peptide. **C.** Western blot assay for 2E peptide detection in brain homogenates after 2E spike-in and IAPP spike-in; Ponceau staining of proteins/peptide load after SDS-PAGE (left), proteins/peptide bands detected by anti-2E 26A12 antibody (right).

Following short-term (4 h) i.p. injections of 2E peptide, Western blot analyses of brain homogenates were conducted (Figure 12A). The anti-2E 26A12 antibody identified bands in the range of 15-30 kDa, exhibiting a dose-dependent response, which, alongside the results from spike-in experiments, implies that these bands likely represent protein complexes or peptide oligomers containing 2E peptide (Figure 12B). Therefore, it can be concluded that after i.p. injection, the 2E peptide successfully penetrates the BBB and distributes within the brain.

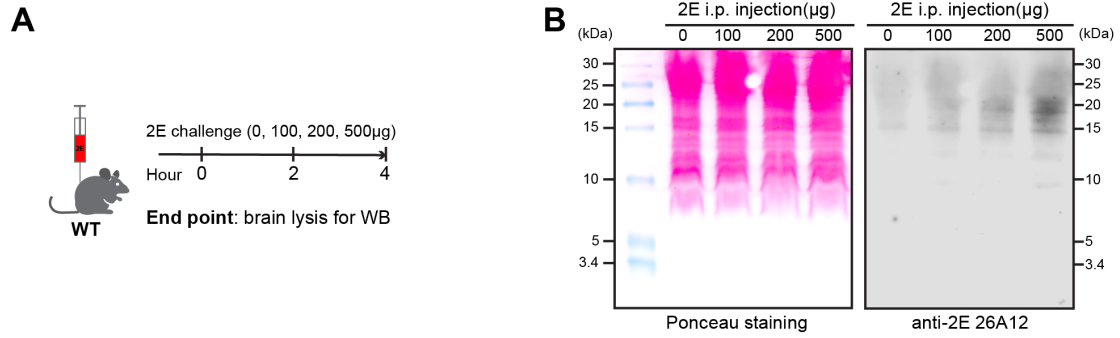


Figure. 12 | 2E distributes within the brain after i.p. injection. A. Schematics of experimental outline for 2E challenge. **B.** Ponceau staining of proteins/peptide load after SDS-PAGE (left), proteins/peptide bands detected by anti-2E 26A12 antibody (right). Each blot contains one sample in order from left to right.

4.5 Chronic 2E treatment improves behavior deficits in 5XFAD mice

To evaluate the effect of 2E peptide on the cognitive functions, we performed Barnes maze with 6-month-old 5XFAD mice from cohort 1 (Figure 13A). Compared with WT mice, 5XFAD group showed notable impairments in spatial learning and memory, evidenced by extended escape latency and longer total distance covered on the platform (Figure 13B-C). Moreover, these 5XFAD mice spent less time and traveled less distance in the target quadrant (Figure 13B-C). Notably, treatment with the 2E peptide effectively mitigated these cognitive deficits in the 5XFAD mice, indicating that chronic administration of 2E significantly improved spatial learning and memory in this AD mouse model and offering the potential therapeutic applications in human AD treatment strategies.

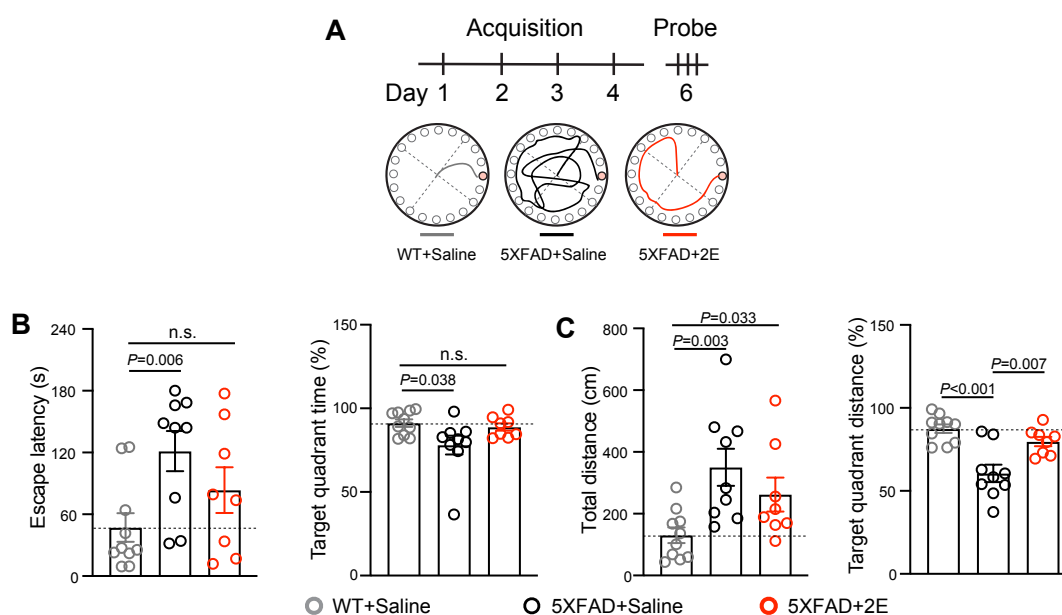


Figure. 13 | 2E improves behavior deficits in 5XFAD mice. **A.** Schematics of Barnes maze experimental outline (upper), representative tracing graphs in platform trials of 6-month-old mice (cohort 1) in Barnes maze (bottom). **B.** Quantification of the escape latency to the target hole (left) and percent of time in target quadrant (right) in probe trial of Barnes maze. **C.** Quantification of the total distance travelled on the platform (left) and percent of distance in target quadrant (right) in probe trial of Barnes maze. Each dot represents one mouse.

In the open field test, 5XFAD mice at 6 months of age exhibited significantly reduced mobility compared to their WT littermates, traveling less distance (Figure 14A-C). Remarkably, post-2E treatment, 5XFAD mice displayed enhanced mobility, travelling distances comparable to the WT group, showing a notable improvement in their activity levels. While there were similar trends in the frequency of entering the center of the open field, these did not reach statistical significance, suggesting no major differences in exploratory behavior among the experimental groups (Figure 14A-C). Additionally, the elevated plus maze test revealed that 2E treatment did not change the stress and anxiety levels in 6-month-old 5XFAD mice (cohort 1), as their performance remained similar to that of the control group (Figure 14D-E). This outcome implies that the observed cognitive improvements in the Barnes maze and enhanced mobility in the open field test were not influenced by changes in anxiety or stress levels, underscoring the specific beneficial effects of 2E treatment on cognitive and locomotor functions in this AD mouse model.

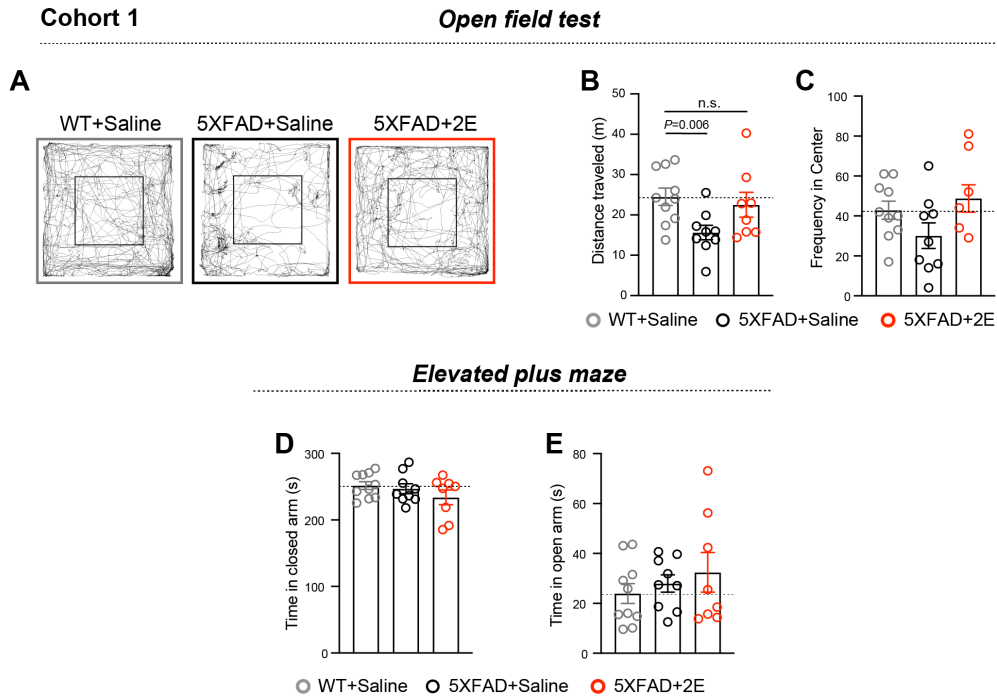


Figure. 14 | 2E improves behavior deficits without changing the anxiety levels in 5XFAD mice. **A.** Illustrative examples of travel paths from WT control mice (left), 5XFAD control mice (middle) and 2E-treated 5XFAD group (right) in the open field (OF) test of 6-month-old mice (cohort 1). **B.** Quantification of distance travelled on the platform in OF. **C.** Quantification of frequency in center in OF. **D.** Quantification of time in the closed arm in elevated plus maze of 6-month-old mice (cohort 1). **E.** Quantification of time in the open arm in elevated plus maze of 6-month-old mice (cohort 1). Each dot represents one mouse.

In the cohort 2 mice, analysis of the open field test and the elevated plus maze revealed no significant differences between the experimental groups, reinforcing the conclusion that there were no changes in anxiety levels (Figure 15A-D). Furthermore, the result showed no distinct gender-related effects on the outcomes, with both male and female mice exhibiting similar behavioral responses across these tests. This consistency across genders and experimental conditions underscores the absence of anxiety alterations in response to the experimental treatments, further supporting the specificity of any observed therapeutic effects to cognitive and motor functions rather than alterations in stress or anxiety levels.

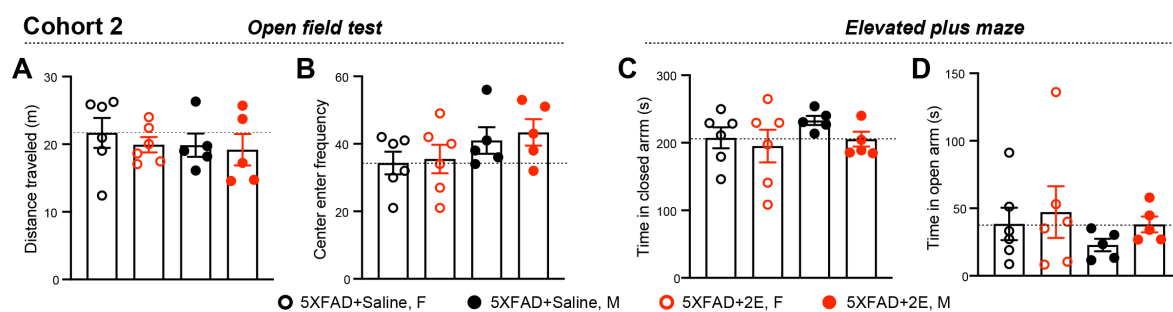


Figure. 15 | 2E has no effects on the anxiety levels of young 5XFAD mice. **A.** Quantification of distance travelled on the platform of 4-month-old mice (cohort 2) in the open field test. **B.** Quantification of frequency in center on the platform of 4-month-old mice (cohort 2) in the open field test. **C.** Quantification of time in the closed arm in elevated plus maze of 4-month-old mice (cohort 2). **D.** Quantification of time in the open arm in elevated plus maze of 4-month-old mice (cohort 2). Each dot represents one mouse.

4.6 Establishment of RNA sequencing with PFA-fixed brain samples

Given the complexity of conducting transcriptomic analyses on mouse brains that have been perfused and fixed with PFA, which typically results in low-quality RNA unsuitable for sequencing, here we developed a novel method to address this challenge. Our method involves the application of proteinase K to digest the proteins and reverse the PFA-induced cross-links in RNA, thereby releasing the RNA (Phan et al., 2021; Thomsen et al., 2016). Subsequently, we employ oligo dT25 magnetic beads to selectively isolate polyA⁺ mRNA from the pool of freed RNA (Picelli et al., 2013), as the steps briefly summarized in Figure 16.

Overview - RNA extraction protocol from PFA-fixed mouse brain



Figure. 16 | Workflow of the main steps of the RNA extraction protocol from PFA-fixed tissue. This figure is part of our published method paper on *Methods Mol Biol*. This figure is part of our published method paper in *Methods Mol Biol*. (Ji et al., 2023:2616:205-212. doi: 10.1007/978-1-0716-2926-0_16.)

To prepare brain tissue samples for RNA sequencing, the targeted brain section is carefully micro-dissected under a microscope using a pipette to gently scratch and isolate the target area, including cortex, hippocampus, and brain stem (Figure 17A). The collected brain tissue is then transferred with the same tip into a tube, where the precipitate can be visually confirmed (Figure 17B).

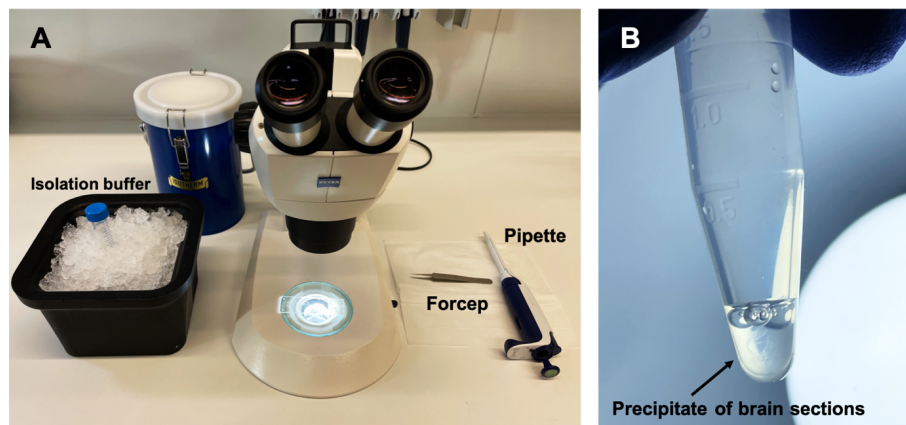


Figure 17. | Isolation of brain tissue for RNA-seq through microdissection. A. The initial preparation of brain section with 200 μ l pipette, and the RNA isolation buffer under a microscope; **B.** Dissected brain sections deposition in the RNA isolation buffer. This figure is part of our published method paper in *Methods Mol Biol.* (Ji et al., 2023:2616:205-212. doi: 10.1007/978-1-0716-2926-0_16.)

To lyse tissue and reverse cross-links, samples are incubated at 56°C for 4 h in a thermal cycler, ensuring to check hourly for sample dissolution. Post-incubation, samples are proceeded for with mRNA purification and elution, where pre-washed dT25 beads are used to mix with samples (Figure 18A), facilitating the reversal of cross-linked RNA. The sample-bead mixture undergoes three washes at RT to ensure thorough cleaning (Figure 18B). Finally, to elute the mRNA, the mixture is heated at 80°C for two minutes and then placed on a magnet at room temperature to separate the beads from the eluted mRNA (Figure 18C).

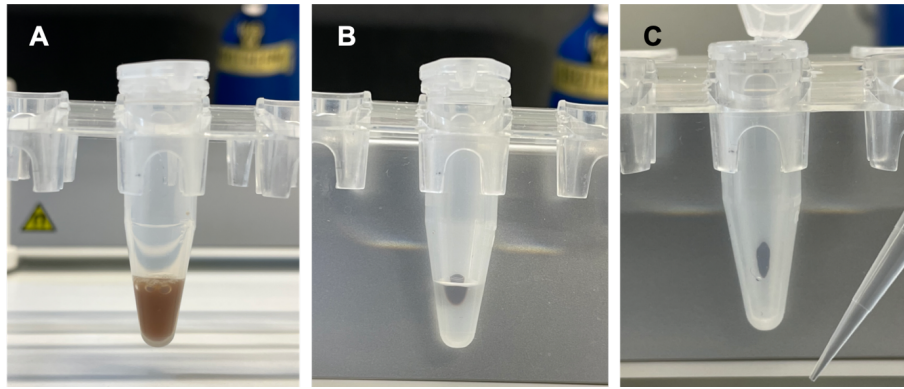


Figure 18. | Purify and elute mRNA using oligo dT25 magnetic beads. **A.** Homogenous sample-bead mixture after fully resuspending; **B.** Bead-sample solution placed on the magnet after incubation period; **C.** Bead-sample pallet in the tube on the magnet after separating the supernatant. This figure is part of our published method paper in *Methods Mol Biol.* (Ji et al., 2023:2616:205-212. doi: 10.1007/978-1-0716-2926-0_16.)

After the quality checks on purified mRNA extracted from brain tissue, we constructed the cDNA library with a modified Smart-seq2 protocol (Ji et al., 2023). To validate the quality and integrity of the cDNA libraries, we verified the peak size of the cDNA fragments, which was found to be around 251 base pairs (bp) (Figure 19). This size fall within the acceptable range of the most sequencing platforms, ensuring the suitability of our libraries for the subsequent sequencing process.

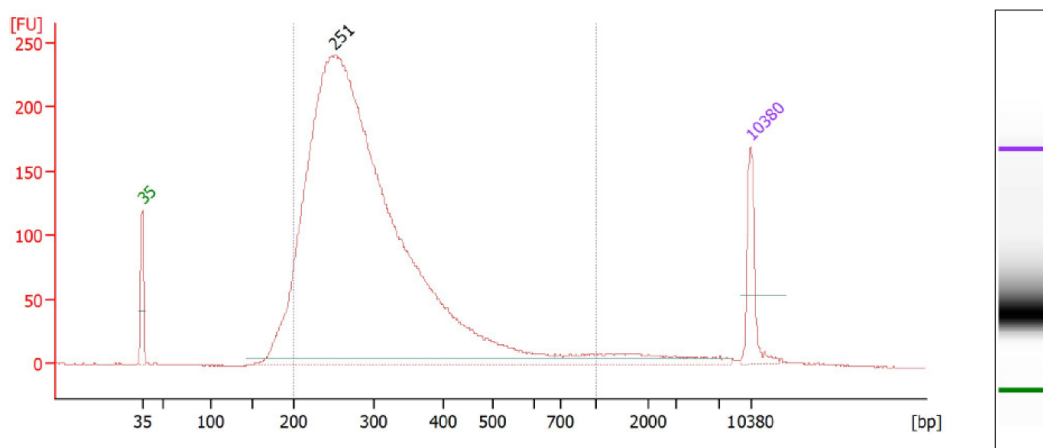


Figure. 19 | Quality check of cDNA libraries before sequencing. The Bioanalyzer data revealed a peaking fragment size of approximately 251 bp for the of the RNA sequencing libraries, with two ladders at 35 bp and 10380 bp as controls. This figure is part of our published method paper in *Methods Mol Biol.* (Ji et al., 2023:2616:205-212. doi: 10.1007/978-1-0716-2926-0_16.)

Prior to conducting differential gene expression analysis and data visualization, we evaluated the quality of our sequencing libraries by examining various sequencing metrics. This assessment included measuring the total number of sequences and the count of RNA species detected, ensuring the percentage of mitochondrial genes did not exceed 0.5%, and confirming that ribosomal genes constituted no more than 10% of the total. Additionally, we evaluated the percentage of ERCC spike-ins (Figure 20). No tissue region effect was detected in above mentioned parameters. These quality checks were applied across multiple brain regions of the mouse to guarantee the reliability and accuracy of our sequencing results.

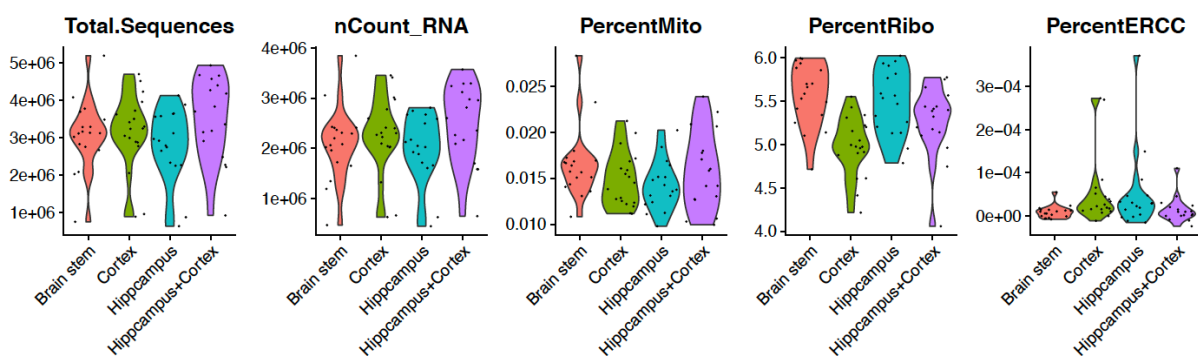


Figure. 20 | Quality assessment of the sequencing data. Violin plots displaying the number of total sequences, number of RNA counts, percentage of mitochondrial and ribosomal genes, and percentage of ERCCs. Samples that did not meet our quality standards were filtered out prior to this analysis. This figure is part of our published method paper in *Methods Mol Biol.* (Ji et al., 2023:2616:205-212. doi: 10.1007/978-1-0716-2926-0_16.)

4.7 2E alters 5XFAD induced gene expression changes

Despite considerable heterogeneity of the mouse AD models, changes in gene expression are consistent across models, providing insights to cell-type specific changes during disease course. To study the impact of the 2E peptide on cellular responses, we isolated RNA from PFA-fixed micro-dissected brain tissues using an optimized protocol and prepared 74 RNA-Seq libraries using a modified SmartSeq2 protocol (Ji et al., 2023) and 3 libraries excluded during quality controls (Figure 21A). Differential gene expression analysis between 5XFAD and WT mice revealed an upregulation of a multitude of genes related to the immune response, inflammation, and microglial and astrocytic activation (Figure 21B), consistent with previous studies in AD mouse models (Habib et al., 2020; Keren-Shaul et al., 2017; K. Srinivasan et al., 2016). We then

compared differentially expressed genes due to 2E treatment in the 5XFAD mice. Multiple genes related to neuronal activity and neurodevelopment such as sodium voltage-gated channel beta subunit 4 (*Scn4b*), proenkephalin (*Penk*), *Rasd2*, and *six3* showed higher expression in saline-treated 5XFAD mice, while 2E treatment was associated with an increase in the expression of many genes including annexin A11 (*Anxa11*), crystallin Mu (*Crym*), and ankyrin repeat and SOCS box containing 18 (*Asb18*) (Figure 21B).

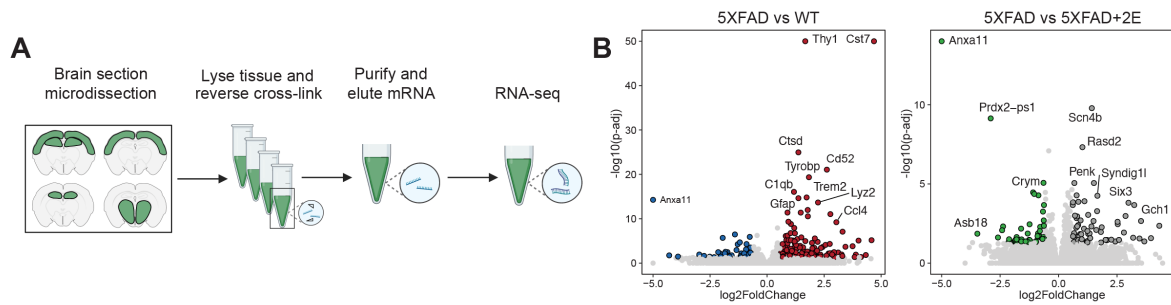


Figure. 21 | RNA-seq experiment summary and differential gene expression analysis. A. Schematics of sample collection for RNA-seq analysis. **B.** Volcano plots showing gene expression differences between 5XFAD and WT (left), and 5XFAD and 5XFAD+2E (right) samples. Highlighted in color are genes with $p\text{-adj} < 0.05$ and $|\log_2 \text{fold-change}| > 0.65$.

We then analyzed global transcriptional similarity of samples using principal component analysis (PCA). First principal component (PC1) separated samples by brain region ($P=4.05E-29$), with most variability originating from differences between brain stem and other regions (Figure 22A). Second principal component (PC2) separated WT samples from 5XFAD samples, and the 2E-treated group showed an increase in the separation (Figure 22A). Consistent with results from DE analysis, among the top PC2 genes were multiple lysosomal genes (*Ctss*, *Ctsb*, *Ctsd*, *Cd68*) and several microglia and astrocytes activation genes (*Trem2*, *Apoe*, *Gfap*, *Serpina3n*). The 2E treatment group had a significantly higher induction of several of the PC2 genes including *Ctsd*, *Trem2*, *Gfap*, and *Cd63*, indicating enhanced microglia and astrocytes activation (Figure 22C). Third principal component (PC3) clustered the 2E-treated 5XFAD and WT samples away from the saline-treated 5XFAD samples, indicating that treatment with 2E prevented 5XFAD-induced transcriptional changes in the genes contributing to PC3 (Figure 22B). Genes with highest loadings to PC3 were mostly associated with neuronal activity and behavior (*Crym*, *Cpne7*, *Scn4b*, *Rasd2*, *Grp*, *Cplx1*, *Pvalb*), in

line with the behavioral rescue of 5XFAD effect noted in the 2E-treated group (Figure 22D).

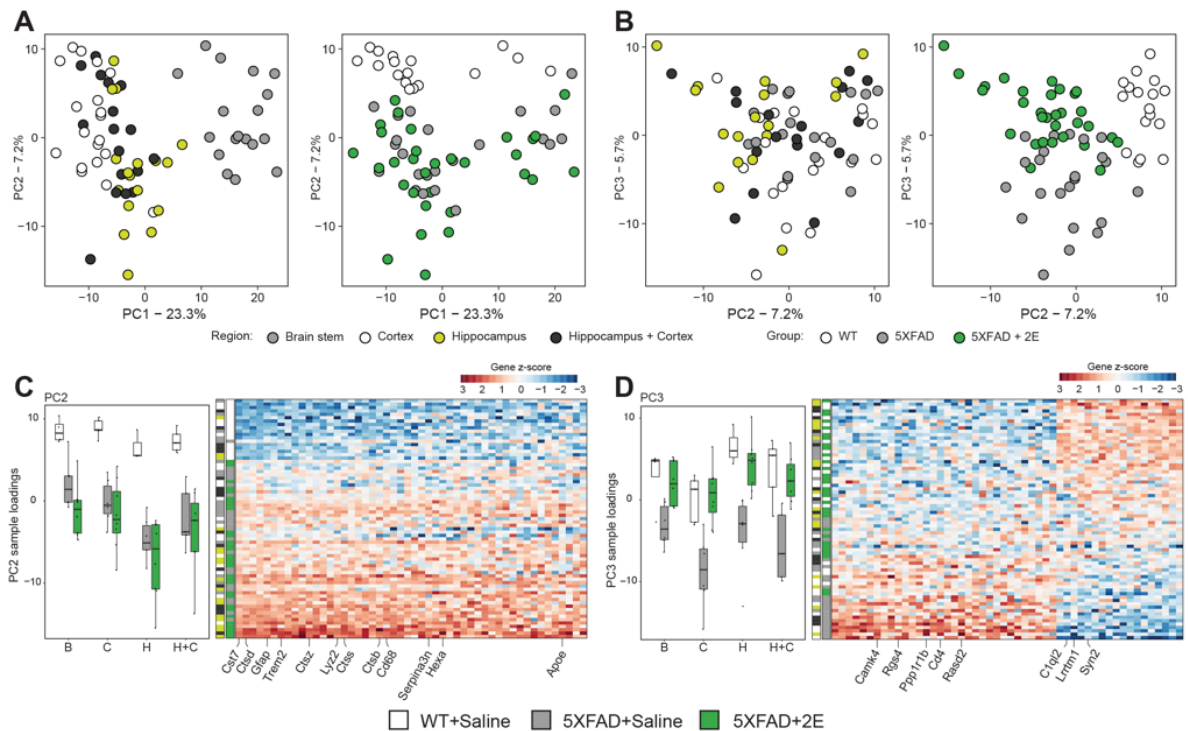


Figure. 22 | 2E alters 5XFAD induced gene expression changes. A/B. PCA plots showing global clustering of individual samples, colored by region (left sub-plots) and by experimental group (right sub-plots). Each dot represents one sample. **C.** Boxplot of PC2 scores for individual mouse. Heatmap shows scaled gene expression of top 50 genes with highest absolute loadings to PC2. Each dot represents one mouse. **D.** Boxplot of PC3 scores for individual mouse. Heatmap shows scaled gene expression of top 50 genes with highest absolute loadings to PC3. Each dot represents one mouse.

To provide functional insight into gene expression signatures, we analyzed enrichment of gene ontology terms, signaling and metabolic pathways using gene set enrichment analysis (GSEA) (Figure 23A-B). When comparing 5XFAD to WT mice, we found a significant upregulation of gene sets related to the immune response and glial activation (Figure 23A). Comparing the saline-treated 5XFAD group with that of the 2E group, revealed a higher enrichment of gene sets related to behavior, neurotransmitter release and transport and membrane polarization in samples from the saline-treated 5XFAD mice, while the 2E-treated mice displayed a higher enrichment of sets associated with myeloid activation, extracellular matrix remodeling, phagocytosis, and lysosomes, suggesting improved processing of amyloid by phagocytic glia and normalization of neuronal activity in 2E-treated 5XFAD mice (Figure 23B). Overall, these findings

highlighted the potential therapeutic effects of the 2E peptide in mitigating the pathological changes associated with AD, including immune response dysregulation, glial activation, amyloid processing, and neuronal dysfunction.

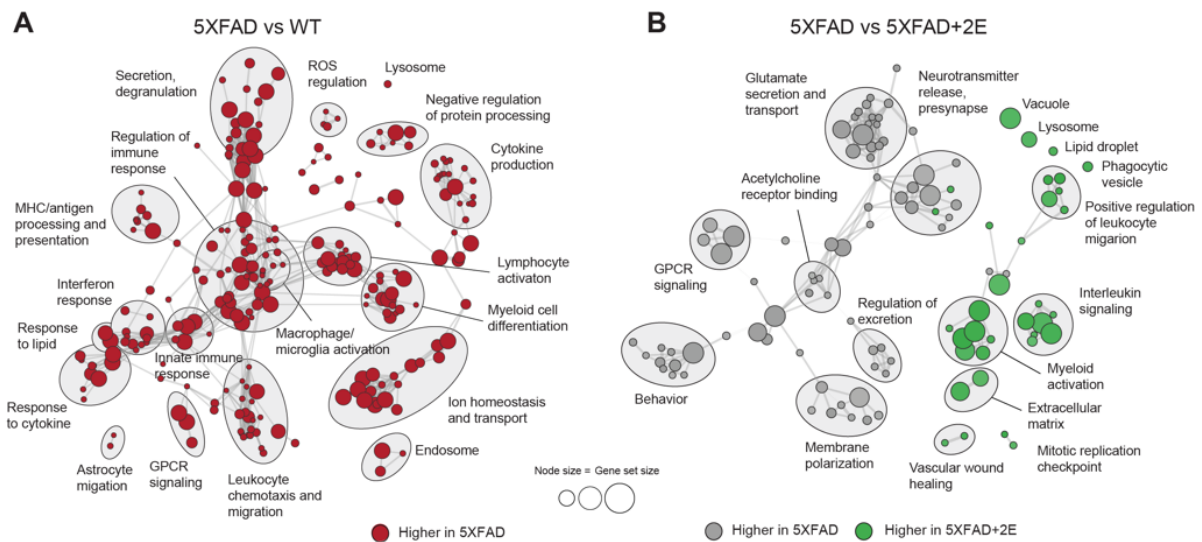


Figure. 23 | Functional analysis of the differentially expressed genes. A. Enrichment map of significantly enriched ($p\text{-adj} < 0.05$) GO terms and pathways in 5XFAD compared to WT samples. Nodes represent gene sets and edges represent degree of overlap between gene sets. **B.** Enrichment map of significantly enriched ($p < 0.05$) GO terms and pathways in 5XFAD compared to 5XFAD+2E samples. Nodes represent gene sets and edges represent degree of overlap between gene sets.

4.8 2E decreases neuronal damage in the brains of 5XFAD mice

Following the beneficial effects in behavioral tests and amyloid pathology in 5XFAD mice after 2E treatment, we investigated its neuroprotective potential. 2E led to a partial reversal of the transcriptional changes induced by 5XFAD that are associated with synaptic transmission, glutamate and neurotransmitter secretion, and behavior (Figure 24A). Notably, several genes implicated in neuronal activity and neurodegeneration, including *Camk4*, *Rgs9*, *Penk*, *Ppp1r1b*, and *Rasd2*, were modified in saline-treated 5XFAD mice (Figure 24B). In contrast, the 2E-treated 5XFAD mice exhibited a pattern of neuronal gene expression that closely resembled that of WT mice, indicating a significant restoration towards normal neuronal function (Figure 24B). This suggests that the 2E treatment not only ameliorates amyloid deposition and improves behavioral outcomes but also exerts a protective effect on neuronal integrity and function in the context of AD.

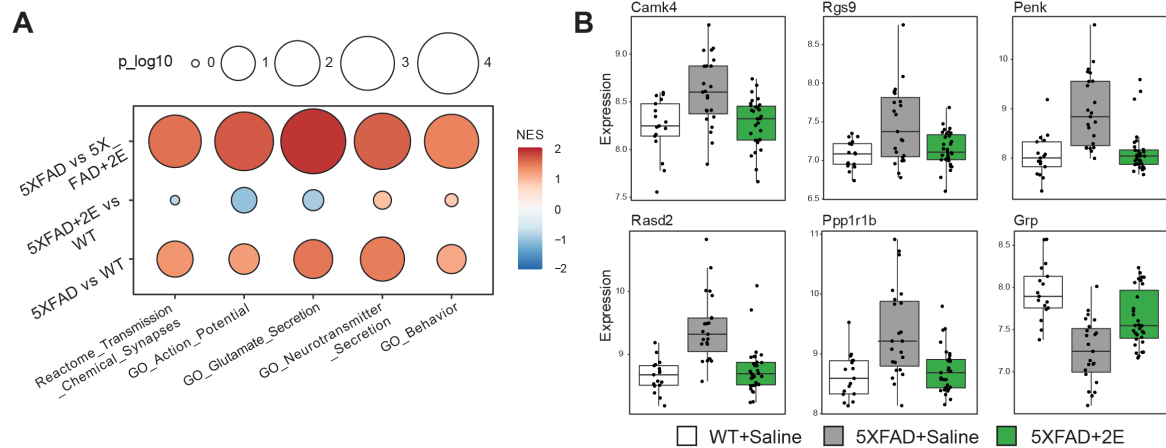


Figure. 24 | 2E mitigates neuronal damage in the brains of 5XFAD mice. A. Enrichment of selected gene sets related Figure 2-8 F. NES = normalized enrichment score. Shades of red mean higher activity in first group in pair-wise contrast. Blue shades represent higher activity in second group in pair-wise contrast. **B.** Boxplots of selected neuron-activity related genes. **C.** Representative confocal microscope images of mouse brain slices stained with a Methoxy-X04 dye (green) and Y188 antibody (red). Scale bar = 50 μ m. **D.** Quantitation of the Y188 intensity coverage (upper) and the coverage per plaque (bottom). **E.** Boxplots of selected neurofilaments related genes. **F.** Standard curve (left) and quantitation (right) of the NFL level in mice serum using Simoa assay. Center shows mean.

To further understand the impact of 2E on neuronal integrity, given the neurotoxic nature of A β plaques, we next examined whether the observed changes in the amyloid plaque profile afforded by 2E treatment influenced neuronal damage. We stained brain sections for the C-terminus of APP using antibody against APP residue Y188 (Jankowsky et al., 2007). As APP accumulates in dystrophic neurites, C-terminal APP positivity is an indication of neuronal damage (Vaillant-Beuchot et al., 2021). We measured C-terminal APP+ neuronal processes within 0-30 μ m spherical shells surrounding A β plaques (Figure 25A). Consistent with its protective effects on plaque deposition, treatment with 2E significantly reduced the total area of dystrophic neurites, as detected by immunostaining with an anti-APP-Y188 antibody (Figure 25B). However, when comparing the extent of dystrophic neurites associated with each plaque, no significant differences were observed between the groups treated with the saline and 2E, suggesting that the remaining plaques in the 2E-treated group retained a similar level of neurotoxicity as those in the saline-treated group (Figure 25C). This indicates that while 2E treatment effectively reduces the overall burden of dystrophic neurites, the intrinsic toxicity of the plaques that do form remains unchanged.

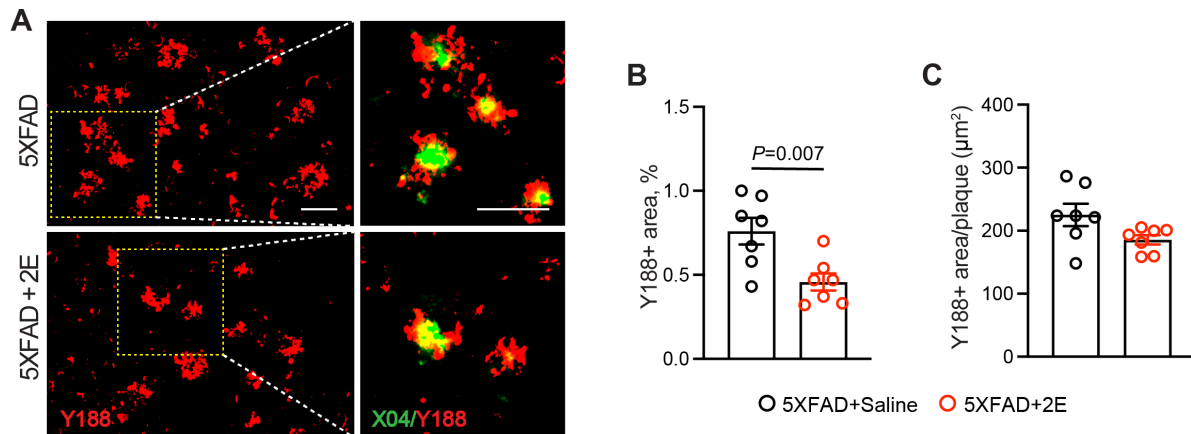


Figure. 25 | 2E mitigates dystrophic neurites in the brains of 5XFAD mice. A. Representative confocal microscope images of mouse brain slices stained with a Methoxy-X04 dye (green) and Y188 antibody (red). Scale bar = 50 μm . **B.** Quantitation of the Y188 intensity coverage. **C.** Quantitation of the Y188 coverage per plaque. Each dot represents one mouse.

NfL, a neuron-specific intermediate filament protein, has gained recognition as a potent blood-based biomarker for neurodegeneration across various neurological conditions, including AD (Preische et al., 2019). In our study, the genes encoding neurofilament proteins, *Nefl* and *Nefm*, exhibited elevated mRNA expression levels in saline-treated 5XFAD mice, but not observed in the 2E-treated group (Figure 26A-B). To quantitatively assess neuro-axonal injury and BBB integrity, we employed the single molecule array (Simoa) technology, a highly sensitive digital immunoassay, to measure serum NfL levels (Abdelhak et al., 2019). Aligning with findings from prior research (Andersson et al., 2020), we detected a significant increase in plasma NfL levels in 6-month-old 5XFAD mice when compared to their WT littermates, indicating heightened neurodegeneration (Figure 26C-D). However, the comparison between 2E- and saline-treated 5XFAD mice revealed no significant differences in plasma NfL levels, only a decreasing trend (Figure 26D). In a related context, clinical studies of the anti-amyloid antibody, donanemab, did not lowered plasma NfL levels, but phosphorylated tau217 and glial fibrillary acidic protein (GFAP) levels (Pontecorvo et al., 2022).

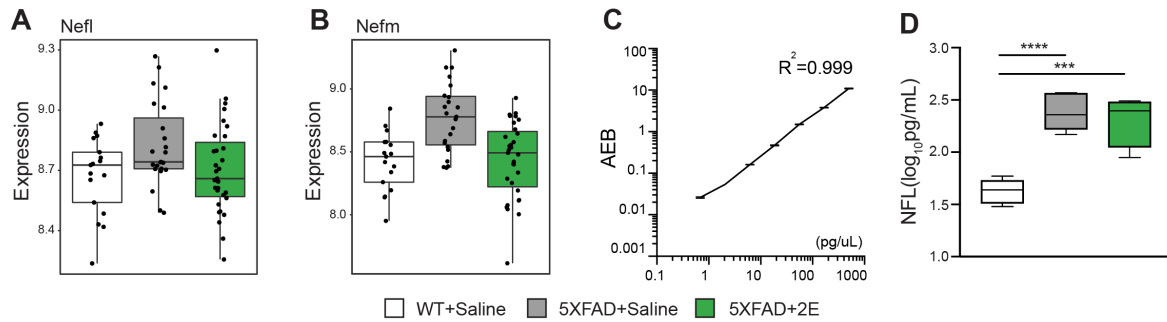


Figure. 26 | 2E decreased the biomarkers of neurodegeneration in 5XFAD mice. A/B. Boxplots of selected neurofilaments related genes. **C.** Standard curve of the NfL level in mice serum using Simoa assay. **D.** Quantification of NfL level in mice serum using Simoa assay.

4.9 2E alters disease-associated glial signatures

To understand the impact of 2E on glial response to A β aggregation, we explored the gene expression of astrocytes and microglia and their spatial relationship with amyloid plaques in the cortex. Staining for GFAP, a marker of astrocyte reactivity, revealed an increase in cortical astrocyte activation following 2E administration (Figure 27A-B). Compared to the control ones, there was a notable enrichment in the number of astrocytes surrounding the plaques (peri-plaque astrocytes) and in their activation level, as evidenced by the GFAP-positive area, when analyzed in conjunction with methoxy-X04-stained amyloid plaques (Figure 27B-C). This suggests that 2E treatment not only affects amyloid plaque deposition but also significantly influences the glial response to these plaques, particularly enhancing astrocyte reactivity in the cortical regions.

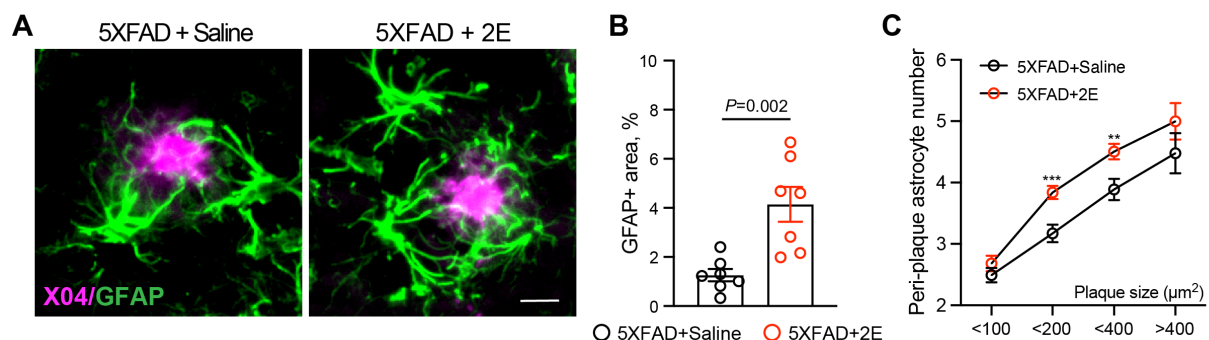


Figure. 27 | 2E activates astrocytes in the brains of 5XFAD mice. A. Representative confocal microscope images of mouse brain slices stained with a Methoxy-X04 dye (magenta) and GFAP antibody (green). Scale bar = 50 μm . **B.** Quantitation of the GFAP+ coverage. **C.** Quantitation of the peri-plaque astrocytes numbers.

Turning to microglia, Iba1 staining was conducted to assess changes in cortical microglia. The analysis showed no significant alterations in the density or morphology of Iba1+ microglia in the cortex following 2E treatment (Figure 28A-B). While there appeared to be a slight increase in the number of microglia surrounding amyloid plaques (peri-plaque microglia), without reaching statistical significance (Figure 28C). This outcome implies that while 2E effectively modulates amyloid pathology, its impact on microglial activation, especially in proximity to plaques, might be limited. It raises the possibility that 2E's influence on the glial response could be mediated by changes in the distribution or forms of A β , particularly oligomeric species, rather than through a direct effect on microglial activation or recruitment.

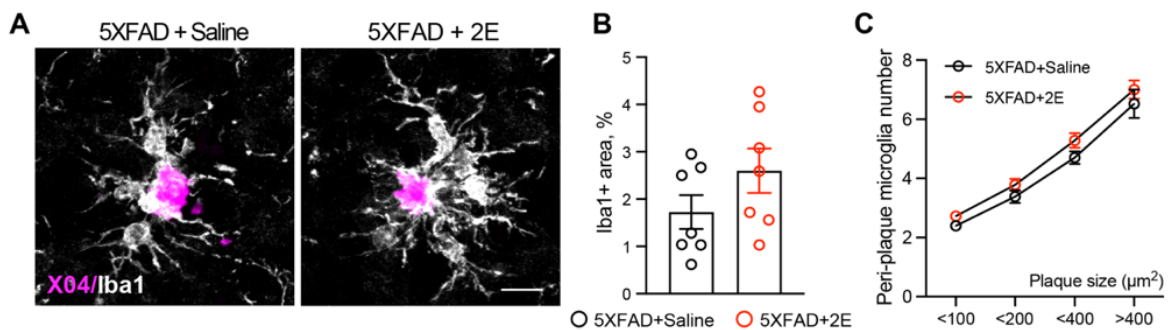


Figure. 28 | 2E partially activates microglia in the brains of 5XFAD mice. A. Representative confocal microscope images of mouse brain slices stained with a Methoxy-X04 dye (magenta) and Iba1 antibody (white). Scale bar = 50μm. **B.** Quantitation of the Iba1+ coverage. **C.** Quantitation of the peri-plaque microglia numbers.

To further corroborate our findings, we performed Western blot analysis using an anti-GFAP antibody to detect activated astrocytes. There was a noticeable increase in total GFAP protein expression after 2E treatment, indicating enhanced astrocyte activation (Figure 29A). Further checking the cellular responses, we analyzed astrocyte and microglia gene expressions using published scRNA-Seq data from models of amyloidosis, focusing on disease-associated astrocytes (DAA) (Habib et al., 2020) and disease-associated microglia (DAM) signatures (Keren-Shaul et al., 2017). The analysis showed that 2E-treated 5XFAD mice exhibited a significantly stronger DAA signature compared to the saline-treated 5XFAD mice, indicating an increased astrocytic response (Figure 29B). Conversely, the expression levels of the DAM gene set were comparable between the two 5XFAD groups, indicating no significant impact

on microglial activation (Figure 29B). This was further supported by the increased levels of the reactive astrocyte markers *Gfap* and *Serpina3n* in 2E-treated 5XFAD mice, in contrast to the saline-treated ones (Figure 29C). These findings compellingly suggest that 2E preferentially targets astrocytic rather than microglial activation in the context of AD pathology.

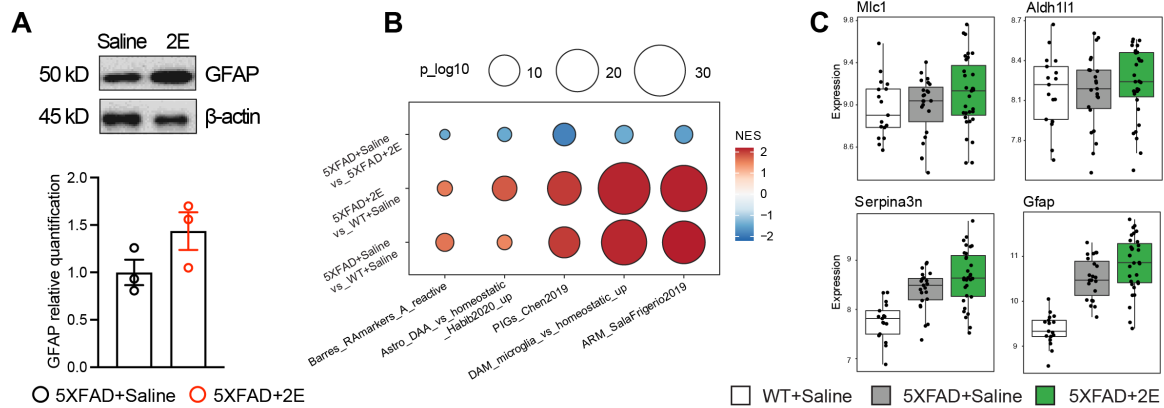


Figure. 29 | 2E preferentially activates astrocytes rather than microglia. A. Representative western plot bands (upper) and quantification (bottom) of GFAP protein expression in the brains of 6-month-old 5XFAD mice. **B.** Bubble plot showing enrichment of DAA and DAM gene signatures among differentially expressed genes, as analyzed by GSEA. NES = normalized enrichment score. **C.** Expression of marker genes for reactive astrocytes, astrocytes, and microglia. Each dot represents one mouse.

To determine whether the observations were attributable to variations in total numbers of microglia or astrocytes, or due to increased transcriptional activation, transcriptome deconvolution using stable marker gene sets was performed. This indicated an elevated microglial presence in 5XFAD mouse samples, which remained unaffected by 2E treatment. The astrocytic stable marker gene set, represented by established astrocytic markers, was consistent across all groups (Figure 30A). Further examination using the cell proliferation marker *Ki67* demonstrated that an enhanced microglial proliferation seen in 5XFAD mice was not affected by the 2E treatment (Figure 30B-C). Collectively, these findings suggest that 2E predominantly activates peri-plaque astrocytes, a contrast to amyloid- β -targeting antibodies known to stimulate microglia via their Fc regions (Bard et al., 2000; Bohrmann et al., 2012; Koenigsnecht-Talboo et al., 2008; Sevigny et al., 2016b).

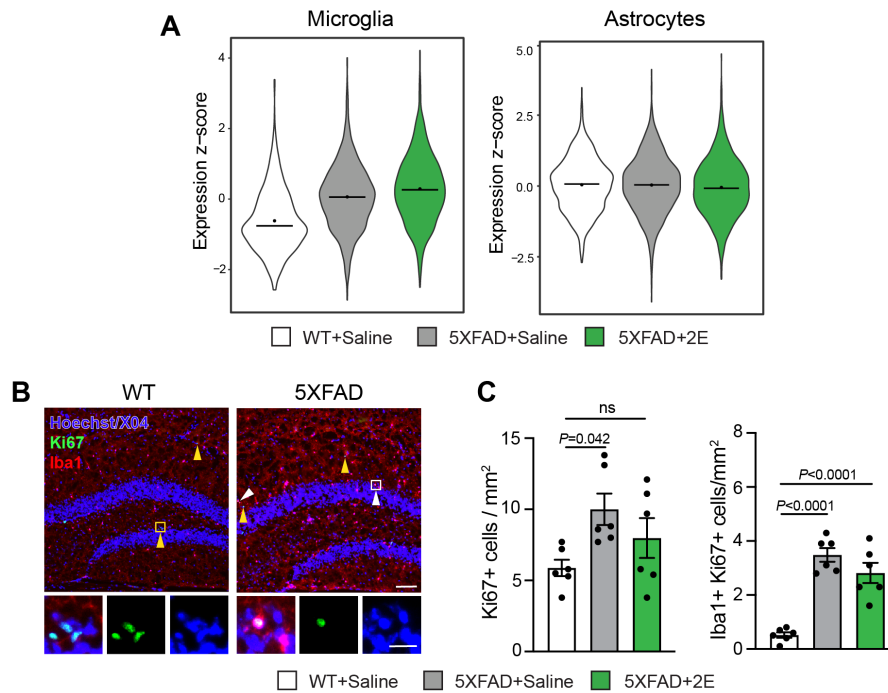


Figure. 30 | 2E has no effects on glial cell numbers in the brains of 5XFAD mice. A. Transcriptome deconvolution with microglia and astrocytes marker gene sets. **B.** Representative confocal microscope images of mouse brain slices stained with Hoechst/Methoxy-X04 dye, Ki67 and Iba1 antibody. Scale bar = 50 μ m. **C.** Quantification of Ki67+ cell numbers and Iba1+Ki67+ cell numbers. Each dot represents one mouse.

Furthermore, samples from 2E-treated mice showed an increased enrichment of several GO terms and pathways related to lysosomal and phagocytic activity (Figure 31A). This observation indicates that 2E may enhance the phagocytic uptake of A β by microglia, suggesting a mechanism by which 2E contributes to the clearance of amyloid plaques. To better assess the phagocytotic activity of microglia, we conducted immunofluorescence analysis using CD68, a marker for phagocytosis. Results showed that the area positive for CD68 was significantly increased in the 2E-treated 5XFAD mice compared to the control ones (Figure 31B-C), signifying enhanced phagocytic activity. Taken together, these findings demonstrate that 2E not only increases the number of plaque-associated astrocytes but also stimulates microglial activation, contributing to a potentially more effective amyloid clearance mechanism.

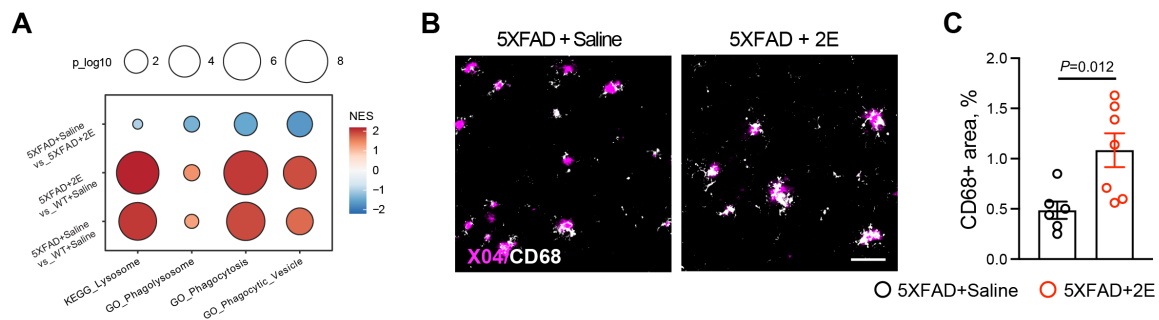


Figure. 31 | 2E increases phagocytic activity of microglia in the brains of 5XFAD mice. A. Enrichment of several GO terms and pathways related to lysosomal and phagocytic activity. **B.** Representative confocal microscope images of mouse brain slices stained with a Methoxy-X04 dye (magenta), CD68 antibody (white). Scale bar = 50 μ m. **C.** Quantitation of the CD68+ coverage.

In summary, the effectiveness of two treatment paradigms of the macrocyclic peptide 2E in mitigating amyloid pathology was examined across both genders of 5XFAD and APPNL-G-F transgenic mice models. The findings demonstrated a notable decrease in amyloid accumulation in the cortex, a lower A β 42/40 ratio in both plasma and cerebrospinal fluid (CSF), a redistribution of amyloid from the brain parenchyma to cerebral blood vessels, reduced neuronal damage, and increased activation of astrocytes following 2E treatment. Additionally, 5XFAD mice treated with 2E showed enhanced memory and motor functions, with no change in anxiety or stress levels. A novel method for performing high-resolution RNA sequencing on paraformaldehyde-fixed tissue sections was developed. RNA-seq data underscored the capacity of 2E to promote astrocyte activation and reverse changes in gene expression related to Alzheimer's disease (AD) in neurons. Crucially, the detection of 2E in the brain post-intra-peritoneal injection underscores its effective biodistribution. Consequently, the macrocyclic peptide 2E holds significant promise as an effective therapeutic, either alone or in conjunction with other anti-amyloid measures, in addressing amyloid-beta-driven AD pathology.

5. Discussion

5.1 Peptide-based inhibitors for A β aggregation

Both animal and human studies highlight the pivotal role of A β misfolding (primarily A β 40 and A β 42) and the resulting processes like oxidative stress and inflammation in AD progression (Cheng et al., 2020; Cummings et al., 2019; Y.-H. Liu et al., 2012). A recent analysis reveals a staggering 99.6% failure rate of AD drug development over the past century since AD's identification (Berchtold & Cotman, 1998). The ineffectiveness of these drugs in enhancing cognitive functions in AD patients is largely due to misguided targeting, adverse drug reactions, and neuroinflammatory responses (Aillaud & Funke, 2023; Y.-H. Liu et al., 2012). Aducanumab, which received expedited FDA approval for AD treatment and targets both soluble and insoluble A β aggregates, is still a subject of debate and requires further evaluation in patients (Karlavish & Grill, 2021). These setbacks underscore the urgency for novel and effective AD treatments and therapies, focusing on precise targeting, reduced immunogenicity, and better biocompatibility.

In the previous ten years, peptide-based medicines have gained significant attention and prominence in the pharmaceutical industry. An example of this is enfuvirtide, a 36 amino acid biomimetic peptide used in HIV-1 treatment (de Castro et al., 2016), and ziconotide, employed for severe chronic pain management (Bourinet & Zamponi, 2017; Deer et al., 2019), and semaglutide used for T2D treatment (Frías et al., 2021). These peptide drugs have found applications in diverse therapeutic fields, including urology, respiratory, pain management, oncology, metabolism, cardiovascular health, and antimicrobial treatments (Fisher et al., 2019; Iyengar et al., 2017; Sloan, 2019; Torres et al., 2019). Currently, over 60 peptide drugs have received FDA approval for disease treatment, with more than 400 in clinical development stages (A. C.-L. Lee et al., 2019). Peptides offer advantages over small molecules and antibodies due to their ease of modification and ability to penetrate tissues and cells, along with high biocompatibility and low immunogenicity, making them promise for AD therapy.

Typically, peptides consist of amino acid chains weighing between 500-5000 Da (Heninot et al., 2018), and their structure and function depend on their amino acid sequences. Their chirality, a critical aspect of peptides, plays a significant role in their

applications (Sidorova et al., 2021). Some studies have concentrated on the chirality of amino acids or peptide-based materials in relation to A β aggregation, as chiral materials can recognize biomolecules and engage in vital physiological processes (Pisarewicz et al., 2005). Other research approaches involve screening specific peptides against target molecules like A β through phase display, aiming to identify peptides with a high affinity to A β , which could be used to alter A β conformation and aggregation. Additionally, strategies have been developed to design functional peptides that inhibit A β aggregation, drawing on knowledge of amyloid fibrosis core sequences and A β structure.

To counteract A β aggregation, most peptide inhibitors have been developed using four key approaches. The first three involve designing inhibitors based on molecular recognition, focusing on 1) amyloid self-assembly, 2) cross-amyloid interactions, and 3) interactions with chaperones or other non-amyloidogenic proteins. The fourth method employs combinatorial libraries and peptide chemistry techniques for inhibitor discovery and optimization. This discussion will focus on the first two methods.

The most widely researched approach involves inhibitors that originate from segments of amyloid self-recognition. These inhibitors, after modifications like N-methylation of amide bonds or cyclization for conformational restriction, incorporate or derive from a “self-recognition” or “amyloid core” region (Funke & Willbold, 2012; Gordon et al., 2001; Goyal et al., 2017; Kapurniotu et al., 2003). A primary example of this strategy is the development of amyloid inhibitors for A β 40(42) derived from its self-recognition segment, A β (16-20).

The second strategy involves designing inhibitors from amyloidogenic polypeptides that cross-interact with the target polypeptide. The interaction partner, either in full-length or as “hot segments,” is utilized. The interaction between islet amyloid polypeptide (IAPP) and A β is a notable instance, where this cross-interaction was harnessed to create cross-amyloid inhibitors (O’Nuallain et al., 2004). Building on IAPP’s cross-amyloid inhibitory function, the macrocyclic 17-residue peptide 2E was engineered to mimic IAPP’s interaction surface with A β (Spanopoulou et al., 2018). Remarkably, 2E demonstrated potent inhibition of A β amyloid self-assembly *in vitro*, showing high proteolytic stability in human plasma and the ability to cross the BBB in an *in vitro* model.

In my thesis, the effectiveness of 2E was evaluated in 5XFAD mice, where two separate experiments showed that 2E treatment significantly reduced the formation of plaques, particularly the smaller ones (Figure 13), paralleling IAPP's *in vivo* effects in 5XFAD mice (Zhu et al., 2015). Moreover, 2E treatment led to a reduction in soluble A β 42 and an increase in A β 40, namely a lower A β 42 to A β 40 ratio, in two AD mouse models, namely 5XFAD and APPNL-G-F mouse models (Figure 14-15). These findings confirmed that less plaque formation after 2E treatment since elevate A β 42/A β 40 ratio could promote plaque formation (Zhang et al., 2023). Furthermore, 2E contributed to the relocation of amyloid deposits from brain parenchyma to blood vessels (Figure 16). Notably, 2E's presence in the brain 4 hours after i.p. injection was confirmed using a monoclonal anti-2E antibody, corroborating its distribution (Figure 17-18) and supporting earlier *in vitro* findings of its stability and ability to penetrate the BBB (Spanopoulou et al., 2018). Behavioral tests revealed that prolonged 2E administration enhanced spatial learning and memory capabilities in 5XFAD mice, without impacting their anxiety levels (Figure 20-21). Collectively, these findings indicate that the 2E, a peptide-based inhibitor, significantly reduces A β accumulation in AD mouse models, underlining its potential as an effective agent for protecting against AD brain pathology.

5.2 Responses of microglia

In AD mouse models, experiments have shown that microglia are responsible for the increased myeloid cell numbers seen in brains with plaque pathology, rather than infiltrating macrophages playing a significant role (Y. Wang et al., 2016). Over the past years, human genetic research, particularly genome-wide association studies (GWAS) via single-nucleotide polymorphisms (SNPs), has made significant progress in identifying genetic risk factors linked to AD (Bateman et al., 2012; Fleisher et al., 2012; Villemagne et al., 2013). A considerable portion of the genetic predisposition to sporadic AD is attributed to variations in the APOE gene, which has three common alleles coding for different forms of APOE: apoE2, apoE3, and apoE4 (Holtzman et al., 2012). ApoE, a major component of lipoproteins including brain-located lipoproteins, is involved in the transport of lipids and cholesterol. It is found in A β plaques and influences both the clearance and accumulation of the A β peptide in the brain (Bien-Ly et al., 2012; Holtzman et al., 2012; Namba et al., 1991; Wisniewski & Frangione, 1992). No-

tably, apoE4 is linked to reduced A β clearance and increased plaque deposition compared to apoE3 (Castellano et al., 2011; Fleisher et al., 2013), although the exact mechanisms of how apoE4 elevates AD risk are not fully understood. One of the critical roles of microglia, facilitated by TREM2, is the engulfment and clearance of cellular debris. This includes the phagocytosis of apoptotic neurons, bacteria, LDL, other lipoproteins, and A β aggregates (Atagi et al., 2015; Yeh et al., 2016). TREM2's efficiency in mediating the uptake of A β , particularly when complexed with lipoproteins like LDL, apoE, and CLU/apoJ, is crucial in Alzheimer's pathology (Yeh et al., 2016). TREM2 deficiencies have shown reduced uptake of A β -lipoprotein complexes, both in vitro and in vivo, indicating a crucial role in A β clearance (Y. Wang et al., 2016; Yeh et al., 2016). The TREM2-apoE axis likely plays a significant role in the microglial clearance of various extracellular and cellular debris, which is vital for minimizing collateral neuronal damage in neurodegenerative diseases. In my thesis work, amyloid plaque load was reduced after 2E treatment, with less plaque formation and relocation of amyloid deposits in different AD mouse models.

Under normal conditions, microglia are highly vigilant cells in the brain, continuously extending and retracting their processes to monitor the environment (Nimmerjahn et al., 2005). However, when β -amyloid accumulates in brain, a hallmark of AD, the activity of these microglial processes diminishes. They tend to form enduring associations with amyloid plaques, and proteins like TREM2, DAP12, and phosphotyrosine accumulate in elevated levels in these areas (Condello et al., 2015; Yuan et al., 2016). Microglia deficient in TREM2 are impaired: they neither cluster around nor proliferate near the plaques, lack characteristic morphological alterations typically seen upon activation, and demonstrate increased cell death (Jay et al., 2015; Mazaheri et al., 2017). Furthermore, TREM2 absence leads to a notable reduction in the microglial gene expression changes triggered by amyloid, emphasizing the crucial role of TREM2 in microglial reactions to amyloid presence (Keren-Shaul et al., 2017; Y. Wang et al., 2015). Recent studies suggest that microglia encase amyloid deposits, compacting the fibrils into denser, less potentially harmful forms, thus inhibiting additional A β accumulation on existing plaques and reducing harm to adjacent neuronal structures (Condello et al., 2015). The integrated outcomes of TREM2 research illuminate the diverse mechanisms through which microglia could impede the accumulation of toxic A β species and the progression of AD. These include the uptake and clearance of soluble A β

species, the phagocytosis of insoluble A β fibrils, the initiation of activation and directed movement towards plaques, and the encapsulation and compression of amyloid plaques.

To study the diverse functional states of microglia, which can change throughout the progression of AD or might coexist at certain disease stage, is crucial for understanding their contribution to neurodegeneration. Recent single-cell RNA-sequencing studies on microglia in AD, have indicated marked changes in gene expression (Keren-Shaul et al., 2017; Orre et al., 2014; K. Srinivasan et al., 2016). These studies highlight the development of a disease-associated microglial (DAM) state characterized by a notable reduction in the expression of "homeostatic" genes like *Cx3cr1*, *P2ry12*, and *Tmem119* and an increase in "neurodegeneration" genes such as *Apoe*, *Axl*, *Csf1*, *Clec7a*, *Cst7*, *Igf1*, *Itgax/CD11c*, *Lilrb4*, *Lpl*, and many major histocompatibility complex class II (MHC-II) genes. When checking activated microglia with single-cell RNA-sequencing, there are slight increases in *Trem2* and *Tyrobp* mRNA expression (Kamphuis et al., 2016; Keren-Shaul et al., 2017; Yin et al., 2017). Significantly, as amyloidosis progresses, the prevalence of DAM cells increases. These DAM cells, located near amyloid plaques, are known to exhibit A β uptake. Computational analysis of DAM genes reveals key insights into vital pathways such as lysosomal activity, phagocytosis, lipid metabolism, and immune response, thus enhancing our understanding of microglia's function in the progression of AD.

In my thesis work, RNA-sequencing showed that the 5XFAD mice exhibited increased expression of numerous genes related to immune responses, inflammation, and the activation of microglia and astrocytes. This aligns with prior RNA-seq research on AD mouse models (Keren-Shaul et al., 2017; K. Srinivasan et al., 2016). A principal component analysis highlighted that the key genes differentiating WT and 5XFAD mice included various lysosomal genes (*Ctss*, *Ctsb*, *Ctsd*, *Cd68*) and genes indicative of microglial and astrocytic activation (*Trem2*, *Apoe*, *Gfap*, *Serpina3n*) (Figure 28A, C). These findings were further supported by our functional analysis (Figure. 29A). Notably, gene alterations following treatment with the 2E peptide predominantly correlated with neuronal activity and behavior (*Crym*, *Cpne7*, *Scn4b*, *Rasd2*, *Grp*, *Cplx1*, *Pvalb*), consistent with the behavioral improvements observed in the 2E-treated 5XFAD mice (Figure 28B, D). Additionally, 2E-treated mice showed enhanced enrichment of gene sets associated with myeloid activation, extracellular matrix remodeling, phagocytosis,

and lysosomal function, suggesting more efficient amyloid processing by phagocytic glia and a normalization of neuronal activity (Figure 29B). For further validation, we observed an increase in microglial activation following 2E treatment, as indicated by Iba1 staining, similar to the trends seen with peri-plaque microglia numbers (Figure 34), while not altering the increased microglial proliferation found in 5XFAD mice (Figure 36). The phagocytic activity of microglia was also heightened post 2E treatment (Figure 37).

5.3 Responses of astrocytes

The role of astrocytes in AD has become a focal point in recent research due to their involvement in the disease's pathophysiological mechanisms (Arranz & De Strooper, 2019; Garwood et al., 2017). Contemporary studies have highlighted astrocytes' roles in neuroinflammation and oxidative stress related to AD (González-Reyes et al., 2017), the complex nature of astrocyte responses in the disease's pathology (Chun & Lee, 2018), their interactions with amyloid (Frost & Li, 2017), and the crucial interactions between astrocytes and neurons in AD (Ibrahim et al., 2020; Nanclares et al., 2021). Various astrocytic functions, such as calcium signaling, glutamate clearance, potassium regulation in the extracellular environment, and energy metabolism, are disrupted in AD (Acosta et al., 2017). Astrocytes in AD also display a diverse range of phenotypic changes, underscoring their cellular heterogeneity in the disease (Monterey et al., 2021). Studies using AD mouse models have revealed that astrocytes, drawn to chemokines like monocyte chemoattractant protein-1 (MCP-1) in A β plaques, migrate to these plaques, absorb, and break down amyloid peptides (Pihlaja et al., 2008; Wyss-Coray et al., 2003). Alongside microglia, astrocytes significantly contribute to the enhanced neuroinflammatory response observed in AD (Singh, 2022). This growing body of evidence highlights the crucial role of astrocytes in AD, underscoring the importance of further exploring AD pathogenesis that involves glial cells. Such insights may lead to the discovery of astrocyte-specific biomarkers for AD (Carter et al., 2019) and the creation of new AD treatments that target astrocytic mechanisms and functions (Fakhoury, 2018; Uddin & Lim, 2022). The therapeutic potential of astrocytes in AD, particularly due to their roles in cellular aging, neuroinflammation, neurotrophic factor release, and A β clearance, has been extensively studied (Pekny & Nilsson, 2005; Valenza et al., 2021).

We found that more peri-plaque astrocytes were found in the 2E group, which indicated the activation of astrocytes (Figure 34). There was a clear trend towards elevated total GFAP protein expression in the brains post-2E treatment (Figure 35A). We then investigated the expression of gene signatures of astrocytes and microglia from published scRNA-Seq studies of amyloid models, encompassing disease-associated astrocytes (DAA) and disease-associated microglia (DAM). The 2E-treated 5XFAD mice demonstrated a more pronounced enrichment of the DAA signature than their saline-treated counterparts, while the DAM gene set expression showed similar enrichment scores for 2E-treated and saline-treated groups (Figure 25B). Concordantly, elevated expression of reactive astrocyte markers *Gfap* and *Serpina3n* was observed in 2E-treated mice relative to the saline-treated 5XFAD group (Figure 25C).

The mechanisms through which the 2E peptide influences astrocytes in AD are not fully elucidated, but our study might suggest that activated astrocytes could interrupt amyloid peptide aggregation and clearance. Astrocytes can directly break down A β 42, the form of A β most prone to aggregation and plaque formation (Wyss-Coray et al., 2003). Moreover, astrocytes secrete ApoE, which plays a critical role in lipid metabolism and also in the degradation of A β . Future experiments will have to address the mechanistic possibility that 2E treatment promotes ApoE secretion from astrocytes. Through the secretion of ApoE, astrocytes enhance the breakdown of A β (Castellano et al., 2011). In addition, astrocytes help in transporting A β from the brain to the bloodstream, primarily through the glymphatic system and perivascular drainage pathways (Iliff et al., 2012; Tarasoff-Conway et al., 2015). These pathways facilitate the clearance of waste from the central nervous system (CNS), including A β . The suppression of astrocyte activation has been associated with accelerated plaque development in AD mouse models, suggesting that active astrocytes play a protective role in the brain (Kraft et al., 2013). When astrocyte activation is reduced, the efficiency of A β clearance is likely impaired, leading to faster plaque accumulation, a hallmark of AD pathology linked to neurodegeneration and cognitive decline. In conclusion, our research underscores the pivotal role of glial cells activation in AD progression. The changes observed in the gene expression and functionality of astrocytes, particularly in response to treatments like the 2E peptide, could be crucial in mitigating AD progression. These findings open avenues for potential therapeutic strategies targeting astrocyte

activation and their A β clearance capabilities, offering hope for slowing down or preventing the progression of AD.

5.4 RNA-seq with PFA-fixed tissue

RNA-seq with PFA-fixed tissue presents unique challenges that hinder the direct use of high-throughput sequencing technologies. PFA fixation, a conventional method for preserving tissue morphology for microscopy, involves cross-linking proteins and nucleic acids (Hoffman et al., 2015; M. Srinivasan et al., 2002). While this process stabilizes tissue structure, it also conceals RNA, complicating its extraction and subsequent sequencing. The cross-linking renders RNA less accessible for reverse transcription, an essential step in RNA-seq workflows, and can fragment RNA and introduce modifications that interfere with cDNA synthesis and amplification.

Recent studies have successfully integrated scRNA-seq with PFA-fixed cells, overcoming the common issue of RNA degradation in archived or hard-to-preserve samples at the single-cell level (Phan et al., 2021; Thomsen et al., 2016). These methods have exposed significant heterogeneity in human radial glial cells and tumor cells, identifying various subpopulations through distinct gene expression profiles. However, these approaches have limitations with more degraded samples, such as PFA-fixed and sectioned tissues on coverslips.

To address this, we have developed a novel method that applies proteinase K to digest proteins and reverse the PFA-induced cross-links in RNA, thereby freeing the RNA. We then use oligo dT25 magnetic beads to selectively isolate polyA⁺ mRNA from the liberated RNA pool. This method avoids the potential RNA damage from laser capturing target regions, which can cause high temperatures (Ong et al., 2020), by microdissecting tissue visually under a microscope. Remarkably, we successfully isolated target tissues, including the cortex, hippocampus, and brain stem, as shown in our results (Figure 23A), and visually confirmed the precipitate in a tube (Figure 23B). Employing Smart-seq2 allowed us to detect picogram levels of mRNA from the samples, making them qualified for RNA-seq (Picelli et al., 2013). Quality checks of RNA-sequencing data showed no effect of tissue region (Figure 26), indicating the establishment of a sensitive and novel method. Current projects are expanding this method to various tissues and cells, such as brain slides, liver, heart, certain cell layers of the

aorta, and cell cultures, highlighting its potential to enhance research on fixed human tissue slides in the future.

5.5 Preclinical randomized controlled trial

In the past few decades, enhanced understanding the pathophysiological mechanisms of ischemic stroke and neurodegeneration has led to numerous experimental studies. Despite many compounds showing promise in neuroprotection, a comprehensive review indicated that none of the more than 49 agents tested in clinical trials successfully transitioned from lab to clinical use (Kidwell et al., 2001). A similar situation exists in the development and validation of AD drugs. Since 2003, the success rate of AD treatment clinical trials has been around 2%, including aducanumab (Kim et al., 2022). This low success rate is attributed to several common issues in these trials, underscoring the complexity of AD as a disease. It's crucial to understand why AD clinical trials often fail and how to address these failures to pave the way for future clinical trials. Three key reasons contribute to the high failure rate in AD clinical trials, alongside possible solutions. Firstly, recruiting suitable participants is challenging, especially when enrolling elderly dementia patients, as it involves their entire families. The lengthy and complex evaluation period for trial eligibility further complicates patient enrollment. Secondly, many issues stem from the design of Alzheimer's clinical trials, such as inappropriate primary clinical outcome measures, inadequate consideration of potential AD subtypes, and late-stage therapeutic interventions. Lastly, the overemphasis on treatments targeting amyloid protein, yielding only modest success, has been a major issue. At least five other causes of neurodegeneration which includes neuroinflammation, mitochondrial dysfunction, lysosomal dysfunction, insulin resistance, and lipid abnormalities - play roles in AD, often in conjunction with amyloid. Amyloid is only part of the problem, not the entirety of it.

The preclinical randomized multicenter trial (pRCT) was developed to address some of these limitations in preclinical studies (Llovera et al., 2015). This approach, mirroring randomized, controlled clinical trials, bridges the gap between animal research and clinical trials. The study evaluated an anti-CD49d antibody, known for its anti-inflammatory properties, in stroke model models. With a meticulous design for statistical analysis and reporting, this method could improve the preclinical efficacy assessment

before progressing to expensive clinical trials. This study is notable for two major reasons: it involved multiple research centers working together to detail the anatomical differences in stroke models, and it found that the anti-CD49d antibody reduced infarct volume only in the permanent occlusion model, suggesting a stronger inflammatory process in this model (Llovera et al., 2015). While it's uncertain if this approach will improve the translation of preclinical stroke studies, it reduces variability and enhances drug effect characterization. Different animal models provide further information for clinical trial planning, such as selecting patients based on their responsiveness to the tested drug, thereby improving the translational process.

In our study, we tested the 2E peptide in two AD mouse models, using both genders of mice, through i.p. and intracerebroventricular injections, conducted by two groups of researchers blinded to the grouping. We examined amyloid pathology at various time points post-treatment, together with behavioral tests of neurological deficits. While this wasn't a standard pRCT conducted across multiple centers, we managed to achieve relatively comprehensive results on the 2E peptide's effects in different AD mouse models. Further research is required to decipher AD's underlying mechanisms and develop new preclinical strategies and animal models for improved translational support. Techniques like amyloid-PET in preclinical mouse models could offer more accurate amyloid pathology assessments and enable longitudinal studies of brain damage in living animals (Chapleau et al., 2022). This method could validate or enhance histological findings using fewer animals and correlate amyloid pathology with neurological deficits. Such methodologies could also be beneficial in clinical trials, enhancing the translation process. Future pRCT studies should utilize the expertise and technologies of varied research groups and adopt this integrated approach.

5.6 Limitations

This study, while providing valuable insights, has several limitations that necessitate further experimental validation to strengthen the presented notions and conclusions. To evaluate the impact of 2E peptides more comprehensively, additional AD mouse models, such as APPPS1, should be employed (Radde et al., 2006). These models will help in better understanding the broad spectrum of 2E peptides' effects across various genetic backgrounds and stages of the disease. A crucial aspect of future research will be to administer short-term, high-dose 2E peptide treatments to advanced-

stage AD mouse models. This approach is essential to assess the therapeutic potential of 2E peptides in later stages of AD progression, where neurodegenerative changes are more pronounced.

Moreover, the development of more sophisticated and reliable techniques for detecting 2E peptides in the brain is critical. Mass spectrometry, for instance, could provide a more precise measurement of 2E peptide concentrations and distribution, thereby confirming its ability to cross the BBB and its bioavailability within the CNS. In parallel, the use of amyloid-PET imaging represents an unbiased and sensitive method for assessing alterations in amyloid pathology within the brains of AD mouse models (Chapleau et al., 2022). This imaging technique will enable a more accurate visualization and quantification of amyloid deposits, offering a clearer understanding of how 2E peptides influence amyloid pathology. Furthermore, comprehensive pharmacokinetic and toxicity testing of the 2E peptides is imperative before any transition to clinical trials. These tests are crucial to ensure the safety and tolerability of the peptides in biological systems, particularly given the complexity and sensitivity of neurodegenerative diseases like AD.

In pursuit of these goals, a series of mechanistic follow-up experiments are already undergoing. These experiments are designed to delve deeper into the molecular pathways and cellular interactions influenced by 2E peptides, thus shedding light on the underlying mechanisms driving their observed effects. By addressing these aspects, the research will move closer to translating these findings from bench to bedside, offering hope for more effective therapeutic strategies in the battle against AD.

5.7 Potential future directions

The encouraging outcomes from our study with the macrocyclic peptide-based inhibitor 2E in AD mouse models pave the way for several vital research directions. Exploring the possibility of combining 2E with other AD treatments, such as anti-amyloid antibodies or neuroprotective agents, could lead to more potent, multi-faceted therapeutic strategies. This combined approach might address various facets of AD pathology more effectively. Developing biomarkers to predict responses to 2E treatment is another key research avenue. Predictive biomarkers could facilitate personalized

treatment approaches in AD, enabling therapies to be tailored to individual patient profiles. Given that protein aggregation is a common feature in various neurodegenerative diseases, it's worthwhile to explore the potential application of 2E in other conditions, such as PD, Huntington's disease, and ALS. For 2E's clinical application, scaling up its synthesis and optimization is imperative. This involves creating cost-effective production methods, ensuring stringent quality control, and establishing reliable storage and delivery systems. Finally, understanding 2E's economic impact, accessibility, and potential to improve patient quality of life will be significant for its widespread adoption and integration into healthcare policies. By following such research pathways in the future, one can build on the foundational findings of this current study.

6. Summary

In my PhD thesis, I have explored the therapeutic potential of the macrocyclic peptide-based inhibitor, 2E, in the context of AD. The research, combining biochemical and behavioral methodologies, has successfully demonstrated that 2E markedly reduces A β accumulation in the brains of 5XFAD aged 4 and 6 months. This reduction in A β accumulation, a key pathological hallmark of AD, is further complemented by a significant alteration in the A β 42 to A β 40 ratio in both plasma and cerebrospinal fluid (CSF). Notably, 2E administration resulted in a decrease in A β 42 levels while simultaneously increasing A β 40 levels, suggesting a therapeutic modulation of amyloidogenic processes. The findings also revealed a profound shift in amyloid deposition patterns in two AD mouse models upon 2E treatment. Through a novel anti-2E monoclonal antibody, we confirmed the ability of 2E to partition into the brain, a critical factor for its efficacy in AD treatment. Functionally, 2E has shown promising results by alleviating learning and memory deficits in 5XFAD mice, without inducing changes in anxiety levels, thereby indicating its neuroprotective effects. This is further supported by RNA-seq analysis, which validated the AD mouse model and highlighted changes in gene expression related to AD pathology post-2E treatment. The study also delved into the impact of 2E treatment on glial cell dynamics, notably observing an activation of astrocytes.

Overall, the work undertaken in this thesis underscores that 2E, initially identified for its *in vitro* inhibition of A β self-assembly, also exhibits significant anti-amyloid activity *in vivo*, and could thus be a candidate for AD therapy. Its ability to enter the brain, modulate amyloid deposition, and enhance cognitive function positions 2E as an alternative AD treatment strategy, complementing antibody-based approaches, especially in targeting early amyloidogenic events and facilitating astrocytic clearance. Future therapeutic approaches combining 2E with anti-amyloid antibodies could thus pave the way for more effective clinical outcomes, potentially also offering cost benefits and reducing side effects. Our study sets the stage for further research, potentially even clinical trials, to explore the full potential of 2E as a novel treatment for AD.

7. List of publications

1. **Hao Ji**, Beatrice Dalla Volta, Peter Androvic, Anna Spanopoulou, Lu Liu, Omar El Bounkari, Chunfang Zan, Katrin Pérez Anderson, Qian Liu, Yijing Wang, Kathleen Hille, Brigitte Nuscher, Johanna Knoferle, Andrew Flatley, Regina Feederle, Jürgen Bernhagen, Aphrodite Kapurniotu[#], Ozgun Gokce[#]. Designed Macrocyclic Peptide Reduces Amyloid Deposition and Neurological Damage in a Murine Alzheimer's Disease Model. Manuscript under revision.
2. Shreeya Kedia*, **Hao Ji***, Ruoqing Feng, Peter Androvic, Lena Spieth, Lu Liu, Jonas Franz, Hanna Zdiarstek, Katrin Perez Anderson, Cem Kaboglu, Qian Liu, Nicola Mattugini, Fatma Cherif, Danilo Prtvar, Ludovico Cantuti-Castelvetri, Arthur Liesz, Martina Schifferer, Christine Stadelmann, Sabina Tahirovic, Ozgun Gokce, Mikael Simons. T cell mediated microglia activation triggers myelin pathology in a model of amyloidosis. *Nature Neuroscience* (2024). <https://doi.org/10.1038/s41593-024-01682-8>
3. **Hao Ji**, Simon Besson-Girard, Peter Androvic, Buket Bulut, Lu Liu, Yijing Wang, Ozgun Gokce. High-resolution RNA sequencing from PFA-fixed microscopy sections. *Methods Mol Biol.* 2023; 2616: 205-212.
4. Tuğberk Kaya*, Nicola Mattugini*, Lu Liu*, **Hao Ji**, Ludovico Cantuti-Castelvetri, Jianping Wu, Martina Schifferer, Janos Groh, Rudolf Martini, Simon Besson-Girard, Seiji Kaji, Arthur Liesz, Ozgun Gokce[#], Mikael Simons[#]. CD8+ T cells induce interferon-responsive oligodendrocytes and microglia in white matter aging. *Nature Neuroscience*. 2022 Nov; 25(11): 1446-1457.
5. Shima Safaiyan*, Simon Besson-Girard*, Tuğberk Kaya, Ludovico Cantuti-Castelvetri, Lu Liu, **Hao Ji**, Martina Schifferer, Garyfallia Gouna, Fumere Usifo, Nirmal Kanaiyan, Dirk Fitzner, Xianyuan Xiang, Moritz J Rossner, Matthias Brendel, Ozgun Gokce[#], Mikael Simons[#]. White matter aging drives microglia diversity. *Neuron*. 2021 Apr 7;109(7): 1100-1117.
6. Peter Androvic*, Martina Schifferer*, Katrin Perez Anderson, Ludovico Cantuti-Castelvetri, Hanyi Jiang, **Hao Ji**, Lu Liu, Garyfallia Gouna, Stefan A Berghoff, Simon

Besson-Girard, Johanna Knoferle, Mikael Simons, Ozgun Gokce. Spatial Transcriptomics-correlated Electron Microscopy maps transcriptional and ultrastructural responses to brain injury. *Nature Communications*. 2023 Jul 11;14(1):4115.

7. Lu Liu, Simon Besson-Girard, **Hao Ji**, Katrin Gehring, Buket Bulut, Tuğberk Kaya, Fumere Usifo, Mikael Simons, Ozgun Gokce. Dissociation of microdissected mouse brain tissue for artifact free single-cell RNA sequencing. *STAR Protocol*. 2021 Jun 10; 2(2): 100590.

8. Christine Krammer*, Bishan Yang*, Sabrina Reichl, Simon Besson-Girard, **Hao Ji**, Verena Bolini, Corinna Schulte, Heidi Noels, Kai Schlepckow, Georg Jocher, Georg Werner, Michael Willem, Omar El Bounkari, Aphrodite Kapurniotu, Ozgun Gokce, Christian Weber, Sarajo Mohanta, Jürgen Bernhagen. Pathways. Linking aging and atheroprotection in Mif-deficient atherosclerotic mice. *FASEB J*. 2023 Mar; 37(3): e 22752.

9. Vini Tiwari, Bharat Prajapati, Yaw Asare, Alkmini Damkou, **Hao Ji**, Garyfallia Gouna, Katarzyna Leszczyńska, Jakub Mieczkowski, Qing Wang, Riki Kawaguchi, Ze Tristan Shi, Vivek Swarup, Daniel H Geschwind, Marco Prinz, Ozgun Gokce, Mikael Simons. Innate immune training restores pro-reparative myeloid functions for remyelination in the aged central nervous system. *Immunity*. 2024. Accepted.

10. Omar El Bounkari*, Chunfang Zan*, Jonas Wagner, Simon Ebert, Bishan Yang, Elina Bugar, Priscila Bourilhon, Christos Kontos, Marlies Zarwel, Dzmitry Sinitski, Jelena Milic, Yvonne Jansen, Wolfgang E. Kempf, Nadja Sachs, Lars Mägdefessel, **Hao Ji**, Ozgun Gokce, Simona Gerra, Adrian Hoffmann, Markus Brandhofer, Richard Bucala, Remco T.A. Megens, Tobias Harm, Dominik Rath, Meinrad Gawaz, Christian Weber, Aphrodite Kapurniotu, Jürgen Bernhagen. An atypical atherogenic chemokine that promotes advanced atherosclerosis and hepatic lipogenesis. Manuscript in revision.

* shared first authorship

shared correspondence

8. References

- 2020 Alzheimer's disease facts and figures. (2020). *Alzheimer's & Dementia: The Journal of the Alzheimer's Association*. <https://doi.org/10.1002/alz.12068>
- 2023 Alzheimer's disease facts and figures. (2023). *Alzheimer's & Dementia: The Journal of the Alzheimer's Association*, 19(4), 1598–1695. <https://doi.org/10.1002/alz.13016>
- A Armstrong, R. (2019). Risk factors for Alzheimer's disease. *Folia Neuropathologica*, 57(2), 87–105. <https://doi.org/10.5114/fn.2019.85929>
- Abdelhak, A., Hottenrott, T., Morenas-Rodríguez, E., Suárez-Calvet, M., Zettl, U. K., Haass, C., Meuth, S. G., Rauer, S., Otto, M., Tumani, H., & Huss, A. (2019). Glial Activation Markers in CSF and Serum From Patients With Primary Progressive Multiple Sclerosis: Potential of Serum GFAP as Disease Severity Marker? *Frontiers in Neurology*, 10, 280. <https://doi.org/10.3389/fneur.2019.00280>
- Acosta, C., Anderson, H. D., & Anderson, C. M. (2017). Astrocyte dysfunction in Alzheimer disease. *Journal of Neuroscience Research*, 95(12), 2430–2447. <https://doi.org/10.1002/jnr.24075>
- Ahmed, S., Venigalla, H., Mekala, H. M., Dar, S., Hassan, M., & Ayub, S. (2017). Traumatic Brain Injury and Neuropsychiatric Complications. *Indian Journal of Psychological Medicine*, 39(2), 114–121. <https://doi.org/10.4103/0253-7176.203129>
- Aillaud, I., & Funke, S. A. (2023). Tau Aggregation Inhibiting Peptides as Potential Therapeutics for Alzheimer Disease. *Cellular and Molecular Neurobiology*, 43(3), 951–961. <https://doi.org/10.1007/s10571-022-01230-7>
- Alonso, A. C., Grundke-Iqbal, I., & Iqbal, K. (1996). Alzheimer's disease hyperphosphorylated tau sequesters normal tau into tangles of filaments and disassembles microtubules. *Nature Medicine*, 2(7), 783–787. <https://doi.org/10.1038/nm0796-783>
- Alzheimer, A., Stelzmann, R. A., Schnitzlein, H. N., & Murtagh, F. R. (1995). An English translation of Alzheimer's 1907 paper, "Über eine eigenartige Erkrankung der Hirnrinde." *Clinical Anatomy (New York, N.Y.)*, 8(6), 429–431. <https://doi.org/10.1002/ca.980080612>

-
- Andersson, E., Janelidze, S., Lampinen, B., Nilsson, M., Leuzy, A., Stomrud, E., Blennow, K., Zetterberg, H., & Hansson, O. (2020). Blood and cerebrospinal fluid neurofilament light differentially detect neurodegeneration in early Alzheimer's disease. *Neurobiology of Aging*, *95*, 143–153. <https://doi.org/10.1016/j.neurobiolaging.2020.07.018>
- Andreetto, E., Malideli, E., Yan, L.-M., Kracklauer, M., Farbiarz, K., Tatarek-Nossol, M., Rammes, G., Prade, E., Neumüller, T., Caporale, A., Spanopoulou, A., Bakou, M., Reif, B., & Kapurniotu, A. (2015). A Hot-Segment-Based Approach for the Design of Cross-Amyloid Interaction Surface Mimics as Inhibitors of Amyloid Self-Assembly. *Angewandte Chemie (International Ed. in English)*, *54*(44), 13095–13100. <https://doi.org/10.1002/anie.201504973>
- Andreetto, E., Yan, L.-M., Tatarek-Nossol, M., Velkova, A., Frank, R., & Kapurniotu, A. (2010). Identification of hot regions of the Abeta-IAPP interaction interface as high-affinity binding sites in both cross- and self-association. *Angewandte Chemie (International Ed. in English)*, *49*(17), 3081–3085. <https://doi.org/10.1002/anie.200904902>
- Androvic, P., Schifferer, M., Perez Anderson, K., Cantuti-Castelvetri, L., Jiang, H., Ji, H., Liu, L., Gouna, G., Berghoff, S. A., Besson-Girard, S., Knoferle, J., Simons, M., & Gokce, O. (2023). Spatial Transcriptomics-correlated Electron Microscopy maps transcriptional and ultrastructural responses to brain injury. *Nature Communications*, *14*(1), 4115. <https://doi.org/10.1038/s41467-023-39447-9>
- Antolini, L., DiFrancesco, J. C., Zedde, M., Basso, G., Arighi, A., Shima, A., Cagnin, A., Caulo, M., Carare, R. O., Charidimou, A., Cirillo, M., Di Lazzaro, V., Ferrarese, C., Giossi, A., Inzitari, D., Marcon, M., Marconi, R., Ihara, M., Nitrini, R., ... Piazza, F. (2021). Spontaneous ARIA-like Events in Cerebral Amyloid Angiopathy-Related Inflammation: A Multicenter Prospective Longitudinal Cohort Study. *Neurology*, *97*(18), e1809–e1822. <https://doi.org/10.1212/WNL.0000000000012778>
- Armiento, V., Spanopoulou, A., & Kapurniotu, A. (2020). Peptide-Based Molecular Strategies To Interfere with Protein Misfolding, Aggregation, and Cell Degeneration. *Angewandte Chemie (International Ed. in English)*, *59*(9), 3372–3384. <https://doi.org/10.1002/anie.201906908>

-
- Arranz, A. M., & De Strooper, B. (2019). The role of astroglia in Alzheimer's disease: Pathophysiology and clinical implications. *The Lancet. Neurology*, *18*(4), 406–414. [https://doi.org/10.1016/S1474-4422\(18\)30490-3](https://doi.org/10.1016/S1474-4422(18)30490-3)
- Atagi, Y., Liu, C.-C., Painter, M. M., Chen, X.-F., Verbeeck, C., Zheng, H., Li, X., Rademakers, R., Kang, S. S., Xu, H., Younkin, S., Das, P., Fryer, J. D., & Bu, G. (2015). Apolipoprotein E Is a Ligand for Triggering Receptor Expressed on Myeloid Cells 2 (TREM2). *The Journal of Biological Chemistry*, *290*(43), 26043–26050. <https://doi.org/10.1074/jbc.M115.679043>
- Attems, J., Yamaguchi, H., Saido, T. C., & Thal, D. R. (2010). Capillary CAA and perivascular A β -deposition: Two distinct features of Alzheimer's disease pathology. *Journal of the Neurological Sciences*, *299*(1–2), 155–162. <https://doi.org/10.1016/j.jns.2010.08.030>
- Bakou, M., Hille, K., Kracklauer, M., Spanopoulou, A., Frost, C. V., Malideli, E., Yan, L.-M., Caporale, A., Zacharias, M., & Kapurniotu, A. (2017). Key aromatic/hydrophobic amino acids controlling a cross-amyloid peptide interaction versus amyloid self-assembly. *The Journal of Biological Chemistry*, *292*(35), 14587–14602. <https://doi.org/10.1074/jbc.M117.774893>
- Bales, K. R., O'Neill, S. M., Pozdnyakov, N., Pan, F., Caouette, D., Pi, Y., Wood, K. M., Volfson, D., Cirrito, J. R., Han, B.-H., Johnson, A. W., Zipfel, G. J., & Samad, T. A. (2016). Passive immunotherapy targeting amyloid- β reduces cerebral amyloid angiopathy and improves vascular reactivity. *Brain: A Journal of Neurology*, *139*(Pt 2), 563–577. <https://doi.org/10.1093/brain/awv313>
- Bard, F., Cannon, C., Barbour, R., Burke, R. L., Games, D., Grajeda, H., Guido, T., Hu, K., Huang, J., Johnson-Wood, K., Khan, K., Kholodenko, D., Lee, M., Lieberburg, I., Motter, R., Nguyen, M., Soriano, F., Vasquez, N., Weiss, K., ... Yednock, T. (2000). Peripherally administered antibodies against amyloid beta-peptide enter the central nervous system and reduce pathology in a mouse model of Alzheimer disease. *Nature Medicine*, *6*(8), 916–919. <https://doi.org/10.1038/78682>
- Bateman, R. J., Xiong, C., Benzinger, T. L. S., Fagan, A. M., Goate, A., Fox, N. C., Marcus, D. S., Cairns, N. J., Xie, X., Blazey, T. M., Holtzman, D. M., Santacruz, A., Buckles, V., Oliver, A., Moulder, K., Aisen, P. S., Ghetti, B., Klunk,

-
- W. E., McDade, E., ... Dominantly Inherited Alzheimer Network. (2012). Clinical and biomarker changes in dominantly inherited Alzheimer's disease. *The New England Journal of Medicine*, 367(9), 795–804.
<https://doi.org/10.1056/NEJMoa1202753>
- Bekris, L. M., Yu, C.-E., Bird, T. D., & Tsuang, D. W. (2010). Genetics of Alzheimer disease. *Journal of Geriatric Psychiatry and Neurology*, 23(4), 213–227.
<https://doi.org/10.1177/0891988710383571>
- Berchtold, N. C., & Cotman, C. W. (1998). Evolution in the conceptualization of dementia and Alzheimer's disease: Greco-Roman period to the 1960s. *Neurobiology of Aging*, 19(3), 173–189. [https://doi.org/10.1016/s0197-4580\(98\)00052-9](https://doi.org/10.1016/s0197-4580(98)00052-9)
- Bertram, L., Lill, C. M., & Tanzi, R. E. (2010). The genetics of Alzheimer disease: Back to the future. *Neuron*, 68(2), 270–281. <https://doi.org/10.1016/j.neuron.2010.10.013>
- Bickeböller, H., Campion, D., Brice, A., Amouyel, P., Hannequin, D., Didierjean, O., Penet, C., Martin, C., Pérez-Tur, J., Michon, A., Dubois, B., Ledoze, F., Thomas-Anterion, C., Pasquier, F., Puel, M., Demonet, J. F., Moreaud, O., Babron, M. C., Meulien, D., ... Clerget-Darpoux, F. (1997). Apolipoprotein E and Alzheimer disease: Genotype-specific risks by age and sex. *American Journal of Human Genetics*, 60(2), 439–446.
- Bien-Ly, N., Gillespie, A. K., Walker, D., Yoon, S. Y., & Huang, Y. (2012). Reducing human apolipoprotein E levels attenuates age-dependent A β accumulation in mutant human amyloid precursor protein transgenic mice. *The Journal of Neuroscience: The Official Journal of the Society for Neuroscience*, 32(14), 4803–4811. <https://doi.org/10.1523/JNEUROSCI.0033-12.2012>
- Bird, T. D. (2008). Genetic aspects of Alzheimer disease. *Genetics in Medicine: Official Journal of the American College of Medical Genetics*, 10(4), 231–239.
<https://doi.org/10.1097/GIM.0b013e31816b64dc>
- Blotenberg, I., Hoffmann, W., & Thyrian, J. R. (2023). Dementia in Germany: Epidemiology and Prevention Potential. *Deutsches Arzteblatt International*, 120(27–28), 470–476. <https://doi.org/10.3238/arztebl.m2023.0100>

-
- Boche, D., Denham, N., Holmes, C., & Nicoll, J. A. R. (2010). Neuropathology after active Aβ₄₂ immunotherapy: Implications for Alzheimer's disease pathogenesis. *Acta Neuropathologica*, *120*(3), 369–384.
<https://doi.org/10.1007/s00401-010-0719-5>
- Bohrmann, B., Baumann, K., Benz, J., Gerber, F., Huber, W., Knoflach, F., Messer, J., Oroszlan, K., Rauchenberger, R., Richter, W. F., Rothe, C., Urban, M., Bardroff, M., Winter, M., Nordstedt, C., & Loetscher, H. (2012). Gantenerumab: A novel human anti-Aβ antibody demonstrates sustained cerebral amyloid-β binding and elicits cell-mediated removal of human amyloid-β. *Journal of Alzheimer's Disease: JAD*, *28*(1), 49–69. <https://doi.org/10.3233/JAD-2011-110977>
- Bourinet, E., & Zamponi, G. W. (2017). Block of voltage-gated calcium channels by peptide toxins. *Neuropharmacology*, *127*, 109–115.
<https://doi.org/10.1016/j.neuropharm.2016.10.016>
- Breijyeh, Z., & Karaman, R. (2020). Comprehensive Review on Alzheimer's Disease: Causes and Treatment. *Molecules (Basel, Switzerland)*, *25*(24), 5789.
<https://doi.org/10.3390/molecules25245789>
- Budd Haeberlein, S., Aisen, P. S., Barkhof, F., Chalkias, S., Chen, T., Cohen, S., Dent, G., Hansson, O., Harrison, K., von Hehn, C., Iwatsubo, T., Mallinckrodt, C., Mummery, C. J., Muralidharan, K. K., Nestorov, I., Nisenbaum, L., Rajagovindan, R., Skordos, L., Tian, Y., ... Sandrock, A. (2022). Two Randomized Phase 3 Studies of Aducanumab in Early Alzheimer's Disease. *The Journal of Prevention of Alzheimer's Disease*, *9*(2), 197–210.
<https://doi.org/10.14283/jpad.2022.30>
- Budson, A. E., & Solomon, P. R. (2012). New criteria for Alzheimer disease and mild cognitive impairment: Implications for the practicing clinician. *The Neurologist*, *18*(6), 356–363. <https://doi.org/10.1097/NRL.0b013e31826a998d>
- Calhoun, M. E., Burgermeister, P., Phinney, A. L., Stalder, M., Tolnay, M., Wiederhold, K. H., Abramowski, D., Sturchler-Pierrat, C., Sommer, B., Staufenbiel, M., & Jucker, M. (1999). Neuronal overexpression of mutant amyloid precursor protein results in prominent deposition of cerebrovascular amyloid. *Proceedings of the National Academy of Sciences of the United States of America*, *96*(24), 14088–14093. <https://doi.org/10.1073/pnas.96.24.14088>

-
- Carter, S. F., Herholz, K., Rosa-Neto, P., Pellerin, L., Nordberg, A., & Zimmer, E. R. (2019). Astrocyte Biomarkers in Alzheimer's Disease. *Trends in Molecular Medicine*, 25(2), 77–95. <https://doi.org/10.1016/j.molmed.2018.11.006>
- Casas, C., Sergeant, N., Itier, J.-M., Blanchard, V., Wirths, O., van der Kolk, N., Vingtdoux, V., van de Steeg, E., Ret, G., Canton, T., Drobecq, H., Clark, A., Bonici, B., Delacourte, A., Benavides, J., Schmitz, C., Tremp, G., Bayer, T. A., Benoit, P., & Pradier, L. (2004). Massive CA1/2 neuronal loss with intraneuronal and N-terminal truncated Abeta42 accumulation in a novel Alzheimer transgenic model. *The American Journal of Pathology*, 165(4), 1289–1300. [https://doi.org/10.1016/s0002-9440\(10\)63388-3](https://doi.org/10.1016/s0002-9440(10)63388-3)
- Castellani, R. J., Lee, H.-G., Zhu, X., Perry, G., & Smith, M. A. (2008). Alzheimer disease pathology as a host response. *Journal of Neuropathology and Experimental Neurology*, 67(6), 523–531. <https://doi.org/10.1097/NEN.0b013e318177eaf4>
- Castellano, J. M., Kim, J., Stewart, F. R., Jiang, H., DeMattos, R. B., Patterson, B. W., Fagan, A. M., Morris, J. C., Mawuenyega, K. G., Cruchaga, C., Goate, A. M., Bales, K. R., Paul, S. M., Bateman, R. J., & Holtzman, D. M. (2011). Human apoE isoforms differentially regulate brain amyloid- β peptide clearance. *Science Translational Medicine*, 3(89), 89ra57. <https://doi.org/10.1126/scitranslmed.3002156>
- Cavanaugh, S. E., Pippin, J. J., & Barnard, N. D. (2014). Animal models of Alzheimer disease: Historical pitfalls and a path forward. *ALTEX*, 31(3), 279–302. <https://doi.org/10.14573/altex.1310071>
- Cecato, J. F., Martinellil, J. E., Bartholomeu, L. L., Basqueira, A. P., Yassuda, M. S., & Aprahamian, I. (2010). Verbal behavior in Alzheimer's disease patients: Analysis of phrase repetition. *Dementia & Neuropsychologia*, 4(3), 202–206. <https://doi.org/10.1590/S1980-57642010DN40300008>
- Chapleau, M., Iaccarino, L., Soleimani-Meigooni, D., & Rabinovici, G. D. (2022). The Role of Amyloid PET in Imaging Neurodegenerative Disorders: A Review. *Journal of Nuclear Medicine: Official Publication, Society of Nuclear Medicine*, 63(Suppl 1), 13S-19S. <https://doi.org/10.2967/jnumed.121.263195>
- Charidimou, A., Boulouis, G., Gurol, M. E., Ayata, C., Bacskai, B. J., Frosch, M. P., Viswanathan, A., & Greenberg, S. M. (2017). Emerging concepts in sporadic

-
- cerebral amyloid angiopathy. *Brain: A Journal of Neurology*, 140(7), 1829–1850. <https://doi.org/10.1093/brain/awx047>
- Cheng, Y., Tian, D.-Y., & Wang, Y.-J. (2020). Peripheral clearance of brain-derived A β in Alzheimer's disease: Pathophysiology and therapeutic perspectives. *Translational Neurodegeneration*, 9(1), 16. <https://doi.org/10.1186/s40035-020-00195-1>
- Chun, H., & Lee, C. J. (2018). Reactive astrocytes in Alzheimer's disease: A double-edged sword. *Neuroscience Research*, 126, 44–52. <https://doi.org/10.1016/j.neures.2017.11.012>
- Cipriani, G., Danti, S., Picchi, L., Nuti, A., & Fiorino, M. D. (2020). Daily functioning and dementia. *Dementia & Neuropsychologia*, 14(2), 93–102. <https://doi.org/10.1590/1980-57642020dn14-020001>
- Condello, C., Yuan, P., Schain, A., & Grutzendler, J. (2015). Microglia constitute a barrier that prevents neurotoxic protofibrillar A β 42 hotspots around plaques. *Nature Communications*, 6, 6176. <https://doi.org/10.1038/ncomms7176>
- Cras, P., Smith, M. A., Richey, P. L., Siedlak, S. L., Mulvihill, P., & Perry, G. (1995). Extracellular neurofibrillary tangles reflect neuronal loss and provide further evidence of extensive protein cross-linking in Alzheimer disease. *Acta Neuropathologica*, 89(4), 291–295. <https://doi.org/10.1007/BF00309621>
- Croisile, B., Auriacombe, S., Etcharry-Bouyx, F., Vercelletto, M., National Institute on Aging (u.s.), & Alzheimer Association. (2012). [The new 2011 recommendations of the National Institute on Aging and the Alzheimer's Association on diagnostic guidelines for Alzheimer's disease: Preclinical stages, mild cognitive impairment, and dementia]. *Revue Neurologique*, 168(6–7), 471–482. <https://doi.org/10.1016/j.neurol.2011.11.007>
- Cummings, J., Feldman, H. H., & Scheltens, P. (2019). The “rights” of precision drug development for Alzheimer's disease. *Alzheimer's Research & Therapy*, 11(1), 76. <https://doi.org/10.1186/s13195-019-0529-5>
- Cummings, J., & Fox, N. (2017). Defining Disease Modifying Therapy for Alzheimer's Disease. *The Journal of Prevention of Alzheimer's Disease*, 4(2), 109–115. <https://doi.org/10.14283/jpad.2017.12>

-
- Cummings, J., Zhou, Y., Lee, G., Zhong, K., Fonseca, J., & Cheng, F. (2023). Alzheimer's disease drug development pipeline: 2023. *Alzheimer's & Dementia (New York, N. Y.)*, 9(2), e12385. <https://doi.org/10.1002/trc2.12385>
- de Castro, N., Braun, J., Charreau, I., Lafeuillade, A., Viard, J.-P., Allavena, C., Aboulker, J.-P., Molina, J.-M., & EASIER ANRS 138 study group. (2016). Incidence and risk factors for liver enzymes elevations in highly treatment-experienced patients switching from enfuvirtide to raltegravir: A sub-study of the ANRS-138 EASIER trial. *AIDS Research and Therapy*, 13, 17. <https://doi.org/10.1186/s12981-016-0101-3>
- Deer, T. R., Pope, J. E., Hanes, M. C., & McDowell, G. C. (2019). Intrathecal Therapy for Chronic Pain: A Review of Morphine and Ziconotide as Firstline Options. *Pain Medicine (Malden, Mass.)*, 20(4), 784–798. <https://doi.org/10.1093/pm/pny132>
- DeKosky, S. T., & Scheff, S. W. (1990). Synapse loss in frontal cortex biopsies in Alzheimer's disease: Correlation with cognitive severity. *Annals of Neurology*, 27(5), 457–464. <https://doi.org/10.1002/ana.410270502>
- DeTure, M. A., & Dickson, D. W. (2019). The neuropathological diagnosis of Alzheimer's disease. *Molecular Neurodegeneration*, 14(1), 32. <https://doi.org/10.1186/s13024-019-0333-5>
- Dickson, D. W. (1997). The pathogenesis of senile plaques. *Journal of Neuropathology and Experimental Neurology*, 56(4), 321–339. <https://doi.org/10.1097/00005072-199704000-00001>
- Doody, R. S., Thomas, R. G., Farlow, M., Iwatsubo, T., Vellas, B., Joffe, S., Kieburtz, K., Raman, R., Sun, X., Aisen, P. S., Siemers, E., Liu-Seifert, H., Mohs, R., Alzheimer's Disease Cooperative Study Steering Committee, & Solanezumab Study Group. (2014). Phase 3 trials of solanezumab for mild-to-moderate Alzheimer's disease. *The New England Journal of Medicine*, 370(4), 311–321. <https://doi.org/10.1056/NEJMoa1312889>
- Du, A. T., Schuff, N., Kramer, J. H., Ganzer, S., Zhu, X. P., Jagust, W. J., Miller, B. L., Reed, B. R., Mungas, D., Yaffe, K., Chui, H. C., & Weiner, M. W. (2004). Higher atrophy rate of entorhinal cortex than hippocampus in AD. *Neurology*, 62(3), 422–427. <https://doi.org/10.1212/01.wnl.0000106462.72282.90>

-
- Du, J., & Murphy, R. M. (2010). Characterization of the interaction of β -amyloid with transthyretin monomers and tetramers. *Biochemistry*, 49(38), 8276–8289. <https://doi.org/10.1021/bi101280t>
- Dubois, B., Hampel, H., Feldman, H. H., Scheltens, P., Aisen, P., Andrieu, S., Bakardjian, H., Benali, H., Bertram, L., Blennow, K., Broich, K., Cavado, E., Crutch, S., Dartigues, J.-F., Duyckaerts, C., Epelbaum, S., Frisoni, G. B., Gauthier, S., Genthon, R., ... Proceedings of the Meeting of the International Working Group (IWG) and the American Alzheimer's Association on "The Pre-clinical State of AD"; July 23, 2015; Washington DC, USA. (2016). Preclinical Alzheimer's disease: Definition, natural history, and diagnostic criteria. *Alzheimer's & Dementia: The Journal of the Alzheimer's Association*, 12(3), 292–323. <https://doi.org/10.1016/j.jalz.2016.02.002>
- Duyckaerts, C., Potier, M.-C., & Delatour, B. (2008). Alzheimer disease models and human neuropathology: Similarities and differences. *Acta Neuropathologica*, 115(1), 5–38. <https://doi.org/10.1007/s00401-007-0312-8>
- Eckman, C. B., Mehta, N. D., Crook, R., Perez-tur, J., Prihar, G., Pfeiffer, E., Graff-Radford, N., Hinder, P., Yager, D., Zenk, B., Refolo, L. M., Prada, C. M., Younkin, S. G., Hutton, M., & Hardy, J. (1997). A new pathogenic mutation in the APP gene (I716V) increases the relative proportion of A beta 42(43). *Human Molecular Genetics*, 6(12), 2087–2089. <https://doi.org/10.1093/hmg/6.12.2087>
- Fakhoury, M. (2018). Microglia and Astrocytes in Alzheimer's Disease: Implications for Therapy. *Current Neuropharmacology*, 16(5), 508–518. <https://doi.org/10.2174/1570159X15666170720095240>
- Fiandaca, M. S., Kapogiannis, D., Mapstone, M., Boxer, A., Eitan, E., Schwartz, J. B., Abner, E. L., Petersen, R. C., Federoff, H. J., Miller, B. L., & Goetzl, E. J. (2015). Identification of preclinical Alzheimer's disease by a profile of pathogenic proteins in neurally derived blood exosomes: A case-control study. *Alzheimer's & Dementia: The Journal of the Alzheimer's Association*, 11(6), 600–607.e1. <https://doi.org/10.1016/j.jalz.2014.06.008>
- Fisher, E., Pavlenko, K., Vlasov, A., & Ramenskaya, G. (2019). Peptide-Based Therapeutics for Oncology. *Pharmaceutical Medicine*, 33(1), 9–20. <https://doi.org/10.1007/s40290-018-0261-7>

-
- Fleisher, A. S., Chen, K., Liu, X., Ayutyanont, N., Roontiva, A., Thiyyagura, P., Protas, H., Joshi, A. D., Sabbagh, M., Sadowsky, C. H., Sperling, R. A., Clark, C. M., Mintun, M. A., Pontecorvo, M. J., Coleman, R. E., Doraiswamy, P. M., Johnson, K. A., Carpenter, A. P., Skovronsky, D. M., & Reiman, E. M. (2013). Apolipoprotein E ϵ 4 and age effects on florbetapir positron emission tomography in healthy aging and Alzheimer disease. *Neurobiology of Aging*, *34*(1), 1–12. <https://doi.org/10.1016/j.neurobiolaging.2012.04.017>
- Fleisher, A. S., Chen, K., Quiroz, Y. T., Jakimovich, L. J., Gomez, M. G., Langois, C. M., Langbaum, J. B. S., Ayutyanont, N., Roontiva, A., Thiyyagura, P., Lee, W., Mo, H., Lopez, L., Moreno, S., Acosta-Baena, N., Giraldo, M., Garcia, G., Reiman, R. A., Huentelman, M. J., ... Reiman, E. M. (2012). Florbetapir PET analysis of amyloid- β deposition in the presenilin 1 E280A autosomal dominant Alzheimer's disease kindred: A cross-sectional study. *The Lancet. Neurology*, *11*(12), 1057–1065. [https://doi.org/10.1016/S1474-4422\(12\)70227-2](https://doi.org/10.1016/S1474-4422(12)70227-2)
- Frías, J. P., Davies, M. J., Rosenstock, J., Pérez Manghi, F. C., Fernández Landó, L., Bergman, B. K., Liu, B., Cui, X., Brown, K., & SURPASS-2 Investigators. (2021). Tirzepatide versus Semaglutide Once Weekly in Patients with Type 2 Diabetes. *The New England Journal of Medicine*, *385*(6), 503–515. <https://doi.org/10.1056/NEJMoa2107519>
- Frost, G. R., & Li, Y.-M. (2017). The role of astrocytes in amyloid production and Alzheimer's disease. *Open Biology*, *7*(12), 170228. <https://doi.org/10.1098/rsob.170228>
- Fu, W., Ruangkittisakul, A., MacTavish, D., Shi, J. Y., Ballanyi, K., & Jhamandas, J. H. (2012). Amyloid β (A β) peptide directly activates amylin-3 receptor subtype by triggering multiple intracellular signaling pathways. *The Journal of Biological Chemistry*, *287*(22), 18820–18830. <https://doi.org/10.1074/jbc.M111.331181>
- Funke, S. A., & Willbold, D. (2012). Peptides for therapy and diagnosis of Alzheimer's disease. *Current Pharmaceutical Design*, *18*(6), 755–767. <https://doi.org/10.2174/138161212799277752>
- Games, D., Adams, D., Alessandrini, R., Barbour, R., Berthelette, P., Blackwell, C., Carr, T., Clemens, J., Donaldson, T., & Gillespie, F. (1995). Alzheimer-type

-
- neuropathology in transgenic mice overexpressing V717F beta-amyloid precursor protein. *Nature*, 373(6514), 523–527. <https://doi.org/10.1038/373523a0>
- Garwood, C. J., Ratcliffe, L. E., Simpson, J. E., Heath, P. R., Ince, P. G., & Wharton, S. B. (2017). Review: Astrocytes in Alzheimer's disease and other age-associated dementias: a supporting player with a central role. *Neuropathology and Applied Neurobiology*, 43(4), 281–298. <https://doi.org/10.1111/nan.12338>
- GBD 2019 Dementia Forecasting Collaborators. (2022). Estimation of the global prevalence of dementia in 2019 and forecasted prevalence in 2050: An analysis for the Global Burden of Disease Study 2019. *The Lancet. Public Health*, 7(2), e105–e125. [https://doi.org/10.1016/S2468-2667\(21\)00249-8](https://doi.org/10.1016/S2468-2667(21)00249-8)
- Goate, A., Chartier-Harlin, M. C., Mullan, M., Brown, J., Crawford, F., Fidani, L., Giuffra, L., Haynes, A., Irving, N., & James, L. (1991). Segregation of a missense mutation in the amyloid precursor protein gene with familial Alzheimer's disease. *Nature*, 349(6311), 704–706. <https://doi.org/10.1038/349704a0>
- Goedert, M., & Jakes, R. (2005). Mutations causing neurodegenerative tauopathies. *Biochimica Et Biophysica Acta*, 1739(2–3), 240–250. <https://doi.org/10.1016/j.bbadis.2004.08.007>
- Goedert, M., & Spillantini, M. G. (2006). A century of Alzheimer's disease. *Science (New York, N. Y.)*, 314(5800), 777–781. <https://doi.org/10.1126/science.1132814>
- Gómez-Isla, T., Hollister, R., West, H., Mui, S., Growdon, J. H., Petersen, R. C., Parisi, J. E., & Hyman, B. T. (1997). Neuronal loss correlates with but exceeds neurofibrillary tangles in Alzheimer's disease. *Annals of Neurology*, 41(1), 17–24. <https://doi.org/10.1002/ana.410410106>
- Gómez-Isla, T., Price, J. L., McKeel, D. W., Morris, J. C., Growdon, J. H., & Hyman, B. T. (1996). Profound loss of layer II entorhinal cortex neurons occurs in very mild Alzheimer's disease. *The Journal of Neuroscience: The Official Journal of the Society for Neuroscience*, 16(14), 4491–4500. <https://doi.org/10.1523/JNEUROSCI.16-14-04491.1996>
- González-Reyes, R. E., Nava-Mesa, M. O., Vargas-Sánchez, K., Ariza-Salamanca, D., & Mora-Muñoz, L. (2017). Involvement of Astrocytes in Alzheimer's Disease from a Neuroinflammatory and Oxidative Stress Perspective. *Frontiers in Molecular Neuroscience*, 10, 427. <https://doi.org/10.3389/fnmol.2017.00427>

-
- Gordon, D. J., Sciarretta, K. L., & Meredith, S. C. (2001). Inhibition of beta-amyloid(40) fibrillogenesis and disassembly of beta-amyloid(40) fibrils by short beta-amyloid congeners containing N-methyl amino acids at alternate residues. *Biochemistry*, *40*(28), 8237–8245. <https://doi.org/10.1021/bi002416v>
- Gottesman, R. F., Albert, M. S., Alonso, A., Coker, L. H., Coresh, J., Davis, S. M., Deal, J. A., McKhann, G. M., Mosley, T. H., Sharrett, A. R., Schneider, A. L. C., Windham, B. G., Wruck, L. M., & Knopman, D. S. (2017). Associations Between Midlife Vascular Risk Factors and 25-Year Incident Dementia in the Atherosclerosis Risk in Communities (ARIC) Cohort. *JAMA Neurology*, *74*(10), 1246–1254. <https://doi.org/10.1001/jamaneurol.2017.1658>
- Goyal, D., Shuaib, S., Mann, S., & Goyal, B. (2017). Rationally Designed Peptides and Peptidomimetics as Inhibitors of Amyloid- β (A β) Aggregation: Potential Therapeutics of Alzheimer's Disease. *ACS Combinatorial Science*, *19*(2), 55–80. <https://doi.org/10.1021/acscombsci.6b00116>
- Grossberg, G. T. (2003). Cholinesterase inhibitors for the treatment of Alzheimer's disease: Getting on and staying on. *Current Therapeutic Research, Clinical and Experimental*, *64*(4), 216–235. [https://doi.org/10.1016/S0011-393X\(03\)00059-6](https://doi.org/10.1016/S0011-393X(03)00059-6)
- Guerreiro, R., & Bras, J. (2015). The age factor in Alzheimer's disease. *Genome Medicine*, *7*, 106. <https://doi.org/10.1186/s13073-015-0232-5>
- Guo, J., Wang, Z., Liu, R., Huang, Y., Zhang, N., & Zhang, R. (2020). Memantine, Donepezil, or Combination Therapy-What is the best therapy for Alzheimer's Disease? A Network Meta-Analysis. *Brain and Behavior*, *10*(11), e01831. <https://doi.org/10.1002/brb3.1831>
- Haass, C., & Selkoe, D. J. (2007). Soluble protein oligomers in neurodegeneration: Lessons from the Alzheimer's amyloid beta-peptide. *Nature Reviews. Molecular Cell Biology*, *8*(2), 101–112. <https://doi.org/10.1038/nrm2101>
- Habib, N., McCabe, C., Medina, S., Varshavsky, M., Kitsberg, D., Dvir-Szternfeld, R., Green, G., Dionne, D., Nguyen, L., Marshall, J. L., Chen, F., Zhang, F., Kaplan, T., Regev, A., & Schwartz, M. (2020). Disease-associated astrocytes in Alzheimer's disease and aging. *Nature Neuroscience*, *23*(6), 701–706. <https://doi.org/10.1038/s41593-020-0624-8>

-
- Hall, A. M., & Roberson, E. D. (2012). Mouse models of Alzheimer's disease. *Brain Research Bulletin*, 88(1), 3–12. <https://doi.org/10.1016/j.brainres-bull.2011.11.017>
- Hempel, H., Hardy, J., Blennow, K., Chen, C., Perry, G., Kim, S. H., Villemagne, V. L., Aisen, P., Vendruscolo, M., Iwatsubo, T., Masters, C. L., Cho, M., Lannfelt, L., Cummings, J. L., & Vergallo, A. (2021). The Amyloid- β Pathway in Alzheimer's Disease. *Molecular Psychiatry*, 26(10), 5481–5503. <https://doi.org/10.1038/s41380-021-01249-0>
- Hempel, H., Mesulam, M.-M., Cuellar, A. C., Farlow, M. R., Giacobini, E., Grossberg, G. T., Khachaturian, A. S., Vergallo, A., Cavado, E., Snyder, P. J., & Khachaturian, Z. S. (2018). The cholinergic system in the pathophysiology and treatment of Alzheimer's disease. *Brain: A Journal of Neurology*, 141(7), 1917–1933. <https://doi.org/10.1093/brain/awy132>
- Haque, A., Engel, J., Teichmann, S. A., & Lönnberg, T. (2017). A practical guide to single-cell RNA-sequencing for biomedical research and clinical applications. *Genome Medicine*, 9(1), 75. <https://doi.org/10.1186/s13073-017-0467-4>
- Hardy, J. A., & Higgins, G. A. (1992). Alzheimer's disease: The amyloid cascade hypothesis. *Science (New York, N.Y.)*, 256(5054), 184–185. <https://doi.org/10.1126/science.1566067>
- Henninot, A., Collins, J. C., & Nuss, J. M. (2018). The Current State of Peptide Drug Discovery: Back to the Future? *Journal of Medicinal Chemistry*, 61(4), 1382–1414. <https://doi.org/10.1021/acs.jmedchem.7b00318>
- Hoffman, E. A., Frey, B. L., Smith, L. M., & Auble, D. T. (2015). Formaldehyde cross-linking: A tool for the study of chromatin complexes. *The Journal of Biological Chemistry*, 290(44), 26404–26411. <https://doi.org/10.1074/jbc.R115.651679>
- Holtzman, D. M., Herz, J., & Bu, G. (2012). Apolipoprotein E and apolipoprotein E receptors: Normal biology and roles in Alzheimer disease. *Cold Spring Harbor Perspectives in Medicine*, 2(3), a006312. <https://doi.org/10.1101/cshperspect.a006312>
- Holtzman, D. M., Morris, J. C., & Goate, A. M. (2011a). Alzheimer's disease: The challenge of the second century. *Science Translational Medicine*, 3(77), 77sr1. <https://doi.org/10.1126/scitranslmed.3002369>

-
- Holtzman, D. M., Morris, J. C., & Goate, A. M. (2011b). Alzheimer's disease: The challenge of the second century. *Science Translational Medicine*, 3(77), 77sr1. <https://doi.org/10.1126/scitranslmed.3002369>
- Honig, L. S., Barakos, J., Dhadda, S., Kanekiyo, M., Reyderman, L., Irizarry, M., Kramer, L. D., Swanson, C. J., & Sabbagh, M. (2023). ARIA in patients treated with lecanemab (BAN2401) in a phase 2 study in early Alzheimer's disease. *Alzheimer's & Dementia (New York, N. Y.)*, 9(1), e12377. <https://doi.org/10.1002/trc2.12377>
- Hsiao, K., Chapman, P., Nilsen, S., Eckman, C., Harigaya, Y., Younkin, S., Yang, F., & Cole, G. (1996). Correlative memory deficits, Abeta elevation, and amyloid plaques in transgenic mice. *Science (New York, N.Y.)*, 274(5284), 99–102. <https://doi.org/10.1126/science.274.5284.99>
- Hutton, M., Lendon, C. L., Rizzu, P., Baker, M., Froelich, S., Houlden, H., Pickering-Brown, S., Chakraverty, S., Isaacs, A., Grover, A., Hackett, J., Adamson, J., Lincoln, S., Dickson, D., Davies, P., Petersen, R. C., Stevens, M., de Graaff, E., Wauters, E., ... Heutink, P. (1998). Association of missense and 5'-splice-site mutations in tau with the inherited dementia FTDP-17. *Nature*, 393(6686), 702–705. <https://doi.org/10.1038/31508>
- Ibrahim, A. M., Pottoo, F. H., Dahiya, E. S., Khan, F. A., & Kumar, J. B. S. (2020). Neuron-glia interactions: Molecular basis of alzheimer's disease and applications of neuroproteomics. *The European Journal of Neuroscience*, 52(2), 2931–2943. <https://doi.org/10.1111/ejn.14838>
- Iliff, J. J., Wang, M., Liao, Y., Plogg, B. A., Peng, W., Gundersen, G. A., Benveniste, H., Vates, G. E., Deane, R., Goldman, S. A., Nagelhus, E. A., & Nedergaard, M. (2012). A paravascular pathway facilitates CSF flow through the brain parenchyma and the clearance of interstitial solutes, including amyloid β . *Science Translational Medicine*, 4(147), 147ra111. <https://doi.org/10.1126/scitranslmed.3003748>
- Itagaki, S., McGeer, P. L., Akiyama, H., Zhu, S., & Selkoe, D. (1989). Relationship of microglia and astrocytes to amyloid deposits of Alzheimer disease. *Journal of Neuroimmunology*, 24(3), 173–182. [https://doi.org/10.1016/0165-5728\(89\)90115-x](https://doi.org/10.1016/0165-5728(89)90115-x)

-
- Iyengar, S., Ossipov, M. H., & Johnson, K. W. (2017). The role of calcitonin gene-related peptide in peripheral and central pain mechanisms including migraine. *Pain, 158*(4), 543–559. <https://doi.org/10.1097/j.pain.0000000000000831>
- Jagust, W., Gitcho, A., Sun, F., Kuczynski, B., Mungas, D., & Haan, M. (2006). Brain imaging evidence of preclinical Alzheimer's disease in normal aging. *Annals of Neurology, 59*(4), 673–681. <https://doi.org/10.1002/ana.20799>
- Jaitin, D. A., Kenigsberg, E., Keren-Shaul, H., Elefant, N., Paul, F., Zaretsky, I., Mildner, A., Cohen, N., Jung, S., Tanay, A., & Amit, I. (2014). Massively parallel single-cell RNA-seq for marker-free decomposition of tissues into cell types. *Science (New York, N.Y.), 343*(6172), 776–779. <https://doi.org/10.1126/science.1247651>
- Jankowsky, J. L., Younkin, L. H., Gonzales, V., Fadale, D. J., Slunt, H. H., Lester, H. A., Younkin, S. G., & Borchelt, D. R. (2007). Rodent A beta modulates the solubility and distribution of amyloid deposits in transgenic mice. *The Journal of Biological Chemistry, 282*(31), 22707–22720. <https://doi.org/10.1074/jbc.M611050200>
- Jawhar, S., Wirths, O., & Bayer, T. A. (2011). Pyroglutamate amyloid- β (A β): A hatchet man in Alzheimer disease. *The Journal of Biological Chemistry, 286*(45), 38825–38832. <https://doi.org/10.1074/jbc.R111.288308>
- Jay, T. R., Miller, C. M., Cheng, P. J., Graham, L. C., Bemiller, S., Broihier, M. L., Xu, G., Margevicius, D., Karlo, J. C., Sousa, G. L., Cotleur, A. C., Butovsky, O., Bekris, L., Staugaitis, S. M., Leverenz, J. B., Pimplikar, S. W., Landreth, G. E., Howell, G. R., Ransohoff, R. M., & Lamb, B. T. (2015). TREM2 deficiency eliminates TREM2+ inflammatory macrophages and ameliorates pathology in Alzheimer's disease mouse models. *The Journal of Experimental Medicine, 212*(3), 287–295. <https://doi.org/10.1084/jem.20142322>
- Ji, H., Besson-Girard, S., Androvic, P., Bulut, B., Liu, L., Wang, Y., & Gokce, O. (2023). High-Resolution RNA Sequencing from PFA-Fixed Microscopy Sections. *Methods in Molecular Biology (Clifton, N.J.), 2616*, 205–212. https://doi.org/10.1007/978-1-0716-2926-0_16

-
- Jonker, C., Geerlings, M. I., & Schmand, B. (2000). Are memory complaints predictive for dementia? A review of clinical and population-based studies. *International Journal of Geriatric Psychiatry*, *15*(11), 983–991.
[https://doi.org/10.1002/1099-1166\(200011\)15:11<983::aid-gps238>3.0.co;2-5](https://doi.org/10.1002/1099-1166(200011)15:11<983::aid-gps238>3.0.co;2-5)
- Joseph-Mathurin, N., Llibre-Guerra, J. J., Li, Y., McCullough, A. A., Hofmann, C., Wojtowicz, J., Park, E., Wang, G., Preboske, G. M., Wang, Q., Gordon, B. A., Chen, C. D., Flores, S., Aggarwal, N. T., Berman, S. B., Bird, T. D., Black, S. E., Borowski, B., Brooks, W. S., ... Dominantly Inherited Alzheimer Network Trials Unit. (2022). Amyloid-Related Imaging Abnormalities in the DIAN-TU-001 Trial of Gantenerumab and Solanezumab: Lessons from a Trial in Dominantly Inherited Alzheimer Disease. *Annals of Neurology*, *92*(5), 729–744.
<https://doi.org/10.1002/ana.26511>
- Kamphuis, W., Kooijman, L., Schetters, S., Orre, M., & Hol, E. M. (2016). Transcriptional profiling of CD11c-positive microglia accumulating around amyloid plaques in a mouse model for Alzheimer’s disease. *Biochimica Et Biophysica Acta*, *1862*(10), 1847–1860. <https://doi.org/10.1016/j.bbadis.2016.07.007>
- Kapurniotu, A., Buck, A., Weber, M., Schmauder, A., Hirsch, T., Bernhagen, J., & Tarek-Nossol, M. (2003). Conformational restriction via cyclization in beta-amyloid peptide Abeta(1-28) leads to an inhibitor of Abeta(1-28) amyloidogenesis and cytotoxicity. *Chemistry & Biology*, *10*(2), 149–159.
[https://doi.org/10.1016/s1074-5521\(03\)00022-x](https://doi.org/10.1016/s1074-5521(03)00022-x)
- Karlawish, J., & Grill, J. D. (2021). The approval of Aduhelm risks eroding public trust in Alzheimer research and the FDA. *Nature Reviews. Neurology*, *17*(9), 523–524. <https://doi.org/10.1038/s41582-021-00540-6>
- Kaur, A., Shuken, S., Yang, A. C., & Iram, T. (2023). A protocol for collection and infusion of cerebrospinal fluid in mice. *STAR Protocols*, *4*(1), 102015.
<https://doi.org/10.1016/j.xpro.2022.102015>
- Kaya, T., Mattugini, N., Liu, L., Ji, H., Cantuti-Castelvetri, L., Wu, J., Schifferer, M., Groh, J., Martini, R., Besson-Girard, S., Kaji, S., Liesz, A., Gokce, O., & Simons, M. (2022). CD8+ T cells induce interferon-responsive oligodendrocytes and microglia in white matter aging. *Nature Neuroscience*, *25*(11), 1446–1457. <https://doi.org/10.1038/s41593-022-01183-6>

-
- Kayed, R., Bernhagen, J., Greenfield, N., Sweimeh, K., Brunner, H., Voelter, W., & Kapurniotu, A. (1999). Conformational transitions of islet amyloid polypeptide (IAPP) in amyloid formation in vitro. *Journal of Molecular Biology*, *287*(4), 781–796. <https://doi.org/10.1006/jmbi.1999.2646>
- Keren-Shaul, H., Spinrad, A., Weiner, A., Matcovitch-Natan, O., Dvir-Szternfeld, R., Ulland, T. K., David, E., Baruch, K., Lara-Astaiso, D., Toth, B., Itzkovitz, S., Colonna, M., Schwartz, M., & Amit, I. (2017). A Unique Microglia Type Associated with Restricting Development of Alzheimer's Disease. *Cell*, *169*(7), 1276–1290.e17. <https://doi.org/10.1016/j.cell.2017.05.018>
- Khoury, R., Rajamanickam, J., & Grossberg, G. T. (2018). An update on the safety of current therapies for Alzheimer's disease: Focus on rivastigmine. *Therapeutic Advances in Drug Safety*, *9*(3), 171–178. <https://doi.org/10.1177/2042098617750555>
- Kidwell, C. S., Liebeskind, D. S., Starkman, S., & Saver, J. L. (2001). Trends in acute ischemic stroke trials through the 20th century. *Stroke*, *32*(6), 1349–1359. <https://doi.org/10.1161/01.str.32.6.1349>
- Kim, C. K., Lee, Y. R., Ong, L., Gold, M., Kalali, A., & Sarkar, J. (2022). Alzheimer's Disease: Key Insights from Two Decades of Clinical Trial Failures. *Journal of Alzheimer's Disease: JAD*, *87*(1), 83–100. <https://doi.org/10.3233/JAD-215699>
- Knowles, R. B., Wyart, C., Buldyrev, S. V., Cruz, L., Urbanc, B., Hasselmo, M. E., Stanley, H. E., & Hyman, B. T. (1999). Plaque-induced neurite abnormalities: Implications for disruption of neural networks in Alzheimer's disease. *Proceedings of the National Academy of Sciences of the United States of America*, *96*(9), 5274–5279. <https://doi.org/10.1073/pnas.96.9.5274>
- Koenigsknecht-Talboo, J., Meyer-Luehmann, M., Parsadanian, M., Garcia-Alloza, M., Finn, M. B., Hyman, B. T., Bacskai, B. J., & Holtzman, D. M. (2008). Rapid microglial response around amyloid pathology after systemic anti-Abeta antibody administration in PDAPP mice. *The Journal of Neuroscience: The Official Journal of the Society for Neuroscience*, *28*(52), 14156–14164. <https://doi.org/10.1523/JNEUROSCI.4147-08.2008>

-
- Köhler, G., & Milstein, C. (1975). Continuous cultures of fused cells secreting antibody of predefined specificity. *Nature*, *256*(5517), 495–497.
<https://doi.org/10.1038/256495a0>
- Kontos, C., El Bounkari, O., Krammer, C., Sinitski, D., Hille, K., Zan, C., Yan, G., Wang, S., Gao, Y., Brandhofer, M., Megens, R. T. A., Hoffmann, A., Pauli, J., Asare, Y., Gerra, S., Bourilhon, P., Leng, L., Eckstein, H.-H., Kempf, W. E., ... Bernhagen, J. (2020). Designed CXCR4 mimic acts as a soluble chemokine receptor that blocks atherogenic inflammation by agonist-specific targeting. *Nature Communications*, *11*(1), 5981. <https://doi.org/10.1038/s41467-020-19764-z>
- Koronyo, Y., Biggs, D., Barron, E., Boyer, D. S., Pearlman, J. A., Au, W. J., Kile, S. J., Blanco, A., Fuchs, D.-T., Ashfaq, A., Frautschy, S., Cole, G. M., Miller, C. A., Hinton, D. R., Verdooner, S. R., Black, K. L., & Koronyo-Hamaoui, M. (2017). Retinal amyloid pathology and proof-of-concept imaging trial in Alzheimer's disease. *JCI Insight*, *2*(16), e93621, 93621.
<https://doi.org/10.1172/jci.insight.93621>
- Kraeuter, A.-K., Guest, P. C., & Sarnyai, Z. (2019). The Elevated Plus Maze Test for Measuring Anxiety-Like Behavior in Rodents. *Methods in Molecular Biology (Clifton, N.J.)*, *1916*, 69–74. https://doi.org/10.1007/978-1-4939-8994-2_4
- Kraft, A. W., Hu, X., Yoon, H., Yan, P., Xiao, Q., Wang, Y., Gil, S. C., Brown, J., Wilhelmsson, U., Restivo, J. L., Cirrito, J. R., Holtzman, D. M., Kim, J., Pekny, M., & Lee, J. (2013). Attenuating astrocyte activation accelerates plaque pathogenesis in APP/PS1 mice. *The FASEB Journal*, *27*(1), 187–198.
<https://doi.org/10.1096/fj.12-208660>
- Krause, D. L., & Müller, N. (2010). Neuroinflammation, microglia and implications for anti-inflammatory treatment in Alzheimer's disease. *International Journal of Alzheimer's Disease*, *2010*, 732806. <https://doi.org/10.4061/2010/732806>
- Kumar-Singh, S., Cras, P., Wang, R., Kros, J. M., van Swieten, J., Lübke, U., Ceuterick, C., Serneels, S., Vennekens, K., Timmermans, J.-P., Van Marck, E., Martin, J.-J., van Duijn, C. M., & Van Broeckhoven, C. (2002). Dense-core senile plaques in the Flemish variant of Alzheimer's disease are vasocentric. *The American Journal of Pathology*, *161*(2), 507–520.
[https://doi.org/10.1016/S0002-9440\(10\)64207-1](https://doi.org/10.1016/S0002-9440(10)64207-1)

-
- Langui, D., Girardot, N., El Hachimi, K. H., Allinquant, B., Blanchard, V., Pradier, L., & Duyckaerts, C. (2004). Subcellular topography of neuronal Abeta peptide in APPxPS1 transgenic mice. *The American Journal of Pathology*, *165*(5), 1465–1477. [https://doi.org/10.1016/s0002-9440\(10\)63405-0](https://doi.org/10.1016/s0002-9440(10)63405-0)
- Lanoiselée, H.-M., Nicolas, G., Wallon, D., Rovelet-Lecrux, A., Lacour, M., Rousseau, S., Richard, A.-C., Pasquier, F., Rollin-Sillaire, A., Martinaud, O., Quillard-Muraine, M., de la Sayette, V., Boutoleau-Bretonniere, C., Etcharry-Bouyx, F., Chauviré, V., Sarazin, M., le Ber, I., Epelbaum, S., Jonveaux, T., ... collaborators of the CNR-MAJ project. (2017). APP, PSEN1, and PSEN2 mutations in early-onset Alzheimer disease: A genetic screening study of familial and sporadic cases. *PLoS Medicine*, *14*(3), e1002270. <https://doi.org/10.1371/journal.pmed.1002270>
- Larson, M. E., & Lesné, S. E. (2012). Soluble A β oligomer production and toxicity. *Journal of Neurochemistry*, *120 Suppl 1*(Suppl 1), 125–139. <https://doi.org/10.1111/j.1471-4159.2011.07478.x>
- Lee, A. C.-L., Harris, J. L., Khanna, K. K., & Hong, J.-H. (2019). A Comprehensive Review on Current Advances in Peptide Drug Development and Design. *International Journal of Molecular Sciences*, *20*(10), 2383. <https://doi.org/10.3390/ijms20102383>
- Lee, D., Slomkowski, M., Hefting, N., Chen, D., Larsen, K. G., Kohegyi, E., Hobart, M., Cummings, J. L., & Grossberg, G. T. (2023). Brexpiprazole for the Treatment of Agitation in Alzheimer Dementia: A Randomized Clinical Trial. *JAMA Neurology*, *80*(12), 1307–1316. <https://doi.org/10.1001/jamaneurol.2023.3810>
- Lesné, S. E., Sherman, M. A., Grant, M., Kuskowski, M., Schneider, J. A., Bennett, D. A., & Ashe, K. H. (2013). Brain amyloid- β oligomers in ageing and Alzheimer's disease. *Brain: A Journal of Neurology*, *136*(Pt 5), 1383–1398. <https://doi.org/10.1093/brain/awt062>
- Lesné, S., Kotilinek, L., & Ashe, K. H. (2008). Plaque-bearing mice with reduced levels of oligomeric amyloid-beta assemblies have intact memory function. *Neuroscience*, *151*(3), 745–749. <https://doi.org/10.1016/j.neuroscience.2007.10.054>
- Leszek, J., Mikhaylenko, E. V., Belousov, D. M., Koutsouraki, E., Szczechowiak, K., Kobusiak-Prokopowicz, M., Mysiak, A., Diniz, B. S., Somasundaram, S. G.,

-
- Kirkland, C. E., & Aliev, G. (2021). The Links between Cardiovascular Diseases and Alzheimer's Disease. *Current Neuropharmacology*, 19(2), 152–169. <https://doi.org/10.2174/1570159X18666200729093724>
- Li, X., & Wang, C.-Y. (2021). From bulk, single-cell to spatial RNA sequencing. *International Journal of Oral Science*, 13(1), 36. <https://doi.org/10.1038/s41368-021-00146-0>
- Lim, Y.-A., Ittner, L. M., Lim, Y. L., & Götz, J. (2008). Human but not rat amylin shares neurotoxic properties with Abeta42 in long-term hippocampal and cortical cultures. *FEBS Letters*, 582(15), 2188–2194. <https://doi.org/10.1016/j.febslet.2008.05.006>
- Liu, C.-C., Liu, C.-C., Kanekiyo, T., Xu, H., & Bu, G. (2013). Apolipoprotein E and Alzheimer disease: Risk, mechanisms and therapy. *Nature Reviews. Neurology*, 9(2), 106–118. <https://doi.org/10.1038/nrneurol.2012.263>
- Liu, Y.-H., Giunta, B., Zhou, H.-D., Tan, J., & Wang, Y.-J. (2012). Immunotherapy for Alzheimer disease: The challenge of adverse effects. *Nature Reviews. Neurology*, 8(8), 465–469. <https://doi.org/10.1038/nrneurol.2012.118>
- Livingston, G., Huntley, J., Sommerlad, A., Ames, D., Ballard, C., Banerjee, S., Brayne, C., Burns, A., Cohen-Mansfield, J., Cooper, C., Costafreda, S. G., Dias, A., Fox, N., Gitlin, L. N., Howard, R., Kales, H. C., Kivimäki, M., Larson, E. B., Ogunniyi, A., ... Mukadam, N. (2020). Dementia prevention, intervention, and care: 2020 report of the Lancet Commission. *Lancet (London, England)*, 396(10248), 413–446. [https://doi.org/10.1016/S0140-6736\(20\)30367-6](https://doi.org/10.1016/S0140-6736(20)30367-6)
- Llovera, G., Hofmann, K., Roth, S., Salas-Pédomo, A., Ferrer-Ferrer, M., Perego, C., Zanier, E. R., Mamrak, U., Rex, A., Party, H., Agin, V., Fauchon, C., Orset, C., Haelewyn, B., De Simoni, M.-G., Dirnagl, U., Grittner, U., Planas, A. M., Plesnila, N., ... Liesz, A. (2015). Results of a preclinical randomized controlled multicenter trial (pRCT): Anti-CD49d treatment for acute brain ischemia. *Science Translational Medicine*, 7(299), 299ra121. <https://doi.org/10.1126/scitranslmed.aaa9853>
- Lue, L. F., Kuo, Y. M., Roher, A. E., Brachova, L., Shen, Y., Sue, L., Beach, T., Kurth, J. H., Rydel, R. E., & Rogers, J. (1999). Soluble amyloid beta peptide concentration as a predictor of synaptic change in Alzheimer's disease. *The*

-
- American Journal of Pathology*, 155(3), 853–862.
[https://doi.org/10.1016/s0002-9440\(10\)65184-x](https://doi.org/10.1016/s0002-9440(10)65184-x)
- Mafi, J. N., Leng, M., Arbanas, J. C., Tseng, C.-H., Damberg, C. L., Sarkisian, C., & Landon, B. E. (2022). Estimated Annual Spending on Aducanumab in the US Medicare Program. *JAMA Health Forum*, 3(1), e214495.
<https://doi.org/10.1001/jamahealthforum.2021.4495>
- Malek-Ahmadi, M., Perez, S. E., Chen, K., & Mufson, E. J. (2016). Neuritic and Diffuse Plaque Associations with Memory in Non-Cognitively Impaired Elderly. *Journal of Alzheimer's Disease: JAD*, 53(4), 1641–1652.
<https://doi.org/10.3233/JAD-160365>
- Manabe, T., Fujikura, Y., Mizukami, K., Akatsu, H., & Kudo, K. (2019). Pneumonia-associated death in patients with dementia: A systematic review and meta-analysis. *PloS One*, 14(3), e0213825. <https://doi.org/10.1371/journal.pone.0213825>
- Manji, Z., Rojas, A., Wang, W., Dingledine, R., Varvel, N. H., & Ganesh, T. (2019). 5xFAD Mice Display Sex-Dependent Inflammatory Gene Induction During the Prodromal Stage of Alzheimer's Disease. *Journal of Alzheimer's Disease: JAD*, 70(4), 1259–1274. <https://doi.org/10.3233/JAD-180678>
- Mazaheri, F., Snaidero, N., Kleinberger, G., Madore, C., Daria, A., Werner, G., Krasemann, S., Capell, A., Trümbach, D., Wurst, W., Brunner, B., Bultmann, S., Tahirovic, S., Kerschensteiner, M., Misgeld, T., Butovsky, O., & Haass, C. (2017). TREM2 deficiency impairs chemotaxis and microglial responses to neuronal injury. *EMBO Reports*, 18(7), 1186–1198.
<https://doi.org/10.15252/embr.201743922>
- Mendez, M. F. (2019). Early-onset Alzheimer Disease and Its Variants. *Continuum (Minneapolis, Minn.)*, 25(1), 34–51.
<https://doi.org/10.1212/CON.0000000000000687>
- Meng, Q., Lin, M.-S., & Tzeng, I.-S. (2020). Relationship Between Exercise and Alzheimer's Disease: A Narrative Literature Review. *Frontiers in Neuroscience*, 14, 131. <https://doi.org/10.3389/fnins.2020.00131>
- Mielke, M. M. (2018). Sex and Gender Differences in Alzheimer's Disease Dementia. *The Psychiatric Times*, 35(11), 14–17.

-
- Monterey, M. D., Wei, H., Wu, X., & Wu, J. Q. (2021). The Many Faces of Astrocytes in Alzheimer's Disease. *Frontiers in Neurology, 12*, 619626. <https://doi.org/10.3389/fneur.2021.619626>
- Mueller, S. G., Weiner, M. W., Thal, L. J., Petersen, R. C., Jack, C., Jagust, W., Trojanowski, J. Q., Toga, A. W., & Beckett, L. (2005). The Alzheimer's disease neuroimaging initiative. *Neuroimaging Clinics of North America, 15*(4), 869–877, xi–xii. <https://doi.org/10.1016/j.nic.2005.09.008>
- Namba, Y., Tomonaga, M., Kawasaki, H., Otomo, E., & Ikeda, K. (1991). Apolipoprotein E immunoreactivity in cerebral amyloid deposits and neurofibrillary tangles in Alzheimer's disease and kuru plaque amyloid in Creutzfeldt-Jakob disease. *Brain Research, 541*(1), 163–166. [https://doi.org/10.1016/0006-8993\(91\)91092-f](https://doi.org/10.1016/0006-8993(91)91092-f)
- Nanclares, C., Baraibar, A. M., Araque, A., & Kofuji, P. (2021). Dysregulation of Astrocyte-Neuronal Communication in Alzheimer's Disease. *International Journal of Molecular Sciences, 22*(15), 7887. <https://doi.org/10.3390/ijms22157887>
- Nelson, P. T., Braak, H., & Markesbery, W. R. (2009). Neuropathology and cognitive impairment in Alzheimer disease: A complex but coherent relationship. *Journal of Neuropathology and Experimental Neurology, 68*(1), 1–14. <https://doi.org/10.1097/NEN.0b013e3181919a48>
- Nimmerjahn, A., Kirchhoff, F., & Helmchen, F. (2005). Resting microglial cells are highly dynamic surveillants of brain parenchyma in vivo. *Science (New York, N.Y.), 308*(5726), 1314–1318. <https://doi.org/10.1126/science.1110647>
- Oakley, H., Cole, S. L., Logan, S., Maus, E., Shao, P., Craft, J., Guillozet-Bongaarts, A., Ohno, M., Disterhoft, J., Van Eldik, L., Berry, R., & Vassar, R. (2006). Intraneuronal beta-amyloid aggregates, neurodegeneration, and neuron loss in transgenic mice with five familial Alzheimer's disease mutations: Potential factors in amyloid plaque formation. *The Journal of Neuroscience: The Official Journal of the Society for Neuroscience, 26*(40), 10129–10140. <https://doi.org/10.1523/JNEUROSCI.1202-06.2006>
- O'Brien, R. J., & Wong, P. C. (2011). Amyloid precursor protein processing and Alzheimer's disease. *Annual Review of Neuroscience, 34*, 185–204. <https://doi.org/10.1146/annurev-neuro-061010-113613>

-
- Olivares, D., Deshpande, V. K., Shi, Y., Lahiri, D. K., Greig, N. H., Rogers, J. T., & Huang, X. (2012). N-methyl D-aspartate (NMDA) receptor antagonists and memantine treatment for Alzheimer's disease, vascular dementia and Parkinson's disease. *Current Alzheimer Research*, 9(6), 746–758.
<https://doi.org/10.2174/156720512801322564>
- Ong, C.-A. J., Tan, Q. X., Lim, H. J., Shannon, N. B., Lim, W. K., Hendrikson, J., Ng, W. H., Tan, J. W. S., Koh, K. K. N., Wasudevan, S. D., Ng, C. C. Y., Rajasegaran, V., Lim, T. K. H., Ong, C. K., Kon, O. L., Teh, B. T., Tan, G. H. C., Chia, C. S., Soo, K. C., & Teo, M. C. C. (2020). An Optimised Protocol Harnessing Laser Capture Microdissection for Transcriptomic Analysis on Matched Primary and Metastatic Colorectal Tumours. *Scientific Reports*, 10(1), 682. <https://doi.org/10.1038/s41598-019-55146-2>
- Onos, K. D., Sukoff Rizzo, S. J., Howell, G. R., & Sasner, M. (2016). Toward more predictive genetic mouse models of Alzheimer's disease. *Brain Research Bulletin*, 122, 1–11. <https://doi.org/10.1016/j.brainresbull.2015.12.003>
- O'Nuallain, B., Williams, A. D., Westermarck, P., & Wetzel, R. (2004). Seeding specificity in amyloid growth induced by heterologous fibrils. *The Journal of Biological Chemistry*, 279(17), 17490–17499.
<https://doi.org/10.1074/jbc.M311300200>
- Orr, A. A., Wördehoff, M. M., Hoyer, W., & Tamamis, P. (2016). Uncovering the Binding and Specificity of β -Wrapins for Amyloid- β and α -Synuclein. *The Journal of Physical Chemistry. B*, 120(50), 12781–12794.
<https://doi.org/10.1021/acs.jpcc.6b08485>
- Orre, M., Kamphuis, W., Osborn, L. M., Jansen, A. H. P., Kooijman, L., Bossers, K., & Hol, E. M. (2014). Isolation of glia from Alzheimer's mice reveals inflammation and dysfunction. *Neurobiology of Aging*, 35(12), 2746–2760.
<https://doi.org/10.1016/j.neurobiolaging.2014.06.004>
- Oskarsson, M. E., Paulsson, J. F., Schultz, S. W., Ingelsson, M., Westermarck, P., & Westermarck, G. T. (2015). In vivo seeding and cross-seeding of localized amyloidosis: A molecular link between type 2 diabetes and Alzheimer disease. *The American Journal of Pathology*, 185(3), 834–846.
<https://doi.org/10.1016/j.ajpath.2014.11.016>

-
- Ostrowitzki, S., Bittner, T., Sink, K. M., Mackey, H., Rabe, C., Honig, L. S., Cassetta, E., Woodward, M., Boada, M., van Dyck, C. H., Grimmer, T., Selkoe, D. J., Schneider, A., Blondeau, K., Hu, N., Quartino, A., Clayton, D., Dolton, M., Dang, Y., ... Doody, R. S. (2022). Evaluating the Safety and Efficacy of Crenzumab vs Placebo in Adults With Early Alzheimer Disease: Two Phase 3 Randomized Placebo-Controlled Trials. *JAMA Neurology*, *79*(11), 1113–1121. <https://doi.org/10.1001/jamaneurol.2022.2909>
- Paterson, R. W., Slattery, C. F., Poole, T., Nicholas, J. M., Magdalinou, N. K., Toombs, J., Chapman, M. D., Lunn, M. P., Heslegrave, A. J., Foiani, M. S., Weston, P. S. J., Keshavan, A., Rohrer, J. D., Rossor, M. N., Warren, J. D., Mummery, C. J., Blennow, K., Fox, N. C., Zetterberg, H., & Schott, J. M. (2018). Cerebrospinal fluid in the differential diagnosis of Alzheimer's disease: Clinical utility of an extended panel of biomarkers in a specialist cognitive clinic. *Alzheimer's Research & Therapy*, *10*(1), 32. <https://doi.org/10.1186/s13195-018-0361-3>
- Pekny, M., & Nilsson, M. (2005). Astrocyte activation and reactive gliosis. *Glia*, *50*(4), 427–434. <https://doi.org/10.1002/glia.20207>
- Perl, D. P. (2010). Neuropathology of Alzheimer's disease. *The Mount Sinai Journal of Medicine, New York*, *77*(1), 32–42. <https://doi.org/10.1002/msj.20157>
- Perrin, R. J., Fagan, A. M., & Holtzman, D. M. (2009). Multimodal techniques for diagnosis and prognosis of Alzheimer's disease. *Nature*, *461*(7266), 916–922. <https://doi.org/10.1038/nature08538>
- Petersen, R. C., Caracciolo, B., Brayne, C., Gauthier, S., Jelic, V., & Fratiglioni, L. (2014). Mild cognitive impairment: A concept in evolution. *Journal of Internal Medicine*, *275*(3), 214–228. <https://doi.org/10.1111/joim.12190>
- Phan, H. V., van Gent, M., Drayman, N., Basu, A., Gack, M. U., & Tay, S. (2021). High-throughput RNA sequencing of paraformaldehyde-fixed single cells. *Nature Communications*, *12*(1), 5636. <https://doi.org/10.1038/s41467-021-25871-2>
- Picelli, S., Björklund, Å. K., Faridani, O. R., Sagasser, S., Winberg, G., & Sandberg, R. (2013). Smart-seq2 for sensitive full-length transcriptome profiling in single cells. *Nature Methods*, *10*(11), 1096–1098. <https://doi.org/10.1038/nmeth.2639>

-
- Picelli, S., Faridani, O. R., Björklund, A. K., Winberg, G., Sagasser, S., & Sandberg, R. (2014). Full-length RNA-seq from single cells using Smart-seq2. *Nature Protocols*, 9(1), 171–181. <https://doi.org/10.1038/nprot.2014.006>
- Pihlaja, R., Koistinaho, J., Malm, T., Sikkilä, H., Vainio, S., & Koistinaho, M. (2008). Transplanted astrocytes internalize deposited beta-amyloid peptides in a transgenic mouse model of Alzheimer's disease. *Glia*, 56(2), 154–163. <https://doi.org/10.1002/glia.20599>
- Pimplikar, S. W. (2009). Reassessing the amyloid cascade hypothesis of Alzheimer's disease. *The International Journal of Biochemistry & Cell Biology*, 41(6), 1261–1268. <https://doi.org/10.1016/j.biocel.2008.12.015>
- Pisarewicz, K., Mora, D., Pflueger, F. C., Fields, G. B., & Marí, F. (2005). Polypeptide chains containing D-gamma-hydroxyvaline. *Journal of the American Chemical Society*, 127(17), 6207–6215. <https://doi.org/10.1021/ja050088m>
- Pitts, M. (2018). Barnes Maze Procedure for Spatial Learning and Memory in Mice. *BIO-PROTOCOL*, 8(5). <https://doi.org/10.21769/BioProtoc.2744>
- Pontecorvo, M. J., Lu, M., Burnham, S. C., Schade, A. E., Dage, J. L., Shcherbinin, S., Collins, E. C., Sims, J. R., & Mintun, M. A. (2022). Association of Donanemab Treatment With Exploratory Plasma Biomarkers in Early Symptomatic Alzheimer Disease: A Secondary Analysis of the TRAILBLAZER-ALZ Randomized Clinical Trial. *JAMA Neurology*, 79(12), 1250–1259. <https://doi.org/10.1001/jamaneurol.2022.3392>
- Preische, O., Schultz, S. A., Apel, A., Kuhle, J., Kaeser, S. A., Barro, C., Gräber, S., Kuder-Buletta, E., LaFougere, C., Laske, C., Vöglein, J., Levin, J., Masters, C. L., Martins, R., Schofield, P. R., Rossor, M. N., Graff-Radford, N. R., Sallo-way, S., Ghetti, B., ... Dominantly Inherited Alzheimer Network. (2019). Serum neurofilament dynamics predicts neurodegeneration and clinical progression in presymptomatic Alzheimer's disease. *Nature Medicine*, 25(2), 277–283. <https://doi.org/10.1038/s41591-018-0304-3>
- Radde, R., Bolmont, T., Kaeser, S. A., Coomaraswamy, J., Lindau, D., Stoltze, L., Calhoun, M. E., Jäggi, F., Wolburg, H., Gengler, S., Haass, C., Ghetti, B., Czech, C., Hölscher, C., Mathews, P. M., & Jucker, M. (2006). Abeta42-driven cerebral amyloidosis in transgenic mice reveals early and robust pathology. *EMBO Reports*, 7(9), 940–946. <https://doi.org/10.1038/sj.embor.7400784>

-
- Reisberg, B., Doody, R., Stöffler, A., Schmitt, F., Ferris, S., Möbius, H. J., & Memantine Study Group. (2003). Memantine in moderate-to-severe Alzheimer's disease. *The New England Journal of Medicine*, *348*(14), 1333–1341. <https://doi.org/10.1056/NEJMoa013128>
- Reish, N. J., Jamshidi, P., Stamm, B., Flanagan, M. E., Sugg, E., Tang, M., Donohue, K. L., McCord, M., Krumpelman, C., Mesulam, M.-M., Castellani, R., & Chou, S. H.-Y. (2023). Multiple Cerebral Hemorrhages in a Patient Receiving Lecanemab and Treated with t-PA for Stroke. *The New England Journal of Medicine*, *388*(5), 478–479. <https://doi.org/10.1056/NEJMc2215148>
- Ren, R., Qi, J., Lin, S., Liu, X., Yin, P., Wang, Z., Tang, R., Wang, J., Huang, Q., Li, J., Xie, X., Hu, Y., Cui, S., Zhu, Y., Yu, X., Wang, P., Zhu, Y., Wang, Y., Huang, Y., ... Wang, G. (2022). The China Alzheimer Report 2022. *General Psychiatry*, *35*(1), e100751. <https://doi.org/10.1136/gpsych-2022-100751>
- Roychaudhuri, R., Yang, M., Hoshi, M. M., & Teplow, D. B. (2009). Amyloid beta-protein assembly and Alzheimer disease. *The Journal of Biological Chemistry*, *284*(8), 4749–4753. <https://doi.org/10.1074/jbc.R800036200>
- Rubio-Perez, J. M., & Morillas-Ruiz, J. M. (2012). A review: Inflammatory process in Alzheimer's disease, role of cytokines. *TheScientificWorldJournal*, *2012*, 756357. <https://doi.org/10.1100/2012/756357>
- Safaiyan, S., Besson-Girard, S., Kaya, T., Cantuti-Castelvetri, L., Liu, L., Ji, H., Schifferer, M., Gouna, G., Usifo, F., Kannaiyan, N., Fitzner, D., Xiang, X., Rossner, M. J., Brendel, M., Gokce, O., & Simons, M. (2021). White matter aging drives microglial diversity. *Neuron*, *109*(7), 1100-1117.e10. <https://doi.org/10.1016/j.neuron.2021.01.027>
- Saito, T., Matsuba, Y., Mihira, N., Takano, J., Nilsson, P., Itohara, S., Iwata, N., & Saido, T. C. (2014). Single App knock-in mouse models of Alzheimer's disease. *Nature Neuroscience*, *17*(5), 661–663. <https://doi.org/10.1038/nn.3697>
- Salloway, S., Farlow, M., McDade, E., Clifford, D. B., Wang, G., Llibre-Guerra, J. J., Hitchcock, J. M., Mills, S. L., Santacruz, A. M., Aschenbrenner, A. J., Hassentab, J., Benzinger, T. L. S., Gordon, B. A., Fagan, A. M., Coalier, K. A., Cruchaga, C., Goate, A. A., Perrin, R. J., Xiong, C., ... Dominantly Inherited

-
- Alzheimer Network–Trials Unit. (2021). A trial of gantenerumab or solanezumab in dominantly inherited Alzheimer's disease. *Nature Medicine*, 27(7), 1187–1196. <https://doi.org/10.1038/s41591-021-01369-8>
- Samudra, N., Lane-Donovan, C., VandeVrede, L., & Boxer, A. L. (2023). Tau pathology in neurodegenerative disease: Disease mechanisms and therapeutic avenues. *The Journal of Clinical Investigation*, 133(12), e168553. <https://doi.org/10.1172/JCI168553>
- Santacruz, K., Lewis, J., Spires, T., Paulson, J., Kotilinek, L., Ingelsson, M., Guimaraes, A., DeTure, M., Ramsden, M., McGowan, E., Forster, C., Yue, M., Orne, J., Janus, C., Mariash, A., Kuskowski, M., Hyman, B., Hutton, M., & Ashe, K. H. (2005). Tau suppression in a neurodegenerative mouse model improves memory function. *Science (New York, N.Y.)*, 309(5733), 476–481. <https://doi.org/10.1126/science.1113694>
- Scheff, S. W., Sparks, L., & Price, D. A. (1993). Quantitative assessment of synaptic density in the entorhinal cortex in Alzheimer's disease. *Annals of Neurology*, 34(3), 356–361. <https://doi.org/10.1002/ana.410340309>
- Schmitz, C., Rutten, B. P. F., Pielen, A., Schäfer, S., Wirths, O., Tremp, G., Czech, C., Blanchard, V., Multhaup, G., Rezaie, P., Korr, H., Steinbusch, H. W. M., Pradier, L., & Bayer, T. A. (2004). Hippocampal neuron loss exceeds amyloid plaque load in a transgenic mouse model of Alzheimer's disease. *The American Journal of Pathology*, 164(4), 1495–1502. [https://doi.org/10.1016/S0002-9440\(10\)63235-X](https://doi.org/10.1016/S0002-9440(10)63235-X)
- Seibenhener, M. L., & Wooten, M. C. (2015). Use of the Open Field Maze to Measure Locomotor and Anxiety-like Behavior in Mice. *Journal of Visualized Experiments*, 96, 52434. <https://doi.org/10.3791/52434>
- Selkoe, D. J., & Hardy, J. (2016). The amyloid hypothesis of Alzheimer's disease at 25 years. *EMBO Molecular Medicine*, 8(6), 595–608. <https://doi.org/10.15252/emmm.201606210>
- Serrano-Pozo, A., Frosch, M. P., Masliah, E., & Hyman, B. T. (2011). Neuropathological alterations in Alzheimer disease. *Cold Spring Harbor Perspectives in Medicine*, 1(1), a006189. <https://doi.org/10.1101/cshperspect.a006189>
- Sevigny, J., Chiao, P., Bussière, T., Weinreb, P. H., Williams, L., Maier, M., Dunstan, R., Salloway, S., Chen, T., Ling, Y., O'Gorman, J., Qian, F., Arastu, M., Li, M.,

-
- Chollate, S., Brennan, M. S., Quintero-Monzon, O., Scannevin, R. H., Arnold, H. M., ... Sandroock, A. (2016a). The antibody aducanumab reduces A β plaques in Alzheimer's disease. *Nature*, 537(7618), 50–56.
<https://doi.org/10.1038/nature19323>
- Sevigny, J., Chiao, P., Bussi re, T., Weinreb, P. H., Williams, L., Maier, M., Dunstan, R., Salloway, S., Chen, T., Ling, Y., O'Gorman, J., Qian, F., Arastu, M., Li, M., Chollate, S., Brennan, M. S., Quintero-Monzon, O., Scannevin, R. H., Arnold, H. M., ... Sandroock, A. (2016b). The antibody aducanumab reduces A β plaques in Alzheimer's disease. *Nature*, 537(7618), 50–56.
<https://doi.org/10.1038/nature19323>
- Sgourakis, N. G., Yan, Y., McCallum, S. A., Wang, C., & Garcia, A. E. (2007). The Alzheimer's peptides Abeta40 and 42 adopt distinct conformations in water: A combined MD / NMR study. *Journal of Molecular Biology*, 368(5), 1448–1457.
<https://doi.org/10.1016/j.jmb.2007.02.093>
- Shin, J.-H. (2022). Dementia Epidemiology Fact Sheet 2022. *Annals of Rehabilitation Medicine*, 46(2), 53–59. <https://doi.org/10.5535/arm.22027>
- Shuster, L. T., Rhodes, D. J., Gostout, B. S., Grossardt, B. R., & Rocca, W. A. (2010). Premature menopause or early menopause: Long-term health consequences. *Maturitas*, 65(2), 161–166. <https://doi.org/10.1016/j.maturitas.2009.08.003>
- Sidorova, A., Bystrov, V., Lutsenko, A., Shpigun, D., Belova, E., & Likhachev, I. (2021). Quantitative Assessment of Chirality of Protein Secondary Structures and Phenylalanine Peptide Nanotubes. *Nanomaterials (Basel, Switzerland)*, 11(12), 3299. <https://doi.org/10.3390/nano11123299>
- Singh, D. (2022). Astrocytic and microglial cells as the modulators of neuroinflammation in Alzheimer's disease. *Journal of Neuroinflammation*, 19(1), 206.
<https://doi.org/10.1186/s12974-022-02565-0>
- Sloan, L. A. (2019). Review of glucagon-like peptide-1 receptor agonists for the treatment of type 2 diabetes mellitus in patients with chronic kidney disease and their renal effects. *Journal of Diabetes*, 11(12), 938–948.
<https://doi.org/10.1111/1753-0407.12969>

-
- Smith, E. E. (2018). Cerebral amyloid angiopathy as a cause of neurodegeneration. *Journal of Neurochemistry*, 144(5), 651–658. <https://doi.org/10.1111/jnc.14157>
- Spanopoulou, A., Heidrich, L., Chen, H., Frost, C., Hrle, D., Malideli, E., Hille, K., Grammatikopoulos, A., Bernhagen, J., Zacharias, M., Rammes, G., & Kapurniotu, A. (2018). Designed Macrocyclic Peptides as Nanomolar Amyloid Inhibitors Based on Minimal Recognition Elements. *Angewandte Chemie International Edition*, 57(44), 14503–14508. <https://doi.org/10.1002/anie.201802979>
- Spires-Jones, T. L., Meyer-Luehmann, M., Osetek, J. D., Jones, P. B., Stern, E. A., Bacskai, B. J., & Hyman, B. T. (2007). Impaired spine stability underlies plaque-related spine loss in an Alzheimer's disease mouse model. *The American Journal of Pathology*, 171(4), 1304–1311. <https://doi.org/10.2353/ajpath.2007.070055>
- Srinivasan, K., Friedman, B. A., Larson, J. L., Lauffer, B. E., Goldstein, L. D., Appling, L. L., Borneo, J., Poon, C., Ho, T., Cai, F., Steiner, P., van der Brug, M. P., Modrusan, Z., Kaminker, J. S., & Hansen, D. V. (2016). Untangling the brain's neuroinflammatory and neurodegenerative transcriptional responses. *Nature Communications*, 7, 11295. <https://doi.org/10.1038/ncomms11295>
- Srinivasan, M., Sedmak, D., & Jewell, S. (2002). Effect of fixatives and tissue processing on the content and integrity of nucleic acids. *The American Journal of Pathology*, 161(6), 1961–1971. [https://doi.org/10.1016/S0002-9440\(10\)64472-0](https://doi.org/10.1016/S0002-9440(10)64472-0)
- Ståhl, P. L., Salmén, F., Vickovic, S., Lundmark, A., Navarro, J. F., Magnusson, J., Giacomello, S., Asp, M., Westholm, J. O., Huss, M., Mollbrink, A., Linnarsson, S., Codeluppi, S., Borg, Å., Pontén, F., Costea, P. I., Sahlén, P., Mulder, J., Bergmann, O., ... Frisén, J. (2016). Visualization and analysis of gene expression in tissue sections by spatial transcriptomics. *Science (New York, N.Y.)*, 353(6294), 78–82. <https://doi.org/10.1126/science.aaf2403>
- Tang, F., Barbacioru, C., Wang, Y., Nordman, E., Lee, C., Xu, N., Wang, X., Bodeau, J., Tuch, B. B., Siddiqui, A., Lao, K., & Surani, M. A. (2009). mRNA-Seq whole-transcriptome analysis of a single cell. *Nature Methods*, 6(5), 377–382. <https://doi.org/10.1038/nmeth.1315>

-
- Tarasoff-Conway, J. M., Carare, R. O., Osorio, R. S., Glodzik, L., Butler, T., Fieremans, E., Axel, L., Rusinek, H., Nicholson, C., Zlokovic, B. V., Frangione, B., Blennow, K., Ménard, J., Zetterberg, H., Wisniewski, T., & de Leon, M. J. (2015). Clearance systems in the brain-implications for Alzheimer disease. *Nature Reviews. Neurology*, *11*(8), 457–470. <https://doi.org/10.1038/nrneurol.2015.119>
- Tarawneh, R., & Holtzman, D. M. (2012). The clinical problem of symptomatic Alzheimer disease and mild cognitive impairment. *Cold Spring Harbor Perspectives in Medicine*, *2*(5), a006148. <https://doi.org/10.1101/cshperspect.a006148>
- Thal, D. R., Ghebremedhin, E., Rüb, U., Yamaguchi, H., Del Tredici, K., & Braak, H. (2002). Two types of sporadic cerebral amyloid angiopathy. *Journal of Neuro pathology and Experimental Neurology*, *61*(3), 282–293. <https://doi.org/10.1093/jnen/61.3.282>
- Thomsen, E. R., Mich, J. K., Yao, Z., Hodge, R. D., Doyle, A. M., Jang, S., Shehata, S. I., Nelson, A. M., Shapovalova, N. V., Levi, B. P., & Ramanathan, S. (2016). Fixed single-cell transcriptomic characterization of human radial glial diversity. *Nature Methods*, *13*(1), 87–93. <https://doi.org/10.1038/nmeth.3629>
- Tjernberg, L. O., Lilliehöök, C., Callaway, D. J., Näslund, J., Hahne, S., Thyberg, J., Terenius, L., & Nordstedt, C. (1997). Controlling amyloid beta-peptide fibril formation with protease-stable ligands. *The Journal of Biological Chemistry*, *272*(19), 12601–12605. <https://doi.org/10.1074/jbc.272.19.12601>
- Tolar, M., Hey, J., Power, A., & Abushakra, S. (2021). Neurotoxic Soluble Amyloid Oligomers Drive Alzheimer’s Pathogenesis and Represent a Clinically Validated Target for Slowing Disease Progression. *International Journal of Molecular Sciences*, *22*(12), 6355. <https://doi.org/10.3390/ijms22126355>
- Torres, M. D. T., Sothiselvam, S., Lu, T. K., & de la Fuente-Nunez, C. (2019). Peptide Design Principles for Antimicrobial Applications. *Journal of Molecular Biology*, *431*(18), 3547–3567. <https://doi.org/10.1016/j.jmb.2018.12.015>
- Tuppo, E. E., & Arias, H. R. (2005). The role of inflammation in Alzheimer’s disease. *The International Journal of Biochemistry & Cell Biology*, *37*(2), 289–305. <https://doi.org/10.1016/j.biocel.2004.07.009>

-
- Uddin, M. S., & Lim, L. W. (2022). Glial cells in Alzheimer's disease: From neuropathological changes to therapeutic implications. *Ageing Research Reviews*, *78*, 101622. <https://doi.org/10.1016/j.arr.2022.101622>
- Vaillant-Beuchot, L., Mary, A., Pardossi-Piquard, R., Bourgeois, A., Lauritzen, I., Eyser, F., Kinoshita, P. F., Cazareth, J., Badot, C., Fragaki, K., Bussiere, R., Martin, C., Mary, R., Bauer, C., Pagnotta, S., Paquis-Flucklinger, V., Buée-Scherrer, V., Buée, L., Lacas-Gervais, S., ... Chami, M. (2021). Accumulation of amyloid precursor protein C-terminal fragments triggers mitochondrial structure, function, and mitophagy defects in Alzheimer's disease models and human brains. *Acta Neuropathologica*, *141*(1), 39–65. <https://doi.org/10.1007/s00401-020-02234-7>
- Valenza, M., Facchinetti, R., Menegoni, G., Steardo, L., & Scuderi, C. (2021). Alternative Targets to Fight Alzheimer's Disease: Focus on Astrocytes. *Biomolecules*, *11*(4), 600. <https://doi.org/10.3390/biom11040600>
- van Dyck, C. H., Swanson, C. J., Aisen, P., Bateman, R. J., Chen, C., Gee, M., Kanekiyo, M., Li, D., Reyderman, L., Cohen, S., Froelich, L., Katayama, S., Sabbagh, M., Vellas, B., Watson, D., Dhadda, S., Irizarry, M., Kramer, L. D., & Iwatsubo, T. (2023). Lecanemab in Early Alzheimer's Disease. *The New England Journal of Medicine*, *388*(1), 9–21. <https://doi.org/10.1056/NEJMoa2212948>
- Vega, J. N., & Newhouse, P. A. (2014). Mild cognitive impairment: Diagnosis, longitudinal course, and emerging treatments. *Current Psychiatry Reports*, *16*(10), 490. <https://doi.org/10.1007/s11920-014-0490-8>
- Verdile, G., Fuller, S. J., & Martins, R. N. (2015). The role of type 2 diabetes in neurodegeneration. *Neurobiology of Disease*, *84*, 22–38. <https://doi.org/10.1016/j.nbd.2015.04.008>
- Vidoni, E. D., Yeh, H.-W., Morris, J. K., Newell, K. L., Alqahtani, A., Burns, N. C., Burns, J. M., & Billinger, S. A. (2016). Cerebral β -Amyloid Angiopathy Is Associated with Earlier Dementia Onset in Alzheimer's Disease. *Neuro-Degenerative Diseases*, *16*(3–4), 218–224. <https://doi.org/10.1159/000441919>
- Villemagne, V. L., Burnham, S., Bourgeat, P., Brown, B., Ellis, K. A., Salvado, O., Szoëke, C., Macaulay, S. L., Martins, R., Maruff, P., Ames, D., Rowe, C. C.,

-
- Masters, C. L., & Australian Imaging Biomarkers and Lifestyle (AIBL) Research Group. (2013). Amyloid β deposition, neurodegeneration, and cognitive decline in sporadic Alzheimer's disease: A prospective cohort study. *The Lancet. Neurology*, *12*(4), 357–367. [https://doi.org/10.1016/S1474-4422\(13\)70044-9](https://doi.org/10.1016/S1474-4422(13)70044-9)
- Viola, K. L., & Klein, W. L. (2015). Amyloid β oligomers in Alzheimer's disease pathogenesis, treatment, and diagnosis. *Acta Neuropathologica*, *129*(2), 183–206. <https://doi.org/10.1007/s00401-015-1386-3>
- Walsh, D. M., & Selkoe, D. J. (2007). A beta oligomers—A decade of discovery. *Journal of Neurochemistry*, *101*(5), 1172–1184. <https://doi.org/10.1111/j.1471-4159.2006.04426.x>
- Wang, X., He, Y., Zhang, Q., Ren, X., & Zhang, Z. (2021). Direct Comparative Analyses of 10X Genomics Chromium and Smart-seq2. *Genomics, Proteomics & Bioinformatics*, *19*(2), 253–266. <https://doi.org/10.1016/j.gpb.2020.02.005>
- Wang, Y., Cella, M., Mallinson, K., Ulrich, J. D., Young, K. L., Robinette, M. L., Gilfillan, S., Krishnan, G. M., Sudhakar, S., Zinselmeyer, B. H., Holtzman, D. M., Cirrito, J. R., & Colonna, M. (2015). TREM2 lipid sensing sustains the microglial response in an Alzheimer's disease model. *Cell*, *160*(6), 1061–1071. <https://doi.org/10.1016/j.cell.2015.01.049>
- Wang, Y., Ulland, T. K., Ulrich, J. D., Song, W., Tzaferis, J. A., Hole, J. T., Yuan, P., Mahan, T. E., Shi, Y., Gilfillan, S., Cella, M., Grutzendler, J., DeMattos, R. B., Cirrito, J. R., Holtzman, D. M., & Colonna, M. (2016). TREM2-mediated early microglial response limits diffusion and toxicity of amyloid plaques. *The Journal of Experimental Medicine*, *213*(5), 667–675. <https://doi.org/10.1084/jem.20151948>
- Wang, Z., Gerstein, M., & Snyder, M. (2009). RNA-Seq: A revolutionary tool for transcriptomics. *Nature Reviews. Genetics*, *10*(1), 57–63. <https://doi.org/10.1038/nrg2484>
- Westermarck, P., Andersson, A., & Westermarck, G. T. (2011). Islet Amyloid Polypeptide, Islet Amyloid, and Diabetes Mellitus. *Physiological Reviews*, *91*(3), 795–826. <https://doi.org/10.1152/physrev.00042.2009>

-
- Wisniewski, T., & Frangione, B. (1992). Apolipoprotein E: A pathological chaperone protein in patients with cerebral and systemic amyloid. *Neuroscience Letters*, *135*(2), 235–238. [https://doi.org/10.1016/0304-3940\(92\)90444-c](https://doi.org/10.1016/0304-3940(92)90444-c)
- Wyss-Coray, T., Loike, J. D., Brionne, T. C., Lu, E., Anankov, R., Yan, F., Silverstein, S. C., & Husemann, J. (2003). Adult mouse astrocytes degrade amyloid-beta in vitro and in situ. *Nature Medicine*, *9*(4), 453–457. <https://doi.org/10.1038/nm838>
- Xiong, M., Jiang, H., Serrano, J. R., Gonzales, E. R., Wang, C., Gratuze, M., Hoyle, R., Bien-Ly, N., Silverman, A. P., Sullivan, P. M., Watts, R. J., Ulrich, J. D., Zipfel, G. J., & Holtzman, D. M. (2021). APOE immunotherapy reduces cerebral amyloid angiopathy and amyloid plaques while improving cerebrovascular function. *Science Translational Medicine*, *13*(581), eabd7522. <https://doi.org/10.1126/scitranslmed.abd7522>
- Yan, L.-M., Tatarek-Nossol, M., Velkova, A., Kazantzis, A., & Kapurniotu, A. (2006). Design of a mimic of nonamyloidogenic and bioactive human islet amyloid polypeptide (IAPP) as nanomolar affinity inhibitor of IAPP cytotoxic fibrillogenesis. *Proceedings of the National Academy of Sciences of the United States of America*, *103*(7), 2046–2051. <https://doi.org/10.1073/pnas.0507471103>
- Yan, L.-M., Velkova, A., Tatarek-Nossol, M., Andreetto, E., & Kapurniotu, A. (2007). IAPP mimic blocks Abeta cytotoxic self-assembly: Cross-suppression of amyloid toxicity of Abeta and IAPP suggests a molecular link between Alzheimer's disease and type II diabetes. *Angewandte Chemie (International Ed. in English)*, *46*(8), 1246–1252. <https://doi.org/10.1002/anie.200604056>
- Yan, L.-M., Velkova, A., Tatarek-Nossol, M., Rammes, G., Sibae, A., Andreetto, E., Kracklauer, M., Bakou, M., Malideli, E., Göke, B., Schirra, J., Storr, M., & Kapurniotu, A. (2013). Selectively N-methylated soluble IAPP mimics as potent IAPP receptor agonists and nanomolar inhibitors of cytotoxic self-assembly of both IAPP and A β 40. *Angewandte Chemie (International Ed. in English)*, *52*(39), 10378–10383. <https://doi.org/10.1002/anie.201302840>
- Yasuhara, O., Kawamata, T., Aimi, Y., McGeer, E. G., & McGeer, P. L. (1994). Two types of dystrophic neurites in senile plaques of Alzheimer disease and elderly non-demented cases. *Neuroscience Letters*, *171*(1–2), 73–76. [https://doi.org/10.1016/0304-3940\(94\)90608-4](https://doi.org/10.1016/0304-3940(94)90608-4)

-
- Yeh, F. L., Wang, Y., Tom, I., Gonzalez, L. C., & Sheng, M. (2016). TREM2 Binds to Apolipoproteins, Including APOE and CLU/APOJ, and Thereby Facilitates Uptake of Amyloid-Beta by Microglia. *Neuron*, *91*(2), 328–340. <https://doi.org/10.1016/j.neuron.2016.06.015>
- Yiannopoulou, K. G., & Papageorgiou, S. G. (2020). Current and Future Treatments in Alzheimer Disease: An Update. *Journal of Central Nervous System Disease*, *12*, 1179573520907397. <https://doi.org/10.1177/1179573520907397>
- Yin, Z., Raj, D., Saiepour, N., Van Dam, D., Brouwer, N., Holtman, I. R., Eggen, B. J. L., Möller, T., Tamm, J. A., Abdourahman, A., Hol, E. M., Kamphuis, W., Bayer, T. A., De Deyn, P. P., & Boddeke, E. (2017). Immune hyperreactivity of A β plaque-associated microglia in Alzheimer's disease. *Neurobiology of Aging*, *55*, 115–122. <https://doi.org/10.1016/j.neurobiolaging.2017.03.021>
- Yuan, P., Condello, C., Keene, C. D., Wang, Y., Bird, T. D., Paul, S. M., Luo, W., Colonna, M., Baddeley, D., & Grutzendler, J. (2016). TREM2 Haplodeficiency in Mice and Humans Impairs the Microglia Barrier Function Leading to Decreased Amyloid Compaction and Severe Axonal Dystrophy. *Neuron*, *90*(4), 724–739. <https://doi.org/10.1016/j.neuron.2016.05.003>
- Zhang, Y., Chen, H., Li, R., Sterling, K., & Song, W. (2023). Amyloid β -based therapy for Alzheimer's disease: Challenges, successes and future. *Signal Transduction and Targeted Therapy*, *8*(1), 248. <https://doi.org/10.1038/s41392-023-01484-7>
- Zhu, H., Wang, X., Wallack, M., Li, H., Carreras, I., Dedeoglu, A., Hur, J.-Y., Zheng, H., Li, H., Fine, R., Mwamburi, M., Sun, X., Kowall, N., Stern, R. A., & Qiu, W. Q. (2015). Intraperitoneal injection of the pancreatic peptide amylin potently reduces behavioral impairment and brain amyloid pathology in murine models of Alzheimer's disease. *Molecular Psychiatry*, *20*(2), 252–262. <https://doi.org/10.1038/mp.2014.17>
- Zolocheska, O., & Tagliatela, G. (2016). Non-Demented Individuals with Alzheimer's Disease Neuropathology: Resistance to Cognitive Decline May Reveal New Treatment Strategies. *Current Pharmaceutical Design*, *22*(26), 4063–4068. <https://doi.org/10.2174/1381612822666160518142110>

9. Acknowledgements

Each doctoral thesis has a long story. This journey, spanning six years and over 8,000 kilometers from China to Germany, was navigated amidst the unprecedented challenges of the COVID-19 pandemic. So many people have offered their support for this story to have a splendid ending. Here, please allow me to acknowledge the invaluable contributions with my sincere gratitude.

Foremost, my gratitude is extended to my supervisor, Univ.-Prof. Dr. Ozgun Gokce, PhD. It was not only amazing be able to follow Oz in developing advanced techniques, but also get to know him, a great scientist full of imaginations and creativities. He wrote the first experiment notes on my notebook and showed me how to use the pipette hand by hand, which motivated me to step into research from a clinical background. Oz always taught me to be open for new knowledge, stay supportive, keep aiming at the future, which the top scientist would always maintain.

Moreover, I also extend my thanks my other thesis committee members, Univ.-Prof. Dr. rer. nat. Jürgen Bernhagen, who also serves as thesis promoter, and Univ.-Prof. Dr. med. Mikael Simons, and my major project supervisor Univ.-Prof. Dr. Aphrodite Kapurniotu. During my research, they gave me valuable opportunities and support to carry projects. More importantly, at times when the path seems unclear, it was their guidance and encourage to rebuild the scientific focus which would profoundly benefit my academic journey.

Moreover, I also extend my thanks my other thesis committee members, Univ.-Prof. Dr. rer. nat. Jürgen Bernhagen, who also serves as thesis promoter, and Univ.-Prof. Dr. med. Mikael Simons, and my major project supervisor Univ.-Prof. Dr. Aphrodite Kapurniotu. During my research, they gave me valuable opportunities and support to carry projects. More importantly, at times when the path seems unclear, it was their guidance and encourage to rebuild the scientific focus which would profoundly benefit my academic journey.

I am deeply grateful to my parents and in-laws for their unlimited support and patience, and to my grandparents for their constant guidance and affection. You have instilled in me the values of respecting others, humility, pragmatism. Your encouragement and oversight have been pivotal in motivating me to pursue my doctoral studies abroad and aim for higher academic goals. I am also thankful to my extended family members,

and friends, whose relationships with me have remained strong despite the barriers of distance and time. I eagerly anticipate our next reunion.

Furthermore, I want to express my heartfelt gratitude to my beloved wife, Dr. med Yishi Qin, for being my constant support and partner for life and doctoral studies. Additionally, I am grateful for our baby son, Yuheng Ji, who has already brought so much joy to our lives in Germany. Your presence is a cherished gift, and we both love you immensely and can't wait to be with you.

Thank you again to all of you for being my companions on this remarkable journey, through moments of joy and tribulation alike. Should I have the chance to be recognized as a qualified scientist one day, a reliable ally, a cherished friend, I would proudly tell you that you are the ones who have guided me.

Affidavit



Affidavit

Ji, Hao

Surname, first name

Nymphenburger Str. 205

Street

80639, Munich, Germany

Zip code, town, country

I hereby declare, that the submitted thesis entitled:
Evaluating the therapeutic effects of a peptide-based inhibitor of amyloid aggregation in mouse models of Alzheimer's disease

.....

is my own work. I have only used the sources indicated and have not made unauthorized use of services of a third party. Where the work of others has been quoted or reproduced, the source is always given.

I further declare that the submitted thesis or parts thereof have not been presented as part of an examination degree to any other university.

Munich, 22-July-2024

place, date

Hao Ji

Signature doctoral candidate

Confirmation of congruency



Confirmation of congruency between printed and electronic version of the doctoral thesis

Ji, Hao

Surname, first name

Nymphenburger Str. 205

Street

80639, Munich, Germany

Zip code, town, country

I hereby declare, that the submitted thesis entitled:

Evaluating the therapeutic effects of a peptide-based inhibitor of amyloid aggregation in mouse models of Alzheimer's disease

.....

is congruent with the printed version both in content and format.

Munich, 22-July-2024

place, date

Hao Ji

Signature doctoral candidate